



**UNIVERSITY OF IOANNINA**

**School of Agriculture  
Department of Agriculture**

**Essential oil loaded collagen hydrogels to battle bacterial  
infections for tissue engineering applications**

**Çağlar Ersanlı**

**Doctoral Thesis**

**Arta**

**2025**

© 2025 Caglar Ersanli

«Η έγκριση της παρούσης Διδακτορικής Διατριβής από το Τμήμα Χημείας της Σχολής Θετικών Επιστημών του Πανεπιστημίου Ιωαννίνων, δεν υποδηλώνει αποδοχή των γνωμών του συγγραφέως (Ν. 5343/1932. Άρθρο 202, παρ.2)»

### **Supervisory Committee**

**Prof. Ioannis Skoufos**, Department of Agriculture, University of Ioannina, Arta, Greece

**Prof. Athina Tzora**, Department of Agriculture, University of Ioannina, Arta, Greece

**Prof. Dimitrios I. Zeugolis**, School of Mechanical and Materials Engineering, University College Dublin, Dublin, Ireland

### **Examining Committee**

**Prof. Ioannis Skoufos**, Department of Agriculture, University of Ioannina, Arta, Greece

**Prof. Athina Tzora**, Department of Agriculture, University of Ioannina, Arta, Greece

**Prof. Dimitrios Zeugolis**, School of Mechanical and Materials Engineering, University College Dublin (UCD), Dublin, Ireland

**Associate Prof. Chrysoula Voidarou**, Department of Agriculture, University of Ioannina, Arta, Greece

**Associate Prof. Eleni K. Efthimiadou**, Department of Chemistry, National and Kapodistrian University of Athens, Panepistimiopolis, Zografou, Athens, Greece

**Senior Resercher Dr. Katerina Gregoriadou**, Institute of Plant Breeding and Genetic Resources, HAO-Demeter, Thessaloniki, Greece

**Prof. Apostolos Avgeropoulos**, Department of Materials Science and Engineering, University of Ioannina, Ioannina, Greece



**UNIVERSITY OF IOANNINA**

**A thesis submitted to the University of Ioannina, Department of Agriculture:**

The present record describes the experimental work development to obtain the Doctor of  
Philosophy (Ph.D.) degree under the title:

**Essential oil loaded collagen hydrogels to battle bacterial infections for tissue engineering  
applications**

**by**

**Çağlar Ersanlı**

**April 2025**

Laboratory of Animal Science, Nutrition and Biotechnology, Department of Agriculture,  
University of Ioannina, 47100 Arta, Greece

Laboratory of Animal Health, Hygiene and Food Quality, Department of Agriculture,  
University of Ioannina, 47100, Arta, Greece

Regenerative, Modular & Developmental Engineering Laboratory (REMODEL), Charles  
Institute of Dermatology, Conway Institute of Biomolecular and Biomedical Research, School of  
Mechanical and Materials Engineering, University College Dublin, D04 V1W8 Dublin, Ireland



European  
Commission

Horizon 2020  
European Union funding  
for Research & Innovation



## **Supervisory Committee**

### **Prof. Ioannis Skoufos**

Department of Agriculture, University of Ioannina, Arta, Greece

### **Prof. Athina Tzora**

Department of Agriculture, University of Ioannina, Arta, Greece

### **Prof. Dimitrios I. Zeugolis**

School of Mechanical and Materials Engineering, University College Dublin, Dublin, Ireland

## **Examining Committee**

### **Prof. Ioannis Skoufos**

Department of Agriculture, University of Ioannina, Arta, Greece

### **Prof. Athina Tzora**

Department of Agriculture, University of Ioannina, Arta, Greece

### **Prof. Dimitrios Zeugolis**

School of Mechanical and Materials Engineering, University College Dublin (UCD), Dublin, Ireland

### **Associate Prof. Chrysoula Voidarou**

Department of Agriculture, University of Ioannina, Arta, Greece

### **Associate Prof. Eleni K. Efthimiadou**

Department of Chemistry, National and Kapodistrian University of Athens, Panepistimiopolis, Zografou, Athens, Greece

### **Senior Resercher Dr. Katerina Gregoriadou,**

Institute of Plant Breeding and Genetic Resources, HAO-Demeter, Thessaloniki, Greece

### **Prof. Apostolos Avgeropoulos**

Department of Materials Science and Engineering, University of Ioannina, Ioannina, Greece

**Funding:** This research has been funded by the European Union, EuroNanoMed3, project nAngioDerm, through the Greek General Secretariat for Research and Innovation ERA-NETS (code 422 number T9EPA3-00022).



*To my brother ınar Ersanlı (RIP) who left us too early ...*

## Table of Contents

Table of Figures .....	5
Table of Tables .....	8
Plagiarism Statement .....	10
List of Abbreviations .....	11
Acknowledgements .....	16
Abstract .....	18
Περίληψη .....	23
Chapter 1: Introduction .....	29
1.1. Introduction .....	30
1.2. Antibacterial collagen biomaterials .....	31
1.3. Current strategies to develop antibacterial collagen biomaterials .....	34
1.3.1. Non-pharmacological approaches .....	35
1.3.2. Pharmacological approaches .....	38
1.3.2.1. Antibiotic-based approaches .....	38
1.3.2.2. Metal-oxide-based approaches .....	44
1.3.2.3. Antimicrobial peptide-based approaches .....	44
1.3.2.4. Plant-derived antimicrobials based approaches .....	45
1.3.3. Combination approaches .....	54
1.4. Project rationale, aims, hypothesis and objectives.....	59
1.4.1. Phase 1 (Chapter 2) .....	60
1.4.2. Phase 2 (Chapter 3) .....	61
1.4.3. Phase 3 (Chapter 3) .....	62

1.5. References .....	63
Chapter 2: Screening of the antimicrobial and anti-biofilm activity of different essential oils .....	77
2.1. Introduction .....	78
2.2. Materials and methods .....	82
2.2.1. Plant material and extraction of essential oils .....	82
2.2.2. Identification of the chemical composition of essential oils .....	82
2.2.3. Antimicrobial susceptibility test and bacterial strains .....	83
2.2.3.1. Antimicrobial activity .....	83
2.2.3.2. Anti-biofilm activity .....	86
2.2.4. Statistical analysis .....	87
2.3. Results .....	88
2.4. Discussion .....	97
2.5. Conclusion .....	101
2.6. References .....	102
Chapter 3: Optimization and development of <i>Thymus sibthorpii</i> EO-loaded collagen hydrogels	109
3.1. Introduction .....	110
3.2. Materials and methods .....	112
3.2.1. Materials .....	112
3.2.2. Fabrication and crosslinking of collagen type I hydrogels .....	112
3.2.3. Screening of the crosslinking efficacy of starPEG crosslinkers on collagen type I hydrogels.....	115
3.2.3.1. Quantification of the free-amine groups .....	115
3.2.3.2. Enzymatic degradation analysis .....	115

3.2.4.	Essential oil-loading and release kinetics analysis .....	115
3.2.5.	Biological activity of essential oil-loaded hydrogels .....	117
3.2.5.1.	Microbiological activity analysis .....	117
3.2.5.2.	Cytocompatibility analysis .....	118
3.2.6.	Statistical analysis .....	118
3.3.	Results .....	119
3.3.1.	Determination of optimal starPEG type and concentration on hydrogel stability .....	119
3.3.2.	EO release profile and release kinetics .....	122
3.3.3.	Biological analyses of the EO-loaded hydrogels .....	126
3.4.	Discussion .....	130
3.5.	Conclusion .....	135
3.6.	References .....	136
Chapter 4:	Summary, limitations and future perspectives .....	143
4.1.	Summary of the study and general conclusions .....	144
4.2.	Future studies .....	147
4.3.	References .....	148
Chapter 5:	Scientific outputs .....	150
5.1.	Published manuscripts .....	151
5.2.	Oral presentations .....	152
5.3.	Poster presentations .....	152
Appendices	.....	153
A.	General workflow .....	154
B.	List of consumables .....	156

C.	List of protocols .....	158
C.1.	Antimicrobial activity .....	158
C.1.1.	Kirby-Bauer disc diffusion assay .....	158
C.1.2.	Broth microdilution assay .....	158
C.2.	Anti-biofilm activity .....	161
C.2.1.	Microtiter plate biofilm assay .....	161
C.3.	Fabrication of collagen type I hydrogels .....	162
C.4.	Quantification of free amines by TNBSA assay .....	164
C.5.	Assessment of the resistance of hydrogels against enzymatic degradation .....	166
C.5.1.	Collagenase assay .....	166
C.5.2.	Pierce™ BCA protein assay .....	167
C.6.	Release profile and release kinetics of essential oil from hydrogels .....	169
C.6.1.	Release profile .....	169
C.6.2.	Release kinetic mathematical model .....	172
C.7.	Cell culture .....	173
C.7.1.	Culture medium for NIH-3T3 fibroblasts .....	173
C.7.2.	Cell thawing and passaging .....	173
C.7.3.	Cell freezing .....	173
C.7.4.	Cell seeding .....	174
C.7.5.	alamarBlue™ assay .....	174
C.7.6.	Quant-iT™ PicoGreen™ dsDNA assay .....	175

## Table of Figures

<b>Figure 1.1.</b> Sources of collagen using biomedical purposes. This figure was created by BioRender.com. ....	32
<b>Figure 1.2.</b> Approaches to developing collagen-based antimicrobial biomaterials for tissue engineering applications. ....	34
<b>Figure 2.1.</b> Experimental summary of the chapter 2. ....	81
<b>Figure 2.2.</b> Schematic illustration of the experimental procedure of (a) disc diffusion and (b) broth microdilution methods. ....	85
<b>Figure 2.3.</b> Qualitative illustration of inhibition zone diameters arising from testing EOs with different concentrations and reference antibiotics against (a) MSSA, (b) MRSA, and (c) <i>S. aureus</i> ATCC 29213. ....	93
<b>Figure 2.4.</b> Comparison of biofilm formation ability of MSSA, MRSA, <i>S. aureus</i> ATCC 29213 ( <i>S. aureus</i> ), <i>S. epidermidis</i> ATCC 12228 ( <i>S. epidermidis</i> (-)), and <i>S. epidermidis</i> ATCC 35984 ( <i>S. epidermidis</i> (+)) regarding their OD values with negative control (TSBG medium only). Each value represents the mean of triplicate experiments with standard deviations (Tukey, $p < 0.05$ ). 95	95
<b>Figure 3.1.</b> Free amine content of non-crosslinked (NCL) and various starPEG crosslinked collagen type I hydrogels (n=3, one-way ANOVA, $p < 0.05$ ). Glutaraldehyde (GTA) was used as a positive control. ....	120
<b>Figure 3.2.</b> The mass of dissolved collagen of various starPEG crosslinked collagen type I hydrogels after (A) 2 h, (B) 4 h, (C) 8 h, (D) 24 h of collagenase digestion (n=3, one-way ANOVA, $p < 0.05$ ). ....	121

**Figure 3.3.** The cumulative release profile of **(A)** 0.5 v%, **(B)** 1 v%, and **(C)** 2 v% of *Thymus sibthorpii* essential oil from optimally crosslinked collagen type I hydrogels in 1x PBS at 37 °C.

.....123

**Figure 3.4.** The qualitative analysis of the antibacterial effect of 0.5 v% (T0.5), 1 v% (T1), and 2 v% (T2) *Thymus sibthorpii* essential loaded optimally crosslinked collagen type I hydrogels against *S. aureus* ATCC 29213, and *E. coli* ATCC 25922. Penicillin and enrofloxacin were used as positive control for *S. aureus*, and *E. coli* strains, respectively. ....127

**Figure 3.5.** Inhibitions zone diameters of 0.5 v% (T0.5), 1 v% (T1), and 2 v% (T2) *Thymus sibthorpii* essential loaded optimally crosslinked collagen type I hydrogels against **(A)** *S. aureus* ATCC 29213, and **(B)** *E. coli* ATCC 25922 (n=3, one-way ANOVA,  $p < 0.05$ ). Penicillin and enrofloxacin were used as positive control for *S. aureus*, and *E. coli* strains, respectively. ....128

**Figure 3.6.** The in vitro **(A)** metabolic activity, and **(B)** DNA content of NIH-3T3 fibroblasts seed on the 0.5 v% *Thymus sibthorpii* essential loaded optimally crosslinked collagen type I hydrogels (n=3, one-way ANOVA,  $p < 0.05$ ). ....129

**Figure A.1.** Objectives and overall workflow of the study. ....154

**Figure A.2.** Schematic illustration of the state of art of the work. ....155

**Figure C.1.2.1.** Indicative experimental procedure of broth microdilution assay. ....160

**Figure C.4. 1.** Calibration curve for TNBSA assay with the known concentrations of glycine. ...165

**Figure C.6.1.1.** The scanning of the wavelength of (A) pure *Thymus sibthorpii* essential oil, (B) 70% v/v ethanol in order to assess the specific wavelength of the essential oil. 365 nm was determined as specific to *Thymus sibthorpii* essential oil which gives the maximum peak. ....170

**Figure C.6.1.2.** Calibration curve for release profile assessment with the known concentrations of *Thymus sibthorpii* essential oil. ....171

## Table of Tables

<b>Table 1.1.</b> Commercially available collagen-based antibacterial products. ....	33
<b>Table 1.2.</b> Illustrative examples of collagen antimicrobial scaffolds designed with non-pharmacological approaches. ....	36
<b>Table 1.3.</b> Illustrative examples of collagen antimicrobial scaffolds designed with antibiotic-based approaches. ....	40
<b>Table 1.4.</b> Illustrative examples of collagen antimicrobial scaffolds designed with non-antibiotic-based approaches. ....	47
<b>Table 1.5.</b> Illustrative examples of collagen antimicrobial scaffolds designed with combination approaches. ....	55
<b>Table 2.1.</b> The essential oil composition of <i>Thymus sibthorpii</i> , <i>Origanum vulgare</i> , <i>Salvia fruticosa</i> , and <i>Crithmum maritimum</i> isolated during the flowering period, including the percentage of components and the experimental (RI) and literature-based (RIL) retention indices. ....	89
<b>Table 2.2.</b> Inhibition zone diameter and minimum inhibition concentration of essential oils and reference antibiotics on treating microorganisms. A 6 mm inhibition zone diameter indicates no activity, and ND means not determined. Each value represents the mean of triplicate experiments with standard deviations. Different superscripts (a-m) in the row differ significantly for each strain (Tukey, $p < 0.05$ ). ....	92
<b>Table 2.3.</b> Biofilm formation inhibition percentages of different concentrations of essential oils and different concentrations of reference antibiotics on treating microorganisms. Each value represents the mean of triplicate experiments with standard deviations. Different superscripts (a-c) in the row differ significantly for each strain (Tukey, $p < 0.05$ ). ....	96
<b>Table 3.1.</b> Six different PEG succinimidyl glutarate crosslinkers used in the study. ....	112

<b>Table 3.2.</b> Regression coefficients ( $R^2$ ) of the five different release kinetic models fitted to the release of three different concentrations of <i>Thymus sibthorpii</i> EO from starPEG-crosslinked collagen type I hydrogels. T0.5, T1, and T2 represent the 0.5, 1, and 2 v% of <i>Thymus sibthorpii</i> essential oil within hydrogels. ....	124
<b>Table C.3. 1.</b> Collagen type I hydrogel preparation. ....	163
<b>Table C.4.1.</b> Standard curve solution preparation for TNBSA assay. ....	165
<b>Table C.5.2.1.</b> Preparation of standard curve solution for Pierce™ BCA protein assay. ....	168
<b>Table C.7.6.1.</b> Preparation of standard curve solution for Quant-iT™ PicoGreen™ dsDNA assay.....	176

## **Plagiarism Statement**

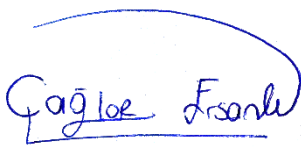
As a Ph.D. student belonging to the University of Ioannina (Greece), concretely to the Department of Agriculture, whose experimental work implementation has been developed mainly in the Laboratory of Animal Science, Nutrition and Biotechnology, Department of Agriculture, University of Ioannina (Greece).

### **I CERTIFY:**

The present dissertation records the progress made for the proposed Ph.D. thesis entitled “Essential oil loaded collagen hydrogels to battle bacterial infections for tissue engineering applications”.

This thesis is entirely the product of my own work, and I have not obtained a degree in this university or elsewhere on the basis of this work.

For the record and for any applicable purposes, I sign this document in Arta (Greece), **29th of April 2025.**



**Signed:** Çağlar Ersanlı

## List of Abbreviations

4SP,pentaerythritol,10 kDa : 4arm PEG Succinimidyl Glutarate, pentaerythritol, 10 kDa

4SP,pentaerythritol,20 kDa: 4arm PEG Succinimidyl Glutarate, pentaerythritol, 20 kDa

8SP,hexaglycerol,10 kDa: 8arm PEG Succinimidyl Glutarate, hexaglycerol, 10 kDa

8SP,hexaglycerol,20 kDa: 8arm PEG Succinimidyl Glutarate, hexaglycerol, 20 kDa

8SP,tripentaerythritol,10 kDa: 8arm PEG Succinimidyl Glutarate, tripentaerythritol, 10 kDa

8SP,tripentaerythritol,20 kDa: 8arm PEG Succinimidyl Glutarate, tripentaerythritol, 20 kDa

AMP: Antimicrobial peptide

AMR: Antimicrobial resistance

ARB: Antibiotic-resistant bacteria

AST: Antimicrobial susceptibility testing

ATCC: American Type Culture Collection

*B. cereus*: *Bacillus cereus*

*B. subtilis*: *Bacillus subtilis*

BA: Blood agar

bFGF: Basic fibroblast growth factor

BG: Bioactive glass

BMSC: Bone marrow mesenchymal stem cell

CaCl<sub>2</sub>: Calcium chloride

CDC: Centre for Disease Control and Prevention

Cef: Cefaclor

CFH: Ciprofloxacin hydrochloride

CFU: Colony forming unit

cHap: Citrate hydroxy apatite

Chi: Chitosan

CLSI: Clinical and Laboratory Standards Institute

CNC: Cellulose nanocrystal

CO<sub>2</sub>: Carbon dioxide

Col: Collagen

CP: Ciprofloxacin

CPO: Calcium peroxide

DMEM: Dulbecco's Modified Eagle Medium

DMSO: Dimethyl sulfoxide

DPBS: Dulbecco's phosphate buffered saline

DXC: Doxycycline hydrochloride

*E. coli: Escherichia coli*

*E. faecalis: Enterococcus faecalis*

EC: Ethyl cellulose

ECDC: European Centre for Disease Prevention and Control

EDC: N-(3-dimethylaminopropyl)-N-ethylcarbodiimide hydrochloride

EGF: Epidermal growth factor

ELP: Elastin-like peptide

EtOH: Ethanol

*F. nucleatum: Fusobacterium nucleatum*

FBS: Fetal bovine serum

GC-MS: Gas chromatography-mass spectrometry

Gel: Gelatin

GO: Graphene oxide

GSP: Gulmohar seed polysaccharide

GTA: Glutaraldehyde

HA: Hyaluronic acid

HaCaT: Spontaneously immortalized, human keratinocyte line

Hap: Hydroxy apatite

hASC: Human adipose-derived stem cell

hBM-MSC: Human bone mar-row-derived stromal cell culture

HCl: Hydrochloric acid

HDF: Human dermal fibroblast

HMDI: Hexamethylene diisocyanate

hUCMSC: Human umbilical cord mesenchymal stem cell

HUVEC: Human umbilical vein endothelial cell

*K. xylinus*: *Komagataeibacter xylinus*

mg: Milligram

MHA: Mueller-Hinton agar

MIC: Minimum inhibitory concentration

mL: Milliliter

mM: Millimolar

MRSA: Methicillin-resistant *Staphylococcus aureus*

MSSA: Methicillin-sensitive *Staphylococcus aureus*

NaHCO<sub>3</sub>: Sodium bicarbonate

NaOH: Sodium hydroxide

NCL: Non-crosslinked

ng: Nanogram

NH<sub>3</sub>: Ammonia

NHS: N-hydroxysuccinimide

nm: Nanometer

NP: Nanoparticle

OBC: Oxidized bacterial cellulose

OD: Optical density

OTC: Oxytetracycline hydrochloride

*P. aeruginosa*: *Pseudomonas aeruginosa*

*P. gingivalis*: *Porphyromonas gingivalis*

*P. putida*: *Pseudomonas putida*

*P. vulgaris*: *Proteus vulgaris*

P/S: Penicillin-streptomycin

PBS: Phosphate buffer saline

PCL: Polycaprolactone

PEO: Polyethylene oxide

PLA: Poly(lactic acid)

PLC: Poly(L-lactide-co- $\epsilon$ -caprolactone)

PLGA: Poly(D,L-lactide-co-glycolic acid)

PVP: Polyvinylpyrrolidone

R<sup>2</sup>: Regression coefficient

Ran: Ranalexin

rASC: Rabbit adipose-derived stem cell

rhBMP-2: Recombinant human bone morphogenetic protein-2

RI: Retention indices

rpm: Revolutions per minute

*S. aureus*: *Staphylococcus aureus*

*S. enterica*: *Salmonella enterica*

*S. epidermidis*: *Staphylococcus epidermidis*

*S. gordonii*: *Streptococcus gordonii*

*S. sanguinis*: *Streptococcus sanguinis*

*S. typhimurium*: *Salmonella typhimurium*

SD: Sprague–Dawley

SDS: Sodium dodecyl sulfate

starPEG: PEG Succinimidyl Glutarate

TB: Tobramycin

TEOS: Tetraethoxysilane

TiO<sub>2</sub>: Titanium dioxide

TNBSA: Trinitrobenzene sulfonic acid

TPP: Sodium tripolyphosphate

TSB: Tryptic soy broth

TSBG: Tryptic soy broth supplemented with glucose

TTC: Triphenyl tetrazolium chloride

UV: Ultraviolet

v: Volume

w: Weight

WHO: World Health Organization

β-TCP: Beta-tricalcium phosphate

μg: Microgram

μL: Microliter

## Acknowledgements

Completing this Ph.D. study has been a journey of intellectual and personal growth, and it would not have been possible without the support and encouragement of many individuals and organizations.

First and foremost, I would like to express my deepest gratitude to my supervisors, Prof. Dimitrios Zeugolis, Prof. Ioannis Skoufos, and Prof. Athina Tzora, for their invaluable guidance, encouragement, and patience throughout this research. Their insightful advice and constructive feedback were instrumental in shaping this thesis and helping me develop as a scientist.

I am also deeply grateful to my professors and colleagues, Prof. Anastasios Tsinas (RIP), Prof. Chrysoula Voidarou, Prof. Eleftherios Bonos, Dr. Konstantina Fotou, Dr. Evangelia Gouva, Achilleas Karamoutsios, Georgios Magklaras, Konstantina Nikolaou, Christos Zacharis, and Katerina Nelli at Laboratory of Animal Science, Nutrition and Biotechnology, University of Ioannina for their collaboration, stimulating discussions, and unwavering support. Besides, I would like to express my thanks to the administrative personnel Ms. Evangelia Tsoumpa, and Ms. Kalliopi Tsitra for being always kind and helpful. A special thanks to Konstantina Fotou, and Achilleas Karamoutsios for being my sister and brother, and for sharing their heart with me as their brother.

I would like to acknowledge the financial support from European Union, EuroNanoMed III, project nAngioDerm, through the Greek General Secretariat for Research and Innovation ERA-NETS (code number T9EPA3-00022) that made this research possible.

I would like to thank to Dr. Eleni Maloupa, and Dr. Katerina Grigoriadou for providing *Thymus sibthorpii* essential oil both working in the Laboratory of Conservation and Evaluation of Native and Floricultural Species, Institute of Plant Breeding and Genetic Resources, Hellenic Agricultural Organization Demeter, Thessaloniki, Greece. Besides, I would like to express my thanks to Prof. Theologos M. Michaelidis, Ms. Despina Makri, and Ms. Eleftheria Sarafi from the Department of Biological Applications and Technology, School of Health Sciences, University of Ioannina for their kind assistance during *in vitro* cell culture experiments.

I would like to extend my heartfelt gratitude to the professors and supervisors from my previous universities who played a pivotal role in shaping my academic foundation and inspiring me to pursue a career in science. To Prof. Şerife Helvacı, Dr. H. Banu Yener, Prof. Berrin İkizler, Prof. Nilay Gizli from Ege University, thank you for your encouragement, insightful lectures, and mentorship during my undergraduate studies, which sparked my passion for science. To Prof. Asli Yüksel Özşen from İzmir Institute of Technology, your rigorous training, and guidance during my M.Sc. project prepared me to face the challenges of scientific research and instilled in me the discipline and curiosity essential for success in academia. To Prof. Funda Tıhminlioğlu, and Dr. Sedef Tamburacı from İzmir Institute of Technology, your invaluable guidance and mentorship prepared me to become a biomaterial scientist with a strong background and open my career path to have this Ph.D. degree. Your influence has been profound, and I am deeply grateful for the knowledge, skills, and values you imparted, which have guided me throughout this journey.

I would like to address a very special thanks to my dear friends Duygu Şengün Baykan, and Deren Daryol who were there all along and have shared my tears of joy, and their heart from the distance. I could not be as strong as I was during my journey if I did not have you as my friends.

A heartfelt thank you goes to my family whose constant encouragement and understanding gave me the strength to persevere. To my mother Güler Eranlı, and my father Berkan Eranlı, thank you for your unconditional love and patience during this demanding journey.

This thesis is the result of the collective efforts of all those who believed in me, and I am deeply grateful to each one of you. Thank you! Teşekkür ederim! Σας ευχαριστώ!

## Abstract

Increased consumption and misuse of antimicrobial agents in both humans and animals have contributed to the spread of antimicrobial resistance, which seriously threatens public and animal health. Whereas infections due to antimicrobial resistance exhibited by bacteria can be adaptive, intrinsic, and acquired, multidrug-resistant bacteria (e.g., methicillin-resistant *Staphylococcus aureus*) cause infections that end up with longer hospitalization periods, remarkable morbidity, and mortality, as well as high healthcare costs. According to Organization of Economic Cooperation and Development (OECD) report, approximately 2.4 million people are expected to die due to this kind of infection in North America, Australia, and Europe over the next three decades, and treatment cost may reach USD 3.5 billion per year.

In general, *S. aureus* is one of the major opportunistic human pathogens, which can escape the immune system. Among the wide variety of infections, *S. aureus* is a well-known bacterium associated with wound infections, where the outermost layer of wounds is colonized. In particular, *S. aureus*-caused infections may be evaluated as a potential risk factor for methicillin-resistant *S. aureus* (MRSA) concern, which has brought about the need for development of alternative antimicrobials to substitute traditional antibiotics. Moreover, *S. aureus* (especially MRSA) has the ability to adhere to living or inert surfaces, secreting an extracellular polymeric substance of proteins, polysaccharides, nucleic acids, and water, known as a biofilm. Subsequently, the biofilm matrix acts as a physical barrier that prevents the permeability of the drug into the bacterial community and helps the microbe resist and minimize the effect of traditional antibiotics. These challenges have given rise to a significant interest in the scientific community in developing herbal-based therapeutics with antimicrobial activity (e.g., essential oils) as a safer and green alternative to antibiotics.

Essential oils (EOs) are colored, aroma-rich, complex hydrophobic liquids, also known as volatile oils. They are defined as the secondary metabolic product of aromatic plants and are found in various plant parts such as flowers, roots, barks, stems, leaves, and seeds. EOs are potential agents to diminish antimicrobial resistance due to their significant therapeutic properties (i.e., antibacterial, antiseptic, and antioxidant activities). For this reason, EOs from pharmaceutical plants have also been examined as potent antimicrobial agents in animal production systems. The

antimicrobial activity of EOs does not only stem from their qualitative chemical composition, but also from the quantitative intensity of every single component that is included in the structure, as well as all plant-based products. Their complex composition mainly includes terpenes (generally monoterpenes and sesquiterpenes) and terpenoids. Even though some of these chemicals are water soluble, most of them are hydrophobic, so EOs are defined as hydrophobic.

In this study, EOs of *Thymus sibthorpii*, *Origanum vulgare*, *Salvia fruticosa*, and *Crithmum maritimum* plants were chosen as the potential antimicrobial agents against various *S. aureus* strains to deal with the antimicrobial resistance problem. All these plant species have already been incorporated in traditional medications due to their potential anti-inflammatory, antimicrobial, antioxidant, and anti-cancer properties. The antimicrobial activities of the above four EOs were screened against methicillin-sensitive *S. aureus* (MSSA), MRSA, and the reference strain *S. aureus* ATCC 29213 applying the Kirby–Bauer disc diffusion and broth microdilution methods. The modified microtiter plate biofilm assay was also performed to assess the biofilm formation ability of tested strains, and the anti-biofilm activity of EOs, as well as reference antimicrobials. *Staphylococcus epidermidis* (*S. epidermidis*) ATCC 12228 and *S. epidermidis* 35984 were used as negative and positive quality control strains, respectively, for this bioassay. Penicillin, enrofloxacin, gentamicin sulfate, tetracycline hydrochloride, and cefaclor were examined as reference antimicrobials in this context. The observed bacterial growth inhibition varied significantly depending on the type and concentration of the antimicrobials. *Thymus sibthorpii* EO was determined as the strongest antimicrobial, with 0.091 mg/mL minimum inhibitory concentration (MIC) and a 14–33 mm diameter inhibition zone at 5% (v/v) concentration. All tested EOs indicated almost 95% inhibition of biofilm formation at their half MIC, while gentamicin sulfate did not show sufficient anti-biofilm activity. None of the methicillin-resistant strains showed resistance to the EOs compared to methicillin-sensitive strains. Thus, *Thymus sibthorpii* and *Origanum vulgare* EOs might be determined potential antimicrobial agent alternatives to overcome the problem of microbial resistance.

Although the strong antimicrobial activity of *Thymus sibthorpii* EO was revealed in the first experimental chapter of this study, a type of administration is needed via a biomaterial system, because of the high sensitivity and volatility of EO. Among a wide variety of biomaterial formulations, collagen hydrogels have been reported as particularly effective for incorporating

essential oils to use in tissue engineering applications. On the other hand, to our best knowledge, *Thymus sibthorpii* EO has not been introduced yet within medical devices in the field of tissue engineering applications according to the literature. Collagen, a fibrous, non-soluble protein, is one of the most prominent polymers for the development of antimicrobial biomaterials, attributable to its superior biocompatibility, excellent biodegradability, hydrophilic nature, reduced cytotoxicity, and high cell attachment affinity. Nevertheless, the fabricated forms of collagen need to be functionalized via *in situ* crosslinking due to a lack of stability. Since physical and biological crosslinking mechanisms have generally resulted in low crosslinking efficacy, carboxyl, and amine terminal crosslinking strategies are favored in research, as arises in literature. Among the above, since carbodiimide and glutaraldehyde often cause cytotoxicity, alternative crosslinkers such as multi-arm, star-shaped poly(ethylene glycol) succinimidyl glutarate (starPEG) have emerged as the subject of research.

At the second experimental part of this study, at first crosslinking efficiency was screened. For this purpose, 300  $\mu$ l collagen type I hydrogels crosslinked with six different starPEG molecules were developed and optimized, followed by assessment of free amine content of the hydrogels using TNBSA assay, and evaluation of their enzymatic degradation profile using collagenase assay. Furthermore, the optimally starPEG-crosslinked collagen hydrogels were loaded with several concentrations (0.5, 1, 2% v/v) of *Thymus sibthorpii* EO and the release profile and kinetics of the EO were investigated. For this purpose, the fabricated EO-loaded hydrogels were soaked into 1 mL of 1x PBS (pH 7.4) at 37 °C using a horizontal shaker incubator. At each defined time point (0, 0.5, 1, 1.5, 2, 2.5, 3, 3.5, 4, 24, and 48 h), 100  $\mu$ L of sample was removed and replaced by 100  $\mu$ L fresh 1x PBS. The linear calibration curve was prepared with different concentrations of *Thymus sibthorpii* EO using 70% v/v ethanol, which was used as a solvent. Then, the absorbance of the supernatant was measured at 365 nm and the concentration of the released *Thymus sibthorpii* EO was determined by using the standard curve to find where their concentration corresponds. After spectrophotometric evaluation, the cumulative release percentage of EO was estimated. Furthermore, we studied the release kinetics according to the release profile of *Thymus sibthorpii* EO. Hence, the zero-order, first-order, Higuchi, Korsmeyer-Peppas, and Hixon-Crowell release kinetics models have been applied to post-burst-release data. Finally, the antimicrobial activity of the developed composite hydrogels was assessed against *S. aureus*, and *Escherichia coli* (*E. coli*)

using Kirby-Bauer disc diffusion method, whilst their cytocompatibility and cytotoxicity was examined on NIH-3T3 fibroblast cell line by alamarBlue cell viability assay, and Quant-iT™ PicoGreen™ dsDNA cell proliferation assay.

starPEG-crosslinked collagen type I hydrogels presented significantly decreased free amine content for all types of crosslinkers with all tested concentrations compared to non-crosslinked hydrogels ( $p < 0.05$ ). An effective plateau was observed between 0.5 and 2 mM, and no statistical difference was noted among 0.5 mM, 1 mM, and 2 mM crosslinked hydrogels ( $p < 0.05$ ). In this plateau, the free amine reduction percentage was between 44.82% and 58.57%. Non-crosslinked hydrogels were completely degraded within a couple of hours. In general perspective, scaffolds showed higher resistance to degradation when crosslinked with glutaraldehyde (GTA), that was used as a positive control. However, hydrogels crosslinked with 0.5 mM of 4SP, pentaerythritol, 10 kDa showed no statistical difference compared to GTA crosslinked hydrogels, whilst 0.5 mM of 4SP, pentaerythritol, 20 kDa, and 8SP, hexaglycerol, 20 kDa displayed the lowest significant difference than all other groups ( $p < 0.05$ ). Therefore, 0.5 mM of the above three crosslinkers were deemed to be optimal conditions for functionalizing collagen hydrogels. The non-crosslinked hydrogels demonstrated burst release and completely released EO within a couple of hours was observed. Although GTA crosslinked scaffolds released almost all loaded quantity of the EO at 0.5% v/v from the polymeric network, the chosen optimized hydrogels crosslinked with 0.5 mM of 4SP, pentaerythritol, 10 kDa, 4SP, pentaerythritol, 20 kDa and 8SP, hexaglycerol, 20 kDa, released  $63.92 \pm 3.31\%$ ,  $75.85 \pm 9.00\%$  and  $57.82 \pm 4.08\%$  of the EO loaded at the same concentration after 48 h. Moreover, the release kinetics was studied by applying five different mathematical models. Hixson-Crowell model did not fit any of the experimental groups, whilst the other four models fitted to different experimental groups. On the other hand, the release exponent (n) values evaluated by the Korsmeyer-Peppas model indicated that the release mechanism of EO from crosslinked hydrogels obeyed the Fickian diffusion. 0.5% v/v EO-loaded collagen type I hydrogels showed adequate antibacterial activity against *S. aureus*. More specifically, hydrogels crosslinked with 0.5 mM 4SP, pentaerythritol, 10 kDa and loaded with 0.5 v% EO demonstrated  $2.83 \pm 0.47$  cm, and  $1.23 \pm 0.15$  cm inhibition zone diameter against *S. aureus*, and *E. coli*, respectively. Moreover, hydrogels containing 0.5% v/v of EO, which was the minor concentration, did not show a statistical difference regarding their antimicrobial activity

compared to positive control penicillin (for gram-positive bacteria), and enrofloxacin (for gram-negative bacteria) ( $p < 0.05$ ). Hence, 0.5% v/v concentration of *Thymus sibthorpii* EO was chosen as the optimal concentration to incorporate into collagen scaffolds. According to cell metabolic activity and proliferation studies, none of the fabricated hydrogels showed any toxicity on NIH-3T3 fibroblast cell line ( $p < 0.05$ ).

In the quest for alternative antibacterial therapies, herein, we developed collagen type I hydrogel systems optimally crosslinked and loaded with *Thymus sibthorpii* essential oil. The proposed antimicrobial agent incorporated into the collagen type I scaffolds showed strong activity against *S. aureus*, demonstrated a sustained release profile, and had no toxicity on fibroblasts. Collectively, the outcomes obtained highlight the importance of *Thymus sibthorpii* essential oil incorporated in collagen type I hydrogels, as an effective and alternative antibacterial therapy for regenerative medicine and tissue engineering purposes and for the reduction of the possible antimicrobial resistance.

## Περίληψη

Η αυξημένη κατανάλωση και η ακατάλληλη χρήση αντιμικροβιακών παραγόντων τόσο στους ανθρώπους όσο και στα ζώα έχουν συνεισφέρει στην εξάπλωση της μικροβιακής αντοχής, η οποία απειλεί σοβαρά τη δημόσια υγεία και την υγεία των ζώων. Ενώ οι λοιμώξεις που οφείλονται σε μικροβιακή αντοχή των βακτηρίων μπορεί να είναι προσαρμοστικές, εγγενείς ή επίκτητες, τα πολυανθεκτικά βακτήρια (π.χ., ο ανθεκτικός στη μεθικιλίνη *Staphylococcus aureus*) προκαλούν λοιμώξεις που οδηγούν σε μεγαλύτερες περιόδους νοσηλείας, σημαντική νοσηρότητα και θνησιμότητα, καθώς και υψηλό κόστος υγειονομικής περίθαλψης. Σύμφωνα με έκθεση του Οργανισμού Οικονομικής Συνεργασίας και Ανάπτυξης (ΟΟΣΑ), περίπου 2,4 εκατομμύρια άνθρωποι αναμένεται να πεθάνουν λόγω αυτού του είδους των λοιμώξεων στη Βόρεια Αμερική, την Αυστραλία και την Ευρώπη κατά τις επόμενες τρεις δεκαετίες, ενώ η θεραπεία μπορεί να κοστίζει έως και 3,5 δισεκατομμύρια δολάρια ΗΠΑ ετησίως.

Γενικά, ο *S. aureus* είναι ένας από τους κύριους ευκαιριακούς παθογόνους μικροοργανισμούς στον άνθρωπο, που μπορεί να διαφεύγει από το ανοσοποιητικό σύστημα. Μεταξύ της μεγάλης ποικιλίας λοιμώξεων, ο *S. aureus* είναι ένα γνωστό βακτήριο που σχετίζεται με μολύνσεις τραυμάτων, αποικίζοντας συνήθως το επιφανειακό στρώμα των τραυμάτων. Συγκεκριμένα, οι λοιμώξεις που προκαλούνται από τον *S. aureus* μπορεί να αξιολογηθούν ως ένας πιθανός παράγοντας κινδύνου για ανησυχία σχετικά με τον ανθεκτικό στη μεθικιλίνη *S. aureus* (methicillin-resistant *S. aureus*, MRSA), γεγονός που έχει οδηγήσει στην ανάγκη για ανάπτυξη εναλλακτικών αντιμικροβιακών, υποκατάστατων των παραδοσιακών αντιβιοτικών. Επιπλέον, ο *S. aureus* (ιδιαίτερα ο MRSA) έχει την ικανότητα να προσκολλάται σε ζωντανές ή αδρανείς επιφάνειες, εκκρίνοντας μια εξωκυτταρική πολυμερική ουσία που αποτελείται από πρωτεΐνες, πολυσακχαρίτες, νουκλεϊκά οξέα και νερό, γνωστή ως βιοϋμένιο (biofilm). Στη συνέχεια, η μήτρα του βιοϋμένιου δρα ως φυσικό εμπόδιο, αποτρέποντας τη διείσδυση του φαρμάκου στην βακτηριακή κοινότητα και βοηθώντας τον μικροοργανισμό να αντιστέκεται και να ελαχιστοποιεί την επίδραση των χορηγούμενων αντιβιοτικών σε αυτήν. Αυτές οι προκλήσεις έχουν προκαλέσει σημαντικό ενδιαφέρον στην επιστημονική κοινότητα για την ανάπτυξη θεραπευτικών προσεγγίσεων με βάση δραστικές ενώσεις φαρμακευτικών/αρωματικών φυτών, που επιδεικνύουν αντιμικροβιακή δράση (αιθέρια έλαια), ως μια ασφαλέστερη και πιο φιλική προς το περιβάλλον εναλλακτική προσέγγιση στα αντιβιοτικά.

Τα αιθέρια έλαια (Essential Oils, EOs) είναι έγχρωμα, αρωματικά, πολύπλοκα υδρόφοβα υγρά, γνωστά επίσης ως πτητικά έλαια. Ορίζονται ως το δευτερεύον μεταβολικό προϊόν των αρωματικών φυτών και βρίσκονται σε διάφορα μέρη των φυτών, όπως τα άνθη, οι ρίζες, οι φλοιοί, οι μίσχοι, τα φύλλα και οι σπόροι. Τα αιθέρια έλαια μπορούν να αποτελέσουν δυνητικά εναλλακτικούς παράγοντες ώστε η χρήση τους να μειώσει την μικροβιακή αντοχή λόγω των σημαντικών θεραπευτικών τους ιδιοτήτων (αντιβακτηριακή, αντισηπτική και αντιοξειδωτική δράση). Για αυτόν τον λόγο, τα αιθέρια έλαια από φαρμακευτικά φυτά έχουν επίσης μελετηθεί ως ισχυροί αντιμικροβιακοί παράγοντες στα συστήματα εκτροφής ζώων. Η αντιμικροβιακή δράση των αιθέριων ελαίων δεν προέρχεται μόνο από την ποιοτική χημική τους σύνθεση, αλλά και από την ποσοτική ένταση κάθε συστατικού που περιλαμβάνεται στη σύστασή τους, όπως και όλων των δραστικών ουσιών που περιέχονται στο φυτικό είδος. Η πολύπλοκη σύνθεσή τους περιλαμβάνει κυρίως τερπένια (συνήθως μονοτερπένια και σεσκιτερπένια) και τερπενοειδή. Παρόλο που ορισμένες από αυτές τις χημικές ουσίες είναι υδατοδιαλυτές, οι περισσότερες είναι υδρόφοβες, συνεπώς τα αιθέρια έλαια ορίζονται γενικά ως υδρόφοβα.

Στην παρούσα μελέτη, τα αιθέρια έλαια των φυτών *Thymus sibthorpii*, *Origanum vulgare*, *Salvia fruticosa* και *Crithmum maritimum* επιλέχθηκαν ως πιθανοί αντιμικροβιακοί παράγοντες κατά διαφόρων στελεχών του *S. aureus*, για την αντιμετώπιση του προβλήματος της μικροβιακής αντοχής. Όλα αυτά τα είδη έχουν ήδη χρησιμοποιηθεί σε παραδοσιακές θεραπείες λόγω των πιθανών αντιφλεγμονωδών, αντιμικροβιακών, αντιοξειδωτικών και αντικαρκινικών ιδιοτήτων τους. Η αντιμικροβιακή δραστηριότητα των τεσσάρων αιθέριων ελαίων ελέγχθηκε κατά των στελεχών του ευαίσθητου στη μεθικιλίνη *S. aureus* (methicillin-sensitive *S. aureus*, MSSA), του ανθεκτικού στη μεθικιλίνη *S. aureus* (MRSA) και του στελέχους αναφοράς *S. aureus* ATCC 29213 εφαρμόζοντας τη μέθοδο διάχυσης δίσκου Kirby–Bauer και τη μέθοδο μικροαραιώσεων σε θρεπτικό υλικό. Επίσης, πραγματοποιήθηκε η τροποποιημένη μέθοδος μικροτιτλοδότησης για την αξιολόγηση της ικανότητας σχηματισμού βιοϋμενίου των εξεταζόμενων στελεχών, καθώς και της αντιβιοϋμενιακής δράσης των αιθέριων ελαίων, όπως και των αντιμικροβιακών παραγόντων αναφοράς. Οι *Staphylococcus epidermidis* (*S. epidermidis*) ATCC 12228 και ο *S. epidermidis* 35984 χρησιμοποιήθηκαν αντίστοιχα ως αρνητικά και θετικά στελέχη αναφοράς για τον ποιοτικό έλεγχο στην βιοδοκιμή. Η πενικιλίνη, η ενροφλοξασίνη, η θειϊκή γενταμυκίνη, η υδροχλωρική τετρακυκλίνη και η κεφακλόρη εξετάστηκαν ως αντιμικροβιακοί παράγοντες αναφοράς στον

συγκεκριμένο πειραματισμό. Η παρατηρούμενη αναστολή της βακτηριακής ανάπτυξης διέφερε σημαντικά ανάλογα με τον τύπο και τη συγκέντρωση των αντιμικροβιακών παραγόντων. Το αιθέριο έλαιο του *Thymus sibthorpii* καθορίστηκε ως το ισχυρότερο σε αντιμικροβιακή δράση, με ελάχιστη ανασταλτική συγκέντρωση (minimum inhibitory concentration, MIC) στα 0,091 mg/mL και ζώνη αναστολής διαμέτρου 14–33 mm σε συγκέντρωση 5% (v/v). Όλα τα εξεταζόμενα αιθέρια έλαια έδειξαν σχεδόν 95% αναστολή του σχηματισμού βιοϋμενίου στο 50% της MIC τους, ενώ η θειϊκή γενταμυκίνη δεν παρουσίασε επαρκή αντιβιοϋμενιική δράση. Κανένα από τα ανθεκτικά στη μεθικιλίνη στελέχη δεν έδειξε αντοχή στα αιθέρια έλαια σε σύγκριση με τα ευαίσθητα στη μεθικιλίνη στελέχη. Συνεπώς, τα αιθέρια έλαια του *Thymus sibthorpii* και του *Origanum vulgare* θα μπορούσαν να προσδιοριστούν ως πιθανοί εναλλακτικοί αντιμικροβιακοί παράγοντες για την αντιμετώπιση του προβλήματος της μικροβιακής αντοχής.

Αν και η ισχυρή αντιμικροβιακή δράση του αιθέριου ελαίου του *Thymus sibthorpii* αποκαλύφθηκε στο πρώτο πειραματικό κεφάλαιο της διατριβής, στο δεύτερο διερευνήθηκε ο τρόπος χορήγησης των αιθέριων ελαίων μέσω εγκλεισμού σε διαφορετικές κατηγορίες βιοϋλικών λόγω της υψηλής ευαισθησίας και πτητικότητας του αιθέριου ελαίου. Μεταξύ ποικίλων βιοϋλικών, τα υδροπηκτώματα κολλαγόνου έχουν αναφερθεί ως ιδιαίτερα αποτελεσματικά για την ενσωμάτωση αιθέριων ελαίων σε εφαρμογές που σχετίζονται με την αναγεννητική ιστών. Από την άλλη πλευρά, σύμφωνα με τη βιβλιογραφία, το αιθέριο έλαιο του *Thymus sibthorpii* δεν έχει έως σήμερα ενσωματωθεί σε βιοϋλικά που να χρησιμοποιούνται στον τομέα της μηχανικής και αναγεννητικής ιστών. Το κολλαγόνο, μια ινώδης, μη διαλυτή πρωτεΐνη, είναι ένα από τα πλέον σημαντικά πολυμερή για την ανάπτυξη αντιμικροβιακών βιοϋλικών, λόγω της εξαιρετικής βιοσυμβατότητάς του, της άριστης βιοαποδομησιμότητας, της υδρόφιλης φύσης του, της μειωμένης κυτταροτοξικότητας και της υψηλής συγγένειας στην κυτταρική του πρόσδεση. Ωστόσο, οι παρασκευασμένες μορφές κολλαγόνου χρειάζονται «ενεργοποίηση» μέσω *in situ* διασύνδεσης (crosslinking) λόγω έλλειψης σταθερότητας. Δεδομένου ότι οι φυσικοί και βιολογικοί μηχανισμοί διασύνδεσης έχουν γενικά χαμηλή αποτελεσματικότητα, οι στρατηγικές crosslinking των καρβοξυλικών και αμινικών άκρων προτιμώνται στην έρευνα, όπως προκύπτει από τη βιβλιογραφία. Μεταξύ αυτών, καθώς οι καρβοδιιμίδες και η γλουταραλδεϋδη προκαλούν συχνά κυτταροτοξικότητα, έχουν αναδειχθεί εναλλακτικοί παράγοντες διασύνδεσης, όπως η πολύ-

βραχιονική, αστροειδούς σχήματος πολυ(αιθυλενογλυκόλη) σουκινιμιδυλική γλουταραλδεΐδη (starPEG), ως αντικείμενο έρευνας για την πειραματική μας δομή.

Στο δεύτερο πειραματικό μέρος αυτής της μελέτης, αρχικά εξετάστηκε η αποτελεσματικότητα της διασύνδεσης. Για το σκοπό αυτό, αναπτύχθηκαν και βελτιστοποιήθηκαν υδροπηκτώματα κολλαγόνου τύπου I, όγκου 300 μl, με διασύνδεση με έξι διαφορετικά μόρια starPEG, και ακολούθησε αξιολόγηση της περιεκτικότητας σε ελεύθερη αμίνη των υδροπηκτωμάτων χρησιμοποιώντας τη δοκιμασία TNBSA και αξιολόγηση του προφίλ ενζυμικής αποικοδόμησής τους χρησιμοποιώντας τη δοκιμασία κολλαγενάσης. Στη συνέχεια, στα υδροπηκτώματα κολλαγόνου, που βελτιστοποιήθηκαν με τη διασύνδεση με starPEG ενσωματώθηκαν διάφορες συγκεντρώσεις (0,5, 1, 2% v/v) αιθέριου ελαίου *Thymus sibthorpii* (EO) και διερευνήθηκαν το προφίλ απελευθέρωσης και η κινητική του αιθέριου ελαίου (EO). Για αυτόν τον σκοπό, τα παρασκευασμένα υδροπηκτώματα που περιείχαν EO τοποθετήθηκαν σε 1 mL διαλύματος PBS 1x (pH 7,4) στους 37°C, χρησιμοποιώντας έναν οριζόντιο αναδευτήρα-επωαστήρα. Σε κάθε καθορισμένο χρονικό σημείο (0, 0,5, 1, 1,5, 2, 2,5, 3, 3,5, 4, 24 και 48 ώρες), αφαιρούνταν 100 μL του δείγματος και αντικαθίσταντο με 100 μL φρέσκου διαλύματος PBS 1x. Η γραμμική καμπύλη βαθμονόμησης παρασκευάστηκε με διαφορετικές συγκεντρώσεις EO *Thymus sibthorpii*, χρησιμοποιώντας 70% v/v αιθανόλη ως διαλύτη. Στη συνέχεια, η απορρόφηση του υπερκείμενου διαλύματος μετρήθηκε στα 365 nm και η συγκέντρωση του απελευθερωμένου EO υπολογίστηκε χρησιμοποιώντας την πρότυπη καμπύλη για να προσδιοριστεί το σημείο αντιστοιχίας της συγκέντρωσης. Μετά τη φασματοφωτομετρική αξιολόγηση, εκτιμήθηκε το ποσοστό σωρευτικής απελευθέρωσης του EO. Επιπλέον, μελετήθηκε η κινητική απελευθέρωσης σύμφωνα με το προφίλ απελευθέρωσης του EO *Thymus sibthorpii*. Συνεπώς, τα μοντέλα κινητικής απελευθέρωσης μηδενικής τάξης, πρώτης τάξης, Higuchi, Korsmeyer-Peppas και Hixon-Crowell εφαρμόστηκαν στα δεδομένα μετά την αρχική ριπή απελευθέρωσης. Τέλος, η αντιμικροβιακή δραστηριότητα των αναπτυγμένων σύνθετων υδροπηκτωμάτων αξιολογήθηκε κατά του *S. aureus* και της *Escherichia coli* (*E. coli*), χρησιμοποιώντας τη μέθοδο διάχυσης δίσκου Kirby-Bauer, ενώ η κυτταροσυμβατότητα τους και η κυτταροτοξικότητα τους αξιολογήθηκε σε κυτταρικές σειρές ινοβλαστών NIH-3T3 με τη δοκιμασία βιωσιμότητας κυττάρων alamarBlue και τη δοκιμασία πολλαπλασιασμού κυττάρων Quant-iT™ PicoGreen™ dsDNA.

Τα υδροπηκτώματα κολλαγόνου τύπου I, διασυνδεδεμένα με starPEG, παρουσίασαν σημαντικά μειωμένη περιεκτικότητα σε ελεύθερες αμίνες για όλους τους τύπους των παραγόντων διασύνδεσης και όλες τις δοκιμασμένες συγκεντρώσεις, σε σύγκριση με τα μη διασυνδεδεμένα υδροπηκτώματα ( $p < 0,05$ ). Ένα αποτελεσματικό πλατό παρατηρήθηκε μεταξύ 0,5 και 2 mM, χωρίς στατιστική διαφορά μεταξύ των υδροπηκτωμάτων διασυνδεδεμένων με 0,5 mM, 1 mM και 2 mM ( $p < 0,05$ ). Στο πλατό αυτό, το ποσοστό μείωσης των ελεύθερων αμινών κυμαινόταν μεταξύ 44,82% και 58,57%. Τα μη διασυνδεδεμένα υδροπηκτώματα αποδομήθηκαν πλήρως μέσα σε λίγες ώρες. Από γενική άποψη, τα ικρίωματα (scaffolds) των υδροπηκτωμάτων έδειξαν υψηλότερη αντοχή στην αποδόμηση όταν διασυνδέθηκαν με γλουταραλδεΐδη (GTA), η οποία χρησιμοποιήθηκε ως θετικό κόντρολ. Ωστόσο, τα υδροπηκτώματα που διασυνδέθηκαν με 0,5 mM 4SP, πενταερυθρίτολη, 10 kDa δεν παρουσίασαν στατιστική διαφορά σε σύγκριση με τα υδροπηκτώματα διασταυρωμένα με GTA, ενώ τα 0,5 mM 4SP, πενταερυθρίτολη, 20 kDa και 8SP, εξαγλυκερόλη, 20 kDa εμφάνισαν τη χαμηλότερη σημαντική διαφορά σε σχέση με όλες τις άλλες ομάδες ( $p < 0,05$ ). Συνεπώς, τα 0,5 mM από τους παραπάνω τρεις παράγοντες διασύνδεσης θεωρήθηκαν οι βέλτιστες συνθήκες για τη λειτουργική τροποποίηση των υδροπηκτωμάτων κολλαγόνου. Τα μη διασυνδεδεμένα υδροπηκτώματα παρουσίασαν αρχική έντονη απελευθέρωση και ολοκλήρωσαν την απελευθέρωση του ΕΟ μέσα σε λίγες ώρες. Αν και τα ικρίωματα του κολλαγόνου που διασυνδέθηκαν με GTA απελευθέρωσαν σχεδόν όλη την ενσωματωμένη ποσότητα ΕΟ σε συγκέντρωση 0,5% v/v από το πολυμερικό δίκτυο, τα επιλεγμένα βελτιστοποιημένα υδροπηκτώματα που διασυνδέθηκαν με 0,5 mM 4SP, πενταερυθρίτολη, 10 kDa, 4SP, πενταερυθρίτολη, 20 kDa και 8SP, εξαγλυκερόλη, 20 kDa, απελευθέρωσαν  $63,92 \pm 3,31\%$ ,  $75,85 \pm 9,00\%$  και  $57,82 \pm 4,08\%$  του ενσωματωμένου ΕΟ στην ίδια συγκέντρωση μετά από 48 ώρες. Επιπλέον, μελετήθηκε η κινητική της απελευθέρωσης εφαρμόζοντας πέντε διαφορετικά μαθηματικά μοντέλα. Το μοντέλο Hixson-Crowell δεν ταίριαξε σε καμία από τις πειραματικές ομάδες, ενώ τα άλλα τέσσερα μοντέλα ταίριαζαν σε διαφορετικές πειραματικές ομάδες. Από την άλλη πλευρά, οι τιμές του εκθέτη απελευθέρωσης ( $n$ ) που αξιολογήθηκαν μέσω του μοντέλου Korsmeyer-Peppas έδειξαν ότι ο μηχανισμός απελευθέρωσης του ΕΟ από τα διασυνδεδεμένα υδροπηκτώματα ακολουθεί τη διάχυση Fickian. Τα υδροπηκτώματα κολλαγόνου τύπου I με φορτωμένο ΕΟ σε συγκέντρωση 0,5% v/v έδειξαν επαρκή αντιβακτηριακή δράση κατά του *S. aureus*. Πιο συγκεκριμένα, τα υδροπηκτώματα που διασυνδέθηκαν με 0,5 mM 4SP, πενταερυθρίτολη, 10 kDa και φορτώθηκαν με 0,5% v/v ΕΟ, παρουσίασαν ζώνη αναστολής με

διάμετρο  $2,83 \pm 0,47$  cm και  $1,23 \pm 0,15$  cm κατά των *S. aureus* και *E. coli*, αντίστοιχα. Επιπλέον, τα υδροπηκτώματα που περιείχαν 0,5% v/v ΕΟ, που ήταν η μικρότερη συγκέντρωση, δεν παρουσίασαν στατιστική διαφορά ως προς την αντιμικροβιακή τους δράση σε σύγκριση με την πενικιλίνη που ήταν το θετικό κοντρόλ (για τα gram-θετικά βακτήρια) και την ενροφλοξασίνη (για τα gram-αρνητικά βακτήρια) αντίστοιχα ( $p < 0,05$ ). Συνεπώς, η συγκέντρωση 0,5% v/v του ΕΟ *Thymus sibthorpii* επιλέχθηκε ως η βέλτιστη συγκέντρωση για ενσωμάτωσή του στα ικρίωματα του κολλαγόνου. Σύμφωνα με τις μελέτες μεταβολικής δραστηριότητας και πολλαπλασιασμού κυττάρων, κανένα από τα διασυνδεδεμένα υδροπηκτώματα δεν παρουσίασε τοξικότητα στην κυτταρική σειρά ινοβλαστών NIH-3T3 που χρησιμοποιήθηκε ( $p < 0,05$ ).

Στο πλαίσιο της αναζήτησης εναλλακτικών αντιβακτηριακών θεραπειών, στην παρούσα μελέτη αναπτύχθηκαν συστήματα υδροπηκτωμάτων κολλαγόνου τύπου I, διασυνδεδεμένα και βελτιστοποιημένα που εμπεριείχαν το αιθέριο έλαιο του *Thymus sibthorpii*. Το προτεινόμενο αιθέριο έλαιο που ενσωματώθηκε στα ικρίωματα κολλαγόνου τύπου I παρουσίασε ισχυρή αντιβακτηριδιακή δράση κατά του *S. aureus*, εμφάνισε προφίλ συνεχούς απελευθέρωσης, ενώ δεν παρουσίασε τοξικότητα στους ινοβλάστες. Συνολικά, τα αποτελέσματα που προέκυψαν είναι πρωτοποριακά, καθώς παρέχουν τη δυνατότητα χρήσης του αιθέριου ελαίου *Thymus sibthorpii* που έχοντας ενσωματωθεί σε υδροπηκτώματα κολλαγόνου τύπου I που έχουν βελτιστοποιηθεί με διασύνδεση με το starPEG, επιδεικνύει αποτελεσματική αντιβακτηριδιακή δράση κατά μικροβιακών στελεχών που εμπλέκονται σε τραύματα ιστών, όντας εναλλακτική θεραπεία για σκοπούς αναγεννητικής ιατρικής και μηχανικής ιστών με στόχο τη μείωση της μικροβιακής αντοχής.

## Chapter 1: Introduction

### Sections of this chapter have been published in:

*Recent advances in collagen antimicrobial biomaterials for tissue engineering applications: a review*, **Ersanli, C.**, Tzora, A., Skoufos, I., Voidarou, C. and Zeugolis, D.I., International Journal of Molecular Sciences, 24(9), 7808, 2023.

Electrospun scaffolds as antimicrobial herbal extract delivery vehicles for wound healing, **Ersanli, C.**, Voidarou, C., Tzora, A., Fotou, K., Zeugolis, D.I., Skoufos, I., Journal of Functional Biomaterials, 14(9), 481, 2023.

## 1.1. Introduction

Microbial infections threaten public health due to the wide range of enervating effects of disease-causing microbes (e.g., bacteria, viruses, and fungi), which have been the primary causatives of the dissemination of pathogenic diseases [1–3]. Antibiotics have been the first choice for infection treatment since the discovery of penicillin in 1928 by Alexander Fleming. Although their low toxicity and great bactericidal features, the usage of antibiotics for a long time led to the burst and release of antibiotic-resistant bacteria (ARB), hence the emergence of antimicrobial resistance (AMR) related diseases [4,5].

Healthcare-associated infections are the major type of AMR-caused infections that may delay discharge from the hospital or cause deaths as well as a rise in healthcare costs, second-line drug costs, and unsuccess in treatments [6]. According to the European Centre for Disease Prevention and Control (ECDC), in Europe, annually, 3.8 million people catch healthcare-associated diseases caused by AMR [7], and 90 thousand people die because of these diseases [8]. Besides, the Centre for Disease Control and Prevention (CDC) reported that more than 2.8 million people suffer from AMR diseases each year, while 35,000 patients die in the US [9]. Moreover, the cost for just one AMR infection case is predicted approximately EUR 9–34 thousand more than non-resistant microbial infections [10], whilst more than EUR 9 billion are required in Europe [11,12]. On the other hand, bacterial resistance itself adds more than USD 20 billion to healthcare costs in the US [9].

In response, a variety of clinical interventions have been employed to combat AMR-related diseases, including the use of combination therapies, strategies aim targeting antimicrobial-resistant enzymes or bacteria, longer treatment durations, and off-label uses [13,14]. Despite these efforts, the development of new and effective antimicrobials has been slow, and the emergence of resistance to these interventions has become incremental. Furthermore, some of these interventions come with their drawbacks, such as an increase in side effects, higher medicinal costs, and longer hospital stays [15]. As such, there is a clinical need for alternative approaches such as biomaterial-based strategies to combat antimicrobial resistance and promote the development of more effective therapies. The various antimicrobial collagen biomaterial strategies have recently come to the fore in the literature within this framework.

## 1.2. Antibacterial collagen biomaterials

Collagen is a fibrous, insoluble protein that is the main component of the extracellular matrix (ECM) of several tissues [16] of humans and many animals, such as bone [17], cartilage [18], tendon [19], skin [20], and muscle [21]. A natural biopolymer, collagen is one of the most abundant proteins in mammals [22] and becomes prominent among the other polymers due to its superior and distinct properties. Excellent biocompatibility, good biodegradability, hydrophilicity, remarkable mechanical properties, low or no antigenicity, hemostatic properties, and cell-binding ability are some of the important features of collagen, which make it important for many biomaterial applications, such as tissue engineering and drug delivery purposes [23–26]. On the other hand, the resistance of collagen to bacteria makes it outstanding to use in the development of antimicrobial biomaterials for many kinds of applications, such as the treatment of wounds and bone infections. Owing to its natural ability to fight infection, collagen contributes to keeping the infection site sterile [26,27]. Moreover, collagen has very high availability since its abundance in mammals and marine organisms as well as its producibility from yeasts, plants, insects, and mammal cells by recombinant protein technology [23,28] (**Figure 1.1**). Despite its proven properties, collagen-based biomaterials need to incorporate bioactive molecules such as antibiotics and plant-based agents in order to increase their biological activities.

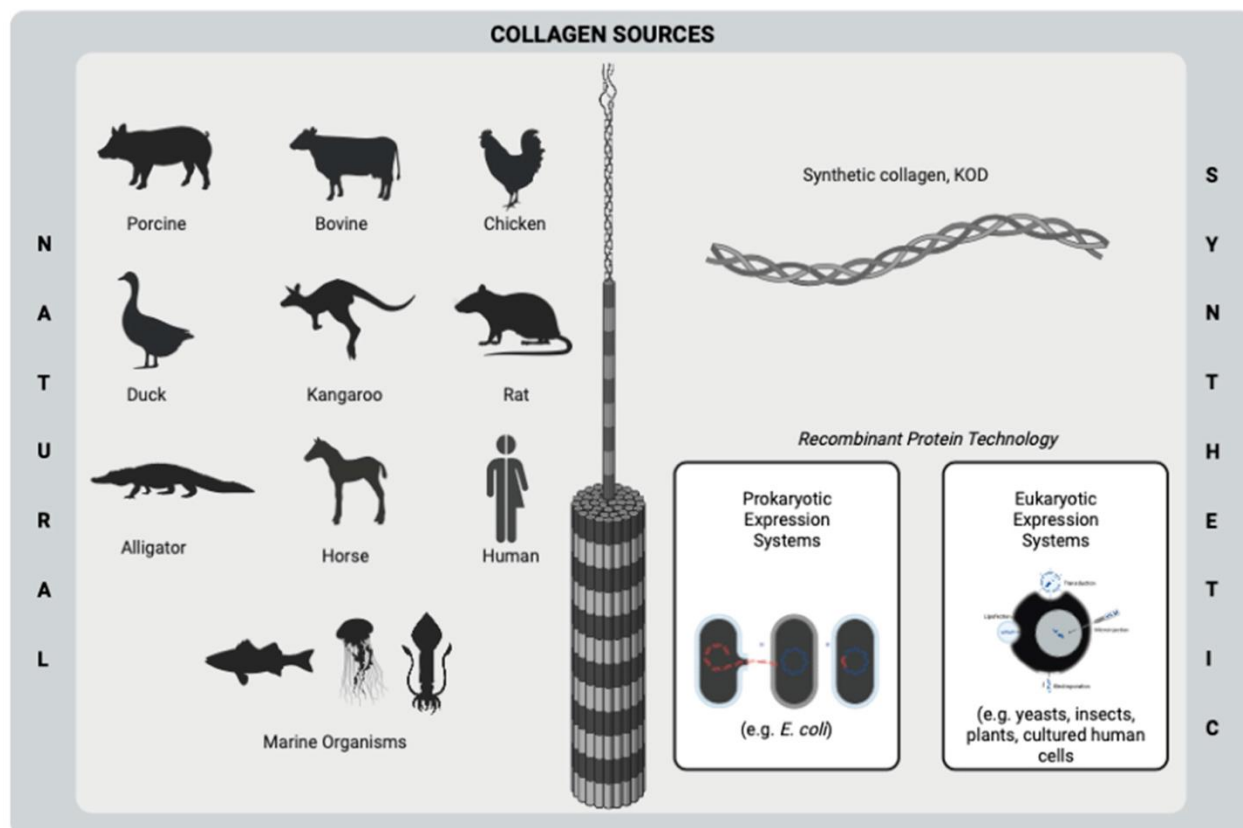


**Figure 1.1.** Sources of collagen using biomedical purposes. This figure was created by BioRender.com.

The use of alternative antimicrobial agents (e.g., herbal extracts, antimicrobial peptides, and metal oxide nanoparticles) as a substitute for antibiotics has started to gain importance in an attempt to overcome the emergence of AMR due to ARB strains [2,29,30]. Even though clinically proven, generally single and limited antibacterial agents (e.g., silver and gentamicin), including collagen-based products, are on the market (**Table 1.1**). Therefore, new modern products are clinically needed to improve treatment efficacy. In this respect, collagen has been widely used as a carrier vehicle for several kinds of bioactive molecules with their ensured biostability owing to its superior biological activities [23–25]. Herein, I briefly reviewed different approaches for designing collagen-based antimicrobial products (**Figure 1.2**) with a particular focus on preclinical studies which have been published in the last decade.

**Table 1.1.** Commercially available collagen-based antibacterial products.

Brand Name	Company	Composition	Collagen Content (w%)	Product Form	Refs.
Promogran Prisma™	3M (Saint Paul, MN, USA)	Collagen, ORC, silver-ORC	55	Pad	[31]
ColActive® Plus Powder Ag	Covalon Technologies (Mississauga, Canada)	Collagen, sodium alginate, CMC, EDTA, AgCl	Not available	Pad	[32]
Septocolla® E	Biomet (Warsaw, IN, USA)	Collagen fleece, gentamicin salts	Not available	Pad	[33]
DermaCol™	DermaRite (North Bergen, NJ, USA)	Collagen, sodium alginate, CMC, EDTA	Not available	Pad	[34]
DermaCol/Ag™	DermaRite	Collagen, sodium alginate, CMC, EDTA, AgCl	Not available	Pad	[35]
SilvaKollagen®	DermaRite	Hydrolyzed collagen, Ag <sub>2</sub> O	Not available	Gel	[36]
Puracol® Plus Ag <sup>+</sup>	Medline (Northfield, IL, USA)	Denatured collagen, CMC, sodium alginate, silver, EDTA	Not available	Pad	[37]
Seeskin® P	Synerheal Pharmaceuticals (Chennai, India)	Collagen	Not available	Powder	[38]
CollaSorb®	Hartmann (Heidenheim an der Brenz, Germany)	Collagen, sodium alginate	90	Pad	[39]
Genta-Coll® resorb	Resorba (Nürnberg, Germany)	Collagen, gentamicin sulfate	58.3	Sponge	[40]
Collamycin	Synerheal Pharmaceuticals	Collagen, gentamicin sulfate	Not available	Gel	[41]
GenColl	ColoGenesis (Salem, India)	Collagen, gentamicin sulfate	Not available	Gel	[42]
Colloskin®M	ColoGenesis	Collagen	Not available	Pad	[43]
Collofiber-MM	ColoGenesis	Collagen, mupirocin, metronidazole	Not available	Powder	[44]
ColoPlug	ColoGenesis	Collagen	Not available	Sponge	[45]
Diacoll-S™	ColoGenesis	Collagen, gentamicin sulfate	Not available	Sponge	[46]

Oxidized regenerated cellulose: ORC; Carboxymethyl cellulose: CMC; Ethylenediamine tetra acetic acid: EDTA; Silver chloride: AgCl; Silver (I) oxide: Ag<sub>2</sub>O.

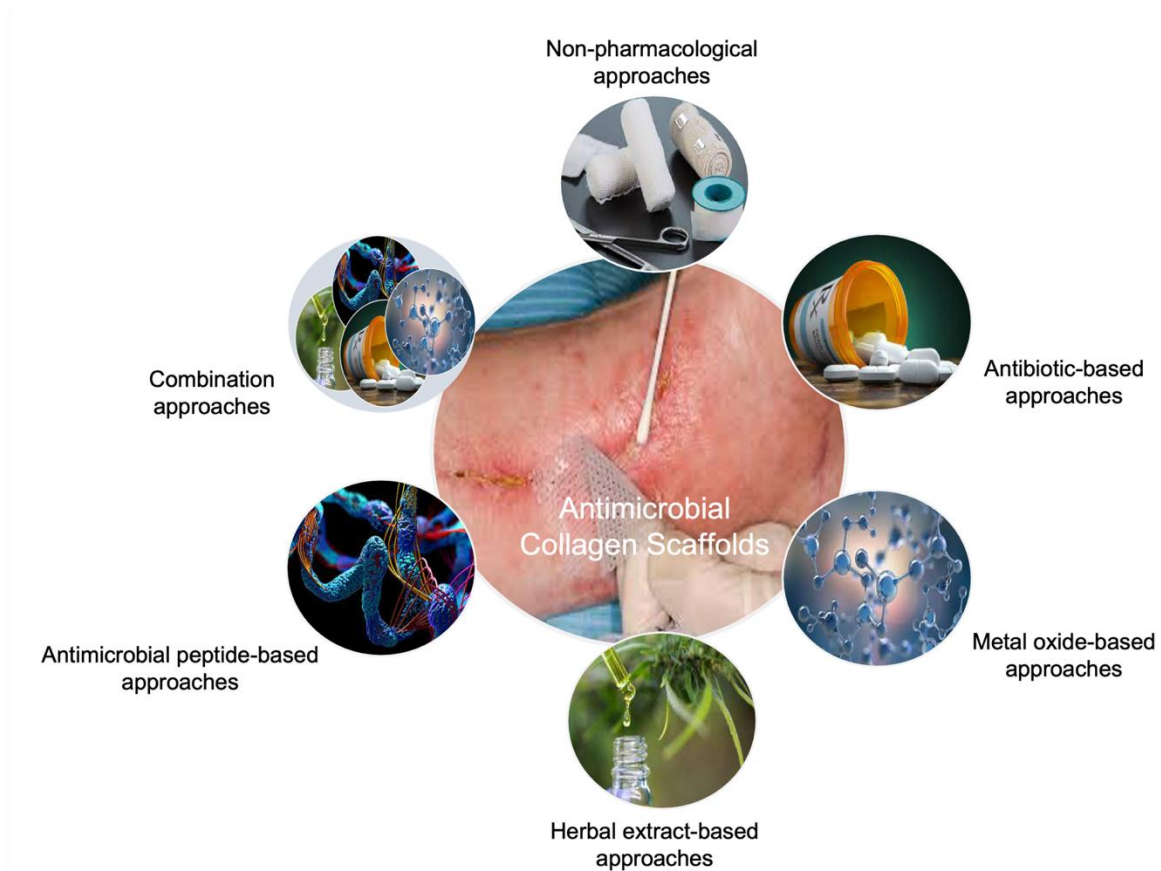


**Figure 1.2.** Approaches to developing collagen-based antimicrobial biomaterials for tissue engineering applications.

### 1.3. Current strategies to develop antibacterial collagen biomaterials

The development of antimicrobial therapeutic strategies has an incremental interest in literature since microbial infections have threatened human health for many years. Biomaterial-based antimicrobial therapies have been considered an alternative and ideal solution for infection treatment because the incorporation of therapeutic bioactive agents into the biomaterial formulation can lead to their controlled and sustained release as well as a decrease in their off-target influences. Moreover, the combination of biomaterials with these molecules' benefits enhancement in bioactivity and stability of therapeutics; hence, therapeutic efficacy could be improved. Collagen is a prominent polymer for the de-signing of antimicrobial scaffolds due to its outstanding biocompatibility, biodegradability, hydrophilicity, remarkable cell-attachment affinity,

and mechanical, hemostatic, low-antigenic, and non-cytotoxic properties. Herein, the recent developments in different collagen-based approaches (**Figure 2.2**) in the treatment of microbial infections using various kinds of bioactive molecules incorporated into collagen-based scaffolds for antimicrobial therapies was reviewed.

### 1.3.1. Non-pharmacological approaches

In the literature, there are several studies concerning collagen-based biomaterial therapies for healing microbial infections without the incorporation of any therapeutics (**Table 1.2**). Chitosan is a commonly used additive polymer for collagen scaffolds to enhance bactericidal effects due to its good antibacterial activity against several Gram-positive and Gram-negative bacterial strains [47]. Chitosan and oxidized bacterial cellulose with composite collagen hemostasis dressings exhibited a faster hemostasis rate (86 s) than commercial gauze (186 s) *in vivo* rat liver trauma model through the collagen to promote platelet and erythrocyte adhesion as well as to improve pro coagulation activity [48]. Collagen hydrolysate wound dressings, including chitosan and tetraethoxysilane (TEOS), accelerated the healing of wounds in the Wistar rats compared to gauze, where the wound recovered completely within 14 days. Besides the augmented healing process, the re-epithelization rate was evaluated as 81% and 55% for composite and control groups, respectively on the 10th post-treatment day. However, despite the successful preclinical findings, developed dressings could not inhibit the growth of *P. aeruginosa*, which is one of the most common causative bacteria for wound infections [49]. On the other hand, some inorganic compounds were incorporated in biomaterial formation to increase targeted tissue regeneration and antimicrobial activity [50–52]. For instance, the association of collagen with bioactive glass (BG) may promote the antibacterial activity of pristine collagen by the increase in osmotic pressure, which is raised proportionally to the released ions (e.g., silicon, calcium, and phosphorous) composed of bioactive glasses. Hence, the growth of bacteria is inhibited because of the formed region by ions. It is reported that collagen/BG scaffolds implanted in Sprague–Dawley (SD) rats' dorsum skin defect healed the wound faster than the clinically used product, Kaltostat, and triggered re-epithelization regarding histologic results [52].

**Table 1.2.** Illustrative examples of collagen antimicrobial scaffolds designed with non-pharmacological approaches.

Composition	Collagen Source	Scaffold Form	Crosslinking	AST	Bacterial Strain/ Cell Line	Antibacterial Activity	Hypothetic Material	Refs.
Col Chi (2% w/v)	Bovine tendon	Bilayer sponge/nanofibers	Not available	Disc diffusion	<i>S. aureus</i> , <i>E. coli</i> No in vitro cell culture	The recovery efficiency of <i>E. coli</i> and <i>S. aureus</i> from composite matrix was evaluated at 52%, and 36%, respectively.	Chronic wound dressing	[53]
Col (8% w/v) BG (10:1 Col/BG)	Tilapia skin	Nanofibrous mat	GTA vapor for 24 h	Antibacterial activity assay	<i>S. aureus</i> HaCaTs, HDFs, HUVECs	Col/BG dressings led to a significant reduction in <i>S. aureus</i> colonies.	Wound dressing	[52]
Col OBC Chi (1:0.9:0.25 w ratio of OBC/Col/Chi)	Fish skin	Sponge	Not available	ISO20743-2007	<i>E. coli</i> , <i>S. aureus</i> , <i>K. xylinus</i> L929 fibroblasts	Developed scaffolds could not completely inhibit the growth of tested bacteria.	Antibacterial hemostatic dressing for internal bleeding control	[48]
Col Chi HA (Various w ratios)	Rat tail	Hydrogel	Genipin (2, 10, 20 mM)	Well diffusion	<i>S. aureus</i> , <i>E. coli</i> MG-63 osteosarcoma cells	Developed hydrogels provided more antibacterial activity against <i>E. coli</i> .	Bone tissue engineering scaffold	[54]
Col Chi Alginate (Various w%)	Tilapia skin	Sponge	Not available	Agar diffusion	<i>S. aureus</i> No in vitro cell culture	Composite sponges did not show an effective inhibitory effect on <i>S. aureus</i> .	Cutaneous wound dressing	[55]
Col Chi Gelatin (40:40:20 Col/Chi/Gelatin w%)	Priacanthus hamrur skin	Sponge	Not available	Disc diffusion	<i>S. aureus</i> , <i>E. coli</i> No in vitro cell culture	The addition of chitosan slightly increased the <i>S. aureus</i> inhibition.	Antibacterial and antioxidant bio-scaffold	[56]
Collagen hydrolysate Chitosan TEOS (0.5–2% w/v)	Bovine tendon	Sponge	Not available	Disc diffusion	<i>B. subtilis</i> , <i>S. aureus</i> , <i>E. coli</i> , <i>P. aeruginosa</i> NIH 3T3 fibroblasts	Developed sponges did not show any antimicrobial activity against <i>P. aeruginosa</i> .	Modern collagen wound dressing against traditional collagen dressings	[49]

Collagen $\beta$ -TCP (9:1 Col/ $\beta$ - TCP w ratio)	Type I (Not Nanofibrous mat specified)	GTA (25, 50 v%)	Turbidimetric method	<i>E. coli</i> , <i>S. aureus</i> BMSCs	Composite mats displayed a more than two-fold higher inhibition rate against <i>E.coli</i> .	Bioactive bone scaffold	[57]	
Collagen (2.5, 5, 10 mg/mL) Na-Alginate microspheres (3% w/v)	Type I (Not specified)	Hydrogel	Not available	Not studied	hUCMSCs	Not studied	Wound dressing	[58]

Antimicrobial susceptibility testing: AST; Collagen: Col; Chitosan: Chi; Weight: w; Volume: v; Spontaneously immortalized, human keratinocyte line: HaCaT; Staphylococcus aureus: *S. aureus*; Escherichia coli: *E. coli*; Komagataeibacter xylinus: *K. xylinus*; Bacillus subtilis: *B. subtilis*; Pseudomonas aeruginosa: *P. aeruginosa*; Bioactive glass: BG; Glutaraldehyde: GTA; Oxidized bacterial cellulose: OBC; Hyaluronic acid: HA; Tetraethoxysilane: TEOS; Beta-tricalcium phosphate:  $\beta$ -TCP; Bone marrow mesenchymal stem cell: BMSC; Human dermal fibroblast: HDF; Human umbilical vein endothelial cell: HUVEC; Human umbilical cord mesenchymal stem cell: hUCMSC.

### 1.3.2. Pharmacological approaches

#### 1.3.2.1. Antibiotic-based approaches

Antibiotics are well-known antimicrobial drugs that have an important role in the treatment of bacterial infections by fighting and preventing the growth of bacteria [59]. The incorporation of various antibiotics, such as aminoglycosides [60–63] and tetracyclines [64–68], into collagen scaffolds have been studied for a long time (**Table 1.3**). These therapeutic agents are generally studied for infected wound and bone defect treatments. For example, when mupirocin was loaded into collagen sponges, complete closure and re-epithelization on full-thickness excision wounds treated with the developed composite scaffold were achieved. Nevertheless, scaffolds could provide significant antibacterial activity against Gram-positive methicillin-resistant *S. aureus* (MRSA) and *B. subtilis* [69]. In another study of a commonly studied antibiotic, doxycycline-loaded collagen-based scaffolds increased the gap closure of bone defects in Wistar rats from 25% to 40% [68]. On the other hand, the concentration of collagen is an effective parameter for the controlled antibiotic release from a biomaterial. An increase in collagen concentration from 20% to 40% (w/w) did not enhance the in vivo healing of mice wounds, treated with cefazolin, including collagen-based nanofibrous mat, due to inadequate release of antibiotics on the wound bed. This outcome indicates the role of polymer concentration in the sustained release of an incorporated antimicrobial agent in a biomaterial formulation [70].

In some strategies, the effect of antibiotics is enhanced by the addition of chitosan into the biomaterial formulation. Chitosan exerts its antibacterial activity by binding to the negatively charged bacterial cell wall, thus initiating a process that leads either to the disruption of bacterial cells or to a change in the bacterial membrane permeability [71]. For instance, minocycline-caged chitosan nanoparticles incorporated into collagen sponges demonstrated almost complete degradation and no remarkable inflammation in the SD rat skull defect model [65]. The antimicrobial activity of biomaterials was also advanced by generating a hypoxic environment by including oxygen-generating additives. Oxygen-generating calcium peroxide particles were coated on the ciprofloxacin-loaded collagen-based sponges by Tripathi et al. to advance the wound healing rate by generating a hypoxic environment. The tested scaffolds on the skin flap model led to less necrosis and displayed almost total wound recovery with the help of the antibacterial activity of the antibiotic and hypoxic conditions, whilst the untreated group showed about 75% of

wound closure within 15 days [72]. Even though good inhibitory effects are re-reported, it is known that long-term use of antibiotics results in the emergence of ARB strains. In the attempt to research a few alternatives, non-antibiotic therapeutic approaches have become inevitable.

**Table 1.3.** Illustrative examples of collagen antimicrobial scaffolds designed with antibiotic-based approaches.

Composition	Collagen Source	Scaffold Form	Crosslinking	Therapeutic Agent	Release Profile	AST	Bacterial Strain/ Cell Line	Antibacterial Activity	Hypothetic Material	Refs.
Col (5% w/v)	Porcine dermis	Sponge	HMDI (0.625–10% w/v)	Cef, Ran (0–500 µg/mL)	10 µg/mL of 90% Cef and 95% Ran released by day 7.	Disc diffusion	<i>E. coli</i> , <i>S. epidermidis</i> Adult HDFs	100 µg/mL of Cef showed activity on tested strains, while Ran did not.	Localized drug delivery vehicle	[73]
Col (1% w/w) Chi (1% w/w) HA (1% w/w)	Rat tail tendon	Thin film	Not available	Gentamicin sulfate (0.4 mg/cm <sup>2</sup> film)	Not studied	Disc diffusion	<i>S. aureus</i> , <i>E. coli</i> , <i>P. aeruginosa</i> No in vitro cell culture	Drug-loaded scaffolds showed approximately 25–30 mm of inhibition zone.	Antibacterial film	[60]
Col (8 w%) Hap (0–15 w%)	Type I (not specified)	Micro/na nostructure d layers	EDC/NHS (4:1 w ratio)	Vancomycin hydrochloride (10 w% of Col)	The max released concentration of vancomycin exceeded the MIC by up to 60–75 times for 4 weeks.	Disc diffusion	MRSA, <i>S. epidermidis</i> , <i>E. faecalis</i> SAOS-2 osteosarcoma cells	Inhibition zone diameters did not differ from standard antibiotic discs significantly.	Local drug carrier	[61]
Col (3 mg/mL)	Bovine tendon	Sponge	Not available	Mupirocin (2 mg/mL) (caged into silica microspheres)	Almost 90% of mupirocin was released within 3 days from sponges.	Broth dilution	<i>B. subtilis</i> , <i>S. aureus</i> , <i>E. coli</i> , <i>P. aeruginosa</i> 3T3-L1 fibroblasts	Drug-loaded wound dressings did not show sufficient antibacterial activity on <i>B. subtilis</i> and <i>E. coli</i> .	Wound dressing	[69]
Col Chi (2% w/v)	Mouse tail tendon	Asymmet ric membrane	TPP (0.2% w/v)	Minocycline (15 µg/mL) (caged into Chi NPs)	Minocycline had sustained release until the 7th day.	Live/dead bacterial double staining	<i>P. gingivalis</i> , <i>F. nucleatum</i> MC3T3-E1 osteoblasts, L929 fibroblasts	Membranes showed 95.3% and 92.1% of bacteriostatic activity against <i>P. gingivalis</i> and <i>F. nucleatum</i> , respectively.	Scaffold for the prevention of infection and guide bone regeneration	[64]

Col hydrolysate (5 mg/mL) PLA (5 mg/mL) cHap (10 mg)	Type I (not specified)	3D-printed porous scaffold	Alkali hydrolysis (1:1 NaOH:EtOH and 0.5% w/v citric acid)	Minocycline hydrochloride (0.5 mg/mL)	A burst release of minocycline was observed within the first hour.	Disc diffusion, biofilm inhibition assay	<i>S. aureus</i> hBM-MSCs	Drug-loaded scaffolds showed smaller inhibition zone than standard antibiotic discs.	Antimicrobial and osteogenic [65] scaffold
Col (10 w%) PLA EC (7:3, 8:2, 9:1 EC/PLA w ratio)	Fish collagen	Nanofibrous mat	Not available	Silver sulfadiazine (0.25, 0.5, 0.75 w%)	28 ppm of silver ions were released from 0.75 w% drug-loaded mats within 96 h.	Disc diffusion	<i>Bacillus</i> , <i>E. coli</i> NIH 3T3 fibroblasts	Only 0.75% of drugs including scaffolds showed antibacterial activity against tested strains.	Wound dressing [74]
Col (10, 20, 40% w/w) PVP (30% w/v) PLA PEO (Shell–Col/PVP, Core: 80:20 PLA/PEO w/w)	Bovine tendon	Nanofibrous mat	Not available	Cefazolin sodium	44.15%, 40.80%, and 37.76% of cefazolin were released for samples containing 10%, 20%, and 30% (w/w) collagen after 6 days.	Disc diffusion	MRSA, <i>E. coli</i> , <i>P. aeruginosa</i> No in vitro cell culture	Fabricated mats showed slightly higher antibacterial activity against <i>P. aeruginosa</i> .	Antibacterial patch for wound healing [70]
Col (10 mg/mL)	Fish collagen	Hydrogel	Alginate dialdehyde (2–10 mg/mL)	Tetracycline hydrochloride (0.01–0.2 mg/mL)	Almost 20% of antibiotics with a concentration equal to or higher than 0.1 mg/mL were released during 600 min.	Zone inhibition	<i>S. aureus</i> 3T3 fibroblasts	Dressings did not show high inhibition rates of <i>S. aureus</i> .	Wound dressing [66]
Col BG (0.5 mg/mL)	Bovine	Membrane (Commercial product)	Not available	Tetracycline hydrochloride (0.05, 0.2, 0.35 mg/mL)	More than 50% of tetracycline releases within the first 6 h, and significant release was observed in 24 h.	Zone inhibition Plate counting	<i>S. aureus</i> (different strains), <i>S. epidermidis</i> MG-63 osteosarcoma cells	Developed scaffolds could significantly inhibit <i>S. aureus</i> growth.	Scaffold for the prevention of biomaterial-related infections [67]

Col (1.5% w/v) Chi (1.5% w/v) CPO (1–4 w%)	Bovine	Sponge	EDC/NHS (3 w%, 2:1 EDC:NHS w ratio)	Ciprofloxacin hydrochloride (1 mg/mL)	Almost 80% of CFH was released from scaffolds including 4% CPO within 200 h.	Zone inhibition	<i>E. coli</i> , <i>S. aureus</i> HDFs	Scaffolds displayed good inhibition zones against both strains.	Skin tissue engineering scaffold	[72]
Col (5% w/v) Hap (10 w%)	Rat tail	Sponge	EDC (0.1 mM)	Doxycycline containing Hap NPs (10 w%)	A sustained release of doxycycline (about 70%) was achieved over 14 days.	Time-kill assay	<i>S. aureus</i> , <i>P. aeruginosa</i> BM-MSCs	Antibiotic addition significantly reduced the number of colonies within 24 h.	Bone tissue engineering scaffold	[68]
Col (1 w%) CNC (5 w%)	Bovine tendon	Sponge	GTA (0.25%)	Gentamicin sulfate (25 mg/mL) impregnated gelatin microspheres	Gentamicin was completely released after 144 h of the incubation period.	Disc diffusion	<i>E. coli</i> , <i>S. aureus</i> NIH-3T3 fibroblasts	Composite scaffolds showed higher antibacterial activity against <i>E. coli</i> than <i>S. aureus</i> .	Antibacterial skin scaffold	[62]
Col Chi (4, 8, 16% total polymer, various Col/Chi w ratio)	Fish	Sponge	Not available	Norfloxacin (1 w%)	An almost complete release of the drug was observed within 20 h.	Not studied	No in vitro cell culture	Not studied	Scaffold for skin regeneration	[75]
Col (6.5 mg/mL)	Bovine tendon	Film	EDC/NHS (1:1:6 w ratio EDC/NHS/Col-Tobramycin)	Tobramycin (15 mg/mL)	The burst release of tobramycin (40%) was observed within the first 4 h.	Plate counting	<i>S. aureus</i> Human corneal epithelial cells	Tobramycin-loaded films showed significantly higher inhibition than pristine films.	Scaffold for corneal repair	[63]
Col Na-Alginate Hap	Cowhide	Sponge	Genipin CaCl <sub>2</sub> (10 w%)	Amoxicillin (0.5, 1, 2 mg/mL)	The long-term drug release effect was investigated.	Zone inhibition	<i>E. coli</i> rASCs	Scaffolds could effectively inhibit <i>E. coli</i> growth.	Composite scaffold for infected bone defects	[76]

Antimicrobial susceptibility testing: AST; Weight: w; Volume: v; Collagen: Col; Chitosan: Chi; Hyaluronic acid: HA; Hexamethylene diisocyanate: HMDI; Cefaclor: Cef; Ranalexin: Ran; Escherichia coli: E. coli; Staphylococcus epidermidis: S. epidermidis; Staphylococcus aureus: S. aureus; Pseudomonas aeruginosa: P. aeruginosa; Enterococcus faecalis: E. faecalis; Methicillin-resistant Staphylococcus aureus: MRSA; Bacillus subtilis: B. subtilis; Porphyromonas gingivalis: P. gingivalis; Fusobacterium nucleatum: F. nucleatum; Hydroxy apatite: Hap; Citrate hydroxy apatite: cHap; N-(3-dimethylaminopropyl)-N-ethylcarbodiimide hydrochloride: EDC; N-hydroxysuccinimide: NHS; Nanoparticle: NP; Sodium tripolyphosphate: TPP; Poly(lactic acid): PLA; Sodium hydroxide: NaOH; Ethanol: EtOH; Polyethylene oxide: PEO; Polycaprolactone: PCL; Ethyl cellulose: EC; Polyvinylpyrrolidone: PVP; Bioactive glass: BG; Glutaraldehyde: GTA; Human bone marrow-derived stromal cell culture: hBM-MSC; Calcium peroxide: CPO; Cellulose nanocrystal: CNC; Ciprofloxacin hydrochloride: CFH; Rabbit adipose-derived stem cell: rASC.

### 1.3.2.2. Metal-oxide-based approaches

In recent years, there has been a great interest in metal oxide nanoparticles (NPs) in enhancing the antimicrobial properties of collagen-based scaffolds due to their great inhibitory effects against broad-spectrum bacteria (**Table 1.4**). They can exert their bactericidal effect by linking to bacterial cell walls via electrostatic interactions [77], hydrophobic forces [78], van der Waals forces [79], and/or ligand binding [80]. Silver NPs are the well-known and most studied NPs in pre-clinical and commercial antimicrobial devices. In one study, silver NPs included collagen nanofibers presented an enhanced healing rate and led to the deposition of more hydroxyproline and collagen on the wound site in the Wistar rat model [81], whereas silver NPs loaded collagen hydrogels contributed to the reduction of pro-inflammatory cytokine IL-6 and inflammatory cytokines CCL24, TIMP1, and sTNFR-2, which indicates the exerted anti-inflammatory properties of silver NPs on the subcutaneous mice model [82]. Similarly, in vivo, 10 ppm silver NPs comprised collagen/chitosan hydrogel applied in full-thickness skin defects in the SD rat model expedited the fibroblast migration by the advance in  $\alpha$ -SMA, upregulated the related macrophage activation, and downregulated inflammatory mediators [83]. However, the addition of silver NPs into collagen scaffolds has not always exhibited a significant impact on wound healing. For example, both silver-loaded and pristine collagen membranes did not show complete wound closure [84], as silver NPs comprised collagen sponges [85]. Besides silver, zinc oxide NPs are also extensively studied in collagen biomaterials, owing to their well-recognized antibacterial and anti-inflammatory properties. For instance, the zinc oxide quantum dots were implicated in collagen/PCL nanofibrous mats for skin regeneration purposes and served as a suitable wound dressing. Both 0.75% (w/v) zinc oxide quantum dots included, pristine mats showed partial wound closure on full-thickness mice wound model at 12-day post-treatment with a wound closure rate of about 90%. Although scaffolds loaded with zinc oxide quantum dots presented a good inhibitory effect against *S. aureus*, their comparison with pristine scaffolds was not reported [86].

### 1.3.2.3. Antimicrobial peptide-based approaches

Antimicrobial peptides are environmentally friendly, small molecular weight, amphiphilic, and polycationic proteins that are composed of less than fifty amino acids in their structure [87–89]. They can cause cell lysis via binding to intercellular targets of negatively charged cell membranes [90,91] and exert bactericidal activity by the modulation of the host immune system [92]. Despite

their good antibacterial action, AMPs have some drawbacks, such as a short half-life (within hours) and high manufacturing costs [93]. Hence, in the literature, the incorporation of AMPs into collagen scaffolds has been less researched than the other therapeutic agents (**Table 1.4**). AMP Tet213 incorporated collagen-based sponge dressings demonstrated almost complete wound healing on *E. coli*- and *S. aureus*-infected wounds on SD rats within 14 days, similar to pristine sponges and commercial silver-including products, in contrast to gauze control. As a result of Sirius red staining, pristine, and Tet213, loaded dressings exhibited around 60% of collagen deposition, which might be contributed by the biocompatibility of collagen. Moreover, according to the samples taken from the SD rat model on day 4, *E. coli* was  $1.8 \times 10^7$  CFU for gauze control, whereas no bacterial colonies were observed on wounds treated with Tet213 dressings [94]. In addition, it was observed that AMPs GL13K [95] and LL37 [96,97] incorporation into the collagen scaffolds increased their antibacterial activity against Gram-negative *E. coli*.

#### **1.3.2.4. Plant derived antimicrobials-based approaches**

Plants have been used for traditional remedies (e.g., bone defects and burn wounds) for centuries [98,99]. The bioactive phytochemicals of herbs, such as phenolic substances, essential oils, vitamins, and phytohormones, gain them tremendous features (e.g., antimicrobial, antifungal, anti-inflammatory, and antioxidant activity) and make them a rising star for antimicrobial therapies as greener and safer therapeutics [100–105].

Almost 70% of people worldwide believe the primary health benefit of herbal compounds, according to the report by the World Health Organization. Herbs present limitless sources to develop alternative, safe, and renewable therapeutics. For instance, among over two hundred and fifty thousand vascular plants, only around 17% of them have been researched for medicinal purposes. Even though herbal components have been known for their excellent biological activities, some shortfalls still appear, such as poor biostability and the inability to reach the target. Hence, there has been a need to develop engineered carrier and delivery vehicle systems (e.g., electrospun nanofibers, hydrogels) to increase the treatment and targeting efficacy. Therefore, there have been a remarkable number of attempts in the literature to incorporate various herbal extracts, such as cinnamon [106], *Cissus quadrangularis* [107], and thymol [108], into collagen

scaffolds to create an ideal and alternative antimicrobial biomaterial strategy for tissue regeneration purposes (**Table 1.4**).

The addition of curcumin into collagen/cellulose nanocrystal sponge dressings advanced epithelization rate and dermal cell proliferation while providing complete wound closure on full thickness burn wounds within 21 days. Moreover, they significantly decreased the level of cytokines IL-1 $\beta$ , IL-6, and TNF- $\alpha$  between the 10th and 21st days and inhibited the NF- $\kappa$ B activity due to the long and sustained release of curcumin with antibacterial, antioxidant, and anti-inflammatory characteristics [109]. Thanks to their complex chemical structure, in some studies, herbal extracts are used as a crosslinker for collagen formulations as well as an antimicrobial therapeutic agent. For example, wheatgrass was studied as both an antimicrobial agent and a green crosslinker for collagen aerogels. The study observed that 2% (w/v) of wheat grass incorporation increased the size reduction of collagen aerogel-treated wounds from 47% to 75% on the 9th post-treatment day and triggered the angiogenesis within 24 h of incubation of the chick embryo model [110]. The concentration of the loaded herbal extract is determined as an effective parameter from the perspective of preclinical studies. To illustrate, the addition of 0.08 g of *Melilotus officinalis* extract exhibited better re-epithelization than 0.04 and 0.02 g on day 18 post-treatment, whereas the 0.08 g extract with collagen-based multilayer nanofibrous mat increased the collagen density *in vivo* from 55% to 82% within 18 days [111].

**Table 1.4.** Illustrative examples of collagen antimicrobial scaffolds designed with non-antibiotic-based approaches.

Composition	Collagen Source	Scaffold Form	Crosslinking	Therapeutic Agent	Release Profile	AST	Bacterial Strain/ Cell Line	Antibacterial Activity	Hypothetic Material	Refs.
<b>Metal-oxide-based approaches</b>										
Col Chi (Various Col/Chi w% ratio)	Goat tendon	Thin film	EDC/NHS (2:1 M ratio)	Silver NPs (0.5 w%)	Not studied	Growth inhibition	<i>E. coli</i> , <i>S. aureus</i> MG-63 osteosarcoma cells	Up to 37% and 27% of growth inhibition was observed against <i>E. coli</i> and <i>S. aureus</i> , respectively.	Composite bone tissue engineering scaffold	[112]
Col FN CS (10:1:3 × 10 <sup>-5</sup> g/g Col/CS/FN)	Bovine tendon	Sponge	GTA (2.5% v/v)	Silver NPs (1 × 10 <sup>-4</sup> g/g polymers)	Not studied	Disc diffusion	<i>F. nucleatum</i> , <i>P. gingivalis</i> Gingival fibroblasts	Hybrid sponges showed slightly higher antimicrobial activity against <i>F. nucleatum</i> .	Oral cavity lesion dressing	[113]
Col (8% w/v)	Fish collagen	Nanofibrou s mat	GTA (50% w/v)	Silver NPs (0.2% w/v)	Cumulatively, almost 100% of silver ions were released within 25 h.	Microdilution, disc diffusion	<i>S. aureus</i> , <i>P. aeruginosa</i> No in vitro cell culture	Approximately 3.2 and 2.3 cm of inhibition zone diameter was observed after 48 h against <i>S. aureus</i> and <i>P. aeruginosa</i> , respectively.	Wound dressing	[81]
Col (10% w/w)	Porcine	Hydrogel	BDDGE	Silver NPs (0.2 μM)	Steady silver concentration was reached within 0.5 h of incubation	Growth inhibition and Time-kill assays	<i>S. aureus</i> , <i>S. epidermidis</i> , <i>E. coli</i> , <i>P. aeruginosa</i> Human epidermal keratinocytes,	Hybrid hydrogels could inhibit the growth of all tested bacteria.	Implantable anti- infective hybrid biomaterial	[82]

								and dermal fibroblasts		
Col (5% w/w) His (0, 1, 2% w/w)	Porcine	Membrane	EDC/NHS (3.55 and 2.13 mg/g)	Silver NPs	Not studied	Disc diffusion, bacterial suspension	<i>P. aeruginosa</i> , <i>S. aureus</i> L929 fibroblasts	Developed membranes did not show sufficient antimicrobial activity against both tested strains.	Dressing for full thickness burn wounds	[84]
Col Chi (9:1 Col/Chi w ratio)	Bovine tendon	Hydrogel	EDC/NHS	Silver NPs (0, 2, 5, 10, 20 ppm)	Not studied	Disc diffusion	<i>E. coli</i> , <i>S. aureus</i> Mouse embryo fibroblasts, HaCaTs	Developed wound dressings showed higher inhibition of <i>S. aureus</i> growth.	Wound dressing	[83]
Col Hap (various w ratio)	Fish scale	Membrane	Genipin (0.003 g)	Silver NPs (0.05 w%)	Not studied	Disc diffusion	<i>E. coli</i> , <i>S. aureus</i> MG-63 osteosarcoma cells	Scaffolds presented less inhibition zone compared to standard ampicillin discs.	Bone filler	[114]
Col (0.5% w/w)	Bovine tendon	Sponge	Dialdehyde xanthan gum (10 mg/mL)	Silver NPs (10 mg/mL)	Not studied	Disc diffusion, bacterial infiltration	<i>E. coli</i> , <i>S. aureus</i> , <i>P. aeruginosa</i> L929 fibroblasts	An increase in silver NP concentration resulted in an increased inhibition rate against tested strains.	Antibacterial wound dressing	[85]
Col Sago starch (1, 2, 3 $\mu$ M)	Fish scale	Sponge	Not available	Sago starch capped silver NPs (1:1 w ratio to Col)	Not studied	Broth dilution	<i>S. aureus</i> , <i>E. coli</i> NIH-3T3 fibroblasts	A lower minimum inhibitory concentration was examined against <i>E. coli</i> .	Scaffold for tissue regeneration applications	[115]
Col (1% w/w) Dextran	Calf hide	Hydrogel	GTA (0.25% v/v)	Zinc oxide NPs	Not studied	Not studied	No in vitro cell culture	Not studied	Wound dressing	[116]
Col (0.7 w%)	Bovine	Hydrogel	GTA (1% v/v)	Zinc oxide NPs (2, 3, 5 w%)	Not studied	Disc diffusion	<i>S. aureus</i> , <i>E. coli</i>	The inhibition zone diameter decreased with	Wound dressing	[117]

							No in vitro cell culture	increasing zinc oxide concentration against <i>S. aureus</i> .		
Col PCL (1:2, 1:1, 2:1, 3:1 w ratio)	Type I (not specified)	Nanofibrous mat	Not available	Zinc oxide quantum dots (0–0.75% w/v)	Not studied	Plate counting	<i>E. coli</i> , <i>S. aureus</i> L929 fibroblasts, 3T3 fibroblasts	The number of living bacteria was significantly reduced by the addition of 0.75% of NPs.	Antibacterial wound dressing	[86]
Col (1% w/w)	Calf hide	Sponge	GTA (0.5 w%)	Zinc titanate	Not studied	Disc diffusion	<i>S. epidermidis</i> , <i>B. cereus</i> , <i>E. coli</i> , <i>S. enterica</i> , <i>P. putida</i> MG-63 osteosarcoma cells, 3T3 fibroblasts HaCaTs	The porous nanocomposites exerted higher antimicrobial activity against <i>S. epidermidis</i> .	Anti-infection biomaterial	[118]
Col (5 mg/mL) Chi (5 mg/mL)	Pig skin	Sponge	GTA (2.5% w/w)	TiO <sub>2</sub> NPs (1–7%)	Not studied	Bacterial culture, SEM imaging	<i>S. aureus</i> Mouse fibroblasts, red blood cells	Increased TiO <sub>2</sub> amount led to reduced <i>S. aureus</i> colonies on the surface of the scaffold.	Wound dressing	[119]
Col (3.47 w%) Chi (3 w%)	Bovine	Nanofibrous mat	GTA (1 w%)	Zinc oxide NPs (1:1:1 w ratio Col:Chi:Zinc oxide)	Not studied	Disc diffusion	<i>S. aureus</i> Hep-2 cells	Membranes showed 4–8 mm of inhibition zone diameter against <i>S. aureus</i> .	Scaffold for skin tissue regeneration	[120]
Col Chi (1:9 Col/Chi w ratio)	Not specified	Sponge	Dehydrothermal crosslink at 105 °C for 24 h	Zinc oxide NPs (1, 3, 5 w%)	Not studied	Disc diffusion	<i>E. coli</i> , <i>S. aureus</i> No in vitro cell culture	<i>S. aureus</i> was found more sensitive to developed scaffolds than <i>E. coli</i> .	Antibacterial product	[121]

Antimicrobial peptide-based approaches										
Col (3 mg/mL)	Bovine	Hydrogel	EDC/NHS (50 mM EDC, 25 mM NHS)	AMP GL13K (1 mM)	Burst release was observed from 21 to 28 days.	ATP bioluminescence, live/dead assays	<i>S. gordonii</i> , <i>E. coli</i> hBM-MSCs	AMP GL13K coating significantly demonstrated less effects on the membrane integrity of <i>S. gordonii</i> .	Scaffold for bone/dental tissue growth and infection prevention	[95]
Col (0.6% w/v) HA (0.5% w/v) Alginate (1.2% w/v)	Type I (not specified)	Sponge	EDC/NHS (0.6 mg/mL EDC, 0.3 mg/mL NHS)	AMP Tet213 (500 µg/mL)	Sustained release (68.4 ± 10.2%) was observed after 14 days.	Zone inhibition, colony counting	<i>E. coli</i> , MRSA, <i>S. aureus</i> NIH-3T3 fibroblasts	The addition of AMP Tet213 into hybrid scaffolds gave rise to almost full inhibition of <i>E. coli</i> and <i>S. aureus</i> .	Mixed-bacteria-infected wound dressing	[94]
Col (2.5–3 mg/mL) HA (1.5 mg/mL)	Rat tail tendon	Polyelectrolyte multilayers	GTA (8% w/v)	AMP LL37 (2, 8, 16 µM)	Sustained release of the AMP killed planktonic bacteria.	Broth dilution, bacterial adhesion test, live/dead assay	<i>E. coli</i> Primary rat hepatocytes	The incorporation of 16 µM of AMP LL37 showed almost 3% of live bacteria on the scaffold surface.	Antimicrobial coating	[96]
Col PLC (14% w/v)	Not specified	Membrane (ready-to-use product)	Not available	AMP LL37 (10–40 µM)	Membranes containing different LL-37 concentrations released LL-37 in the same quantity.	Not studied	L929 fibroblasts	Not studied	Collagen membrane for guided bone regeneration	[97]
Plant-derived antimicrobials-based approaches										
Col (2% w/v)	Bovine skin	Membrane	Not available	Propolis NPs (200 µg/mL)	Not studied	Not studied	HDFs	Not studied	Dermal patch	[122]
Col CNC (7 w%)	Bovine tendon	Sponge	Not available	Curcumin (5 mg/mL)	99.3% of curcumin was	Disc diffusion	<i>E. coli</i> , <i>S. aureus</i> , <i>P. aeruginosa</i>	Curcumin significantly enhanced the	Full thickness burn dressing	[109]

					released within the first 24 h.		No in vitro cell culture	antimicrobial activity of pristine porous scaffolds.		
Col (1% w/w) Col/Gel microparticles (50, 125, 250 mg)	Bovine	Sponge	GTA (0.02% v/v)	<i>Calendula officinalis</i> extract (1% v/v)	Incomplete release of the extract was observed within 14 days at pH 5.5 and 7.4.	Not studied	L929 fibroblasts	Not studied	Dermal substitute	[123]
Col	Goat tendon	Aerogel	Wheatgrass (1, 2, 3% w/v)	Wheatgrass (1, 2, 3% w/v)	Not studied	Agar diffusion	<i>E. coli</i> , <i>B. subtilis</i> Swiss 3T6 fibroblasts, HaCaTs	Hybrid aerogels showed smaller inhibition zones than commercial ampicillin discs against <i>B. subtilis</i> .	Wound dressing	[110]
Col (10 mg/mL) GSP (25–100 w% to Col)	Cowhide trimming waste	Sponge	Chloroform extract of cinnamon bark (14.28% v/v)	Cinnamon bark powder (2 g)	Not studied	Broth dilution	<i>B. subtilis</i> , <i>S. aureus</i> , <i>E. coli</i> No in vitro cell culture	The addition of cinnamon bark powder led to great inhibition of all tested strains.	Antimicrobial wound dressing	[106]
Col (9 mg/mL)	Type I (Not specified)	Sponge	Not available	Berberine-oleanolic acid (1–5%)	All samples released about 70% of the drug within 1 h.	Filter paper diffusion	<i>S. aureus</i> , <i>E. coli</i> MG-63 osteosarcoma cells	Gram-positive bacteria were found more sensitive to developed scaffolds than Gram-negative bacteria.	Scaffold for postoperative bacterial bone infection	[124]
Col (1% w/v) Chi (1% w/v) Hap (5% w/v) PCL (20–80 mg/mL) PVA (0.5–3% w/v)	Bovine tendon	Sponge	GTA (0.1% v/v)	<i>Cissus quadrangularis</i> caged PCL nanoparticles	Cumulatively more than 80% of the extract was released within 21 days.	Not studied	MC3T3-E1 osteoblasts	Not studied	Bone tissue engineering scaffold	[107]

Col (1% w/v)	Rat tail tendon	Film	Not available	Thymol (0.25–4 mg/cm <sup>2</sup> )	Not studied	Dehydrogenase activity assay, ATP bioluminescence, microbial penetration assay	<i>S. aureus</i> , <i>E. coli</i> , <i>P. aeruginosa</i> Red blood cells	4 mg/cm <sup>2</sup> of thymol including films indicated almost full inhibition of all tested strains.	Antibacterial film for wound care applications	[108]
Col (11 w% middle layers; 10 w% inner layers) PCL (10 w% outer layers; 11 w% middle layer)	Rat tail	Nanofibrous mat	Not available	<i>Melilotus officinalis</i> (2, 4, 8% w/w)	Not studied	Not studied	L929 fibroblasts	Not studied	Diabetic foot ulcer dressing	[111]
Col Lipid NPs (10:1 w ratio Col/Lipid NPs)	Bovine tendon	Sponge	Not available	Curcumin into lipid NPs	The complete release of curcumin-loaded NPs was observed within 25 days.	Not studied	NIH 3T3 fibroblasts, HaCaTs	Not studied	Composite cryostructure for wound healing	[125]
Col (10 mg/mL) <i>Annona polysaccharide</i> (7.5 mg/mL)	Bovine Achilles tendon	Sponge	Chloroform extract of cinnamon bark	Tetrahydrocurcumin microspheres	28.95 ± 1.7% of the drug was released within 12 h from the composite scaffold.	Disc diffusion	<i>B. subtilis</i> , <i>P. aeruginosa</i> , <i>S. aureus</i> NIH 3T3 fibroblasts	Approximately 20 mm and 10 mm inhibition zone diameters were evaluated against <i>S. aureus</i> around the positive control and composite scaffold, respectively.	Antimicrobial wound dressing	[126]
Col (60% v/v in shell) PVA (50% v/v in core)	Type I (Not specified)	Nanofibrous core-shell mat	Not available	Licorice roots (50% v/v in core, and 40% v/v in shell)	Not studied	Disc diffusion	<i>S. aureus</i> , <i>P. aeruginosa</i> No in vitro cell culture	Bio-nano scaffolds did not show any activity on the inhibition of <i>P. aeruginosa</i> growth.	Hybrid bio-nano wound dressing	[127]

Antimicrobial susceptibility testing: AST; Weight: w; Volume: v; Collagen: Col; Chitosan: Chi; Nanoparticle: NP; Fibronectin: FN; Chondroitin 4-sulfate: CS; 1,4-Butanediol diglycidyl ether: BDDGE; Histidine: His; Hydroxy apatite: Hap; N-(3-dimethylaminopropyl)-N-ethylcarbodiimide hydrochloride: EDC; N-hydroxysuccinimide: NHS; Poly-caprolactone: PCL; Glutaraldehyde: GTA; Titanium dioxide: TiO<sub>2</sub>; Antimicrobial peptide: AMP; Hyaluronic acid: HA; Poly(L-lactide-co-ε-caprolactone): PLC; Cellulose nanocrystal: CNC; Gelatin: Gel; Gulmohar seed polysaccharide: GSP; Poly(vinyl alcohol): PVA; Escherichia coli: E. coli; Staphylococcus epidermidis: S. epidermidis; Staphylococcus aureus: S. aureus; Pseudomonas aeruginosa: P. aeruginosa; Bacillus subtilis: B. subtilis; Bacillus cereus: B. cereus; Salmonella enterica: S. enterica; Pseudomonas putida: P. putida; Porphyromonas gingivalis: P. gingivalis; Fusobacterium nucleatum: F. nucleatum; Streptococcus gordonii: S. gordonii; Methicillin-resistant Staphylococcus aureus: MRSA; Spontaneously immortalized, human keratinocyte line: HaCaT; Human bone marrow-derived stromal cell culture: hBM-MSC; Human dermal fibroblast: HDF.

### 1.3.3. Combination approaches

The combination of antimicrobial bioactive agents has been studied to increase the treatment efficacy of collagen-based antimicrobial biomaterial therapies in addition to their single use by taking advantage of synergetic effects of different therapeutics. For this purpose, the simultaneous incorporation of herbal extracts, metal oxides, AMPs, antibiotics, growth factors, and other bioactive molecules into antimicrobial collagen scaffolds has been extensively investigated (**Table 1.5**). For example, the synergism of 60 mg/mL of lemon balm and dill essential oils enhanced the antimicrobial activity of collagen-based nanofibers on various Gram-positive and Gram-negative bacterial strains and showed *in vivo* biocompatibility on Swiss adult mouse model without any causative effect [102]. In the literature, the combination of metal oxide NPs and phytochemicals in biomaterial formulation exhibited advanced tissue regeneration and antimicrobial activity. In a study, the administration of silver NPs and silymarin raised the contraction rate of collagen/chitosan bilayer sponges treated wounds on Wistar rats from 55% to almost complete contraction within 10 days with a thin crust appearance [128]. Similarly, 0.5 w% curcumin-loaded graphene oxide NP (2 mg/mL)-reinforced sponge dressings accelerated the wound closure of the open wounds *in vivo* due to the superior anti-inflammatory and antibacterial features of curcumin and graphene oxide [129], while the cumulative effect of silver NPs and plumbagin led to complete healing of open excision wounds on Wistar rats on the 15th post-treatment day as well as a significant bactericidal effect on both Gram-positive and Gram-negative bacteria [130].

In some cases, the application of antibiotics could not prevent the re-growing of antibiotic-resistant bacterial strains. Although vancomycin-loaded collagen hydrogels were effective in reducing bacterial luminescence on luminescent MRSA, which infected *in vivo* wounds on the first day, re-growing of bacteria was reported on the 2nd post-treatment day. To overcome this problem, collagen-mimetic-peptide-tethered vancomycin was chosen, and complete inhibition of bacterial growth was achieved by their synergetic effect [131]. Apart from this, the combination of antibiotics with growth factors may ameliorate the rate of wound healing. Silver sulfadiazine, and epidermal and basic fibroblast growth factors, including collagen-based multi-layered nanofibers, presented ideal healing for *in vivo* full-thickness wounds thanks to the slow release of growth factors, neutralizing and anti-growth impact of antibiotics, which supported granulation tissue formation as well normal interactions of collagen fibers and fibroblasts with ECM [132].

**Table 1.5.** Illustrative examples of collagen antimicrobial scaffolds designed with combination approaches.

Composition	Collagen Source	Scaffold Form	Crosslinking	Therapeutic Agent	Release Profile	AST	Bacterial Strain/Cell Line	Antibacterial Activity	Hypothetic Material	Refs.
Col hydrolysate (2.66% w/v) Chi (1.5% w/v)	Bovine tendon Rabbit skin	Nanofibrous mat	Not available	Lemon balm and Dill EOs (60 mg/mL each, 1:1 ratio)	Not studied	Disc diffusion	<i>S. aureus</i> , <i>E. coli</i> , <i>E. faecalis</i> , <i>S. typhimurium</i> No <i>in vitro</i> cell culture	While EOs only did not show efficient antimicrobial activity, EO-including membranes, showed significantly higher activity against tested strains.	Medical wound dressing	[102]
Col (5% w/v)	Not specified	Sponge	GTA (2.5% v/v)	AMPs Pac-525 and KSL-W (1.5 mg/mL) into PLGA microspheres	Burst release of AMPs occurred within 2 days in both microspheres and scaffolds.	Oxford cup disc diffusion	<i>S. aureus</i> , <i>E. coli</i> MC-3T3 fibroblasts	Lower doses of AMPs could not lead to inhibition of <i>S. aureus</i> and <i>E. coli</i> growth.	Scaffold for infective bone defect repair	[133]
Col (3.5% w/v) Chi (1.5% w/v)	Hydrolyzed peptide	Bilayer sponge	GTA (0.025% v/v)	Silymarin (0.5, 1, 2% w/w), and silver NPs (3% w/w)	A sustained release of antioxidants was observed over 120 h.	Not studied	Cos-7 fibroblasts	Not studied	Antioxidant and antibacterial wound dressing	[128]
Col	Rat tail tendon	Hydrogel	Incubation of Col solution in saturated NH <sub>3</sub> chamber	Silver NPs (67, 6.7, 0.67 mg/g), and <i>Cannabis sativa</i> oil (0.15 mL)	Only 1.5 g of the silver content is released after 24 h.	Disc diffusion, broth dilution	<i>S. aureus</i> , <i>P. aeruginosa</i> MDCK epithelial cells	Inhibition zone diameter of 67 mg/g silver-NP-including hydrogels increased from 1.45 to 1.75 cm with the addition of EO.	Wound dressing	[134]

Col (1% w/v)	Fish scale	Sponge	EDC/NHS (1:2:2 GO:EDC:NHS molar ratio)	Curcumin (0.5 w%), and GO NPs (2 mg/mL)	82.5% of loaded curcumin was released within 96 h.	Disc diffusion	<i>P. aeruginosa</i> , <i>S. aureus</i> NIH-3T3 fibroblasts	The inhibition zone diameters around hybrid scaffolds were evaluated as approximately 16 and 15 mm against <i>S. aureus</i> , and <i>P. aeruginosa</i> , respectively.	Wound dressing	[129]
Col	Rat tail tendon	Membrane	Curcumin caged silver NPs (10, 20 μM)	Curcumin (20–100 μM) caged silver NPs	Not studied	Broth dilution	<i>E. coli</i> , <i>B. subtilis</i> HaCaTs	20 μM curcumin-caged silver NPs showed 95% growth inhibition of <i>E. coli</i> .	Scaffold for biomedical engineering	[135]
Col (3 mg/mL)	Rat tail tendon	Sponge	Plumbagin (1–5 μM)	Plumbagin (1–5 μM) caged silver NPs	Not studied	Disc diffusion, broth microdilution	<i>E. coli</i> <i>B. subtilis</i> No in vitro cell culture	Hybrid scaffolds presented better antimicrobial activity against <i>B. subtilis</i> .	Wound dressing	[130]
Col (8 w%) Hap (0, 5, 15 w%)	Type I (Not specified)	Nanofibrous mat	EDC/NHS (4:1 w ratio EDC:NHS)	Vancomycin hydrochloride, gentamicin sulfate (10 w% total, 1:1 w ratio)	High concentrations of vancomycin and gentamicin were released for 21 days.	Disc diffusion	MRSA, <i>S. epidermidis</i> , <i>E. faecalis</i> SAOS-2 osteosarcoma cells	The synergetic effect of two antibiotics yielded increased inhibition zone diameters on MRSA.	Scaffold for the treatment of prosthetic joint infection	[136]
Col (2, 3, 4 mg/mL) Fibrinogen (1.25 mg/mL) Thrombin (0.156 IU/mL)	Bovine	Hydrogel	Not available	Collagen mimetic peptide tethered vancomycin (1.25 mg/gel) into liposomes (30 μg/gel)	Complete vancomycin release was achieved within 12 h.	Broth dilution	<i>S. aureus</i> , MRSA NIH-3T3 fibroblasts	Hybrid hydrogels presented higher antimicrobial activity than pristine hydrogels with less than 10 <sup>4</sup> CFU/wound up to the 9th day.	Scaffold for the MRSA-associated treatment	[131]
Col (1% w/v)	Fish scale	Sponge	GTA (0.25% v/v)	Mupirocin (1:1 w ratio) and <i>Macrotyloma uniflorum</i> extract (10% v/v)	94% of mupirocin was released within 72 h.	Disc diffusion	<i>B. subtilis</i> , <i>S. aureus</i> , <i>P. vulgaris</i> , <i>E. coli</i> NIH-3T3 fibroblasts, HaCaTs	The highest antimicrobial activity of composite dressings was observed on <i>S. aureus</i> .	Burn wound dressing	[137]

Col (20 w%) PCL Zein (15 w% PCL/Zein with various ratios)	Fish	Nanofibrous mat	Not available	Zinc oxide NPs (1 w%) and <i>Aloe vera</i> (5, 8 w%)	Approximately 70% of zinc oxide NPs are released within 30 days.	Disc diffusion	<i>S. aureus</i> , <i>E. coli</i> Human gingival fibroblasts	The combination of zinc oxide NPs with <i>Aloe vera</i> increased the growth inhibition rate of both bacteria.	Wound dressing	[138]
Col (0.5% w/v)	Rat tail	Bilayer sponge	GTA (25% v/v)	Fibrinogen and silver NPs	50% of the included fibrinogen was released within 5 days.	Zone inhibition	<i>E. coli</i> No in vitro cell culture	The one-fold increase in silver NPs concentration did not enhance the antimicrobial activity of scaffolds significantly.	Skin tissue engineering scaffold	[139]
Col (6 mg/mL) Elastin-like peptide (18 mg/mL) (1:3 Col/ELP)	Rat tail tendon	Hydrogel	EDC/NHS	rhBMP-2 (0.005% w/v) doxycycline hydrate (0.5% w/w)	Bi-phasic release of doxycycline was observed with an initial burst release followed by a sustained release.	Zone inhibition	<i>E. coli</i> , <i>P. aeruginosa</i> , <i>S. sanguinis</i> hASCs	The developed hydrogels could not exert effective activity against <i>E. coli</i> .	Bone regenerative hydrogel	[140]
Col (2 w%) PCL (15 w%) Chi (2 w%) PEO (5 w%)	Type I (not specified)	3-layered nanofibrous mat	Not available	Silver sulfadiazine (3 mg/mL), EGF, and bFGF (25 µg/mL each)	Between days 5 and 20, the sustained release was achieved with a cumulative release of about 80%.	Antibiotic tube dilution	<i>P. aeruginosa</i> , <i>S. aureus</i> HDFs	Minimum inhibitory concentration was evaluated as 15 and 30 µg/mL against <i>P. aeruginosa</i> and <i>S. aureus</i> , respectively.	Wound dressing	[132]
Col (1% w/v)	Bovine skin	Sponge	GTA (0–1% w/v)	OTC (1 g/L) DXC (1 g/L)	About 70% of OTC was released from 0.5% of GTA crosslinked scaffolds within 600 min.	Broth dilution	<i>E. coli</i> , <i>E. faecalis</i> , <i>S. aureus</i> Dermal fibroblasts of mouse cell line	Oxytetracycline led to more inhibition of growth of tested bacteria.	Dressing for prevention and treatment of infections at the application site	[141]

Col PVA (1:3 w/w PVA/Col)	Bovine tendon	Membrane	Not available	Ciprofloxacin and tobramycin (0.3% w/v for soaking method, 5% w/w for mixing method)	CP showed more sustained and controlled release. 95% of CP was released after 48 h.	Microdilution, time-kill assay	<i>S. aureus</i> , <i>E. coli</i> No in vitro cell culture	The efficacy of membranes to kill the tested bacteria was found independent of their release profile.	Ulcerative keratitis dressing	[142]
Col (4 mg/mL)	Not specified	Sponge	Triphenyl phosphate (10% v/v)	Mupirocin (50 mg) in 5% w/v Chi microspheres and <i>Piper betle</i> extract (5% v/v)	More than 50% of both drugs are released at the end of 12 h.	Agar disc diffusion	<i>E. coli</i> , <i>S. aureus</i> No in vitro cell culture	The combination of two antimicrobials slightly increased the antimicrobial activity against both strains.	Wound dressing	[143]
Col (1.06 mg/mL)	<i>Rapana venosa</i>	Sponge	Not available	<i>Salvia officinalis</i> extract loaded mesoporous silica NPs (10, 20 mg/mL)	Not studied	Broth microdilution	<i>P. aeruginosa</i> , <i>S. aureus</i> HaCaTs, Human Mel-Juso skin carcinoma cells	The hybrid scaffolds showed at least a two-fold higher minimum inhibitory concentration for <i>P. aeruginosa</i> .	Wound dressing	[144]

Antimicrobial susceptibility testing: AST; Weight: w; Volume: v; Collagen: Col; Chitosan: Chi; Essential oil: EO; poly(D,L-lactide-co-glycolic acid): PLGA; Polycaprolactone: PCL; Antimicrobial peptide: AMP; Nanoparticle: NP; Ammonia: NH<sub>3</sub>; Graphene oxide: GO; Hydroxy apatite: Hap; Elastin-like peptide: ELP; Epidermal growth factor: EGF; Basic fibroblast growth factor: bFGF; Oxytetracycline hydrochloride: OTC; Doxycycline hydrochloride: DXC; Ciprofloxacin: CP; Tobramycin: TB; N-(3-dimethylaminopropyl)-N-ethylcarbodiimide hydrochloride: EDC; N-hydroxysuccinimide: NHS; Glutaraldehyde: GTA; Escherichia coli: E. coli; Staphylococcus aureus: S. aureus; Enterococcus faecalis: E. faecalis; Salmonella typhimurium: S. typhimurium; Methicillin-resistant Staphylococcus aureus: MRSA; Pseudo-monas aeruginosa: P. aeruginosa; Bacillus subtilis: B. subtilis; Proteus vulgaris: P. vulgaris; Streptococcus sanguinis: S. sanguinis; Spontaneously immortalized human keratinocyte line: HaCaT; Recombinant human bone morphogenetic protein-2: rhBMP-2; Human adipose-derived stem cell: hASC; Human dermal fibroblast: HDF.

#### 1.4. Project rationale, aims, hypothesis and objectives

Antimicrobial resistance poses a significant global health challenge following cardiac problems, as microorganisms like bacteria, viruses, fungi, and parasites adapt to withstand the impact of medications. Since the discovery of penicillin in 1928 by Alexander Fleming, antibiotics have been the preferred choice for treating infections. Despite their low toxicity and potent bactericidal properties, prolonged use of antibiotics has led to the proliferation and spread of antibiotic-resistant bacteria, giving rise to diseases related to antimicrobial resistance. This adaptation renders standard treatments ineffective and complicates the management of infections. Consequently, antimicrobial resistance results in prolonged illness, heightened mortality rates, and places a substantial strain on healthcare systems. Consequently, the emergence of new antimicrobial treatment strategies using alternative and safer antimicrobial agents has been getting attention. Essential oils are one of the promising alternative antimicrobial agents substitute for commercial antibiotics thanks to their broad range of biological activities. However, their high volatility and sensitivity requires their use within a carrier system.

Herein, the ultimate goal of this study was to develop an optimally functionalized antibacterial collagen hydrogel systems incorporated with an effective essential oil in order to treat infected tissues by aiming to combat antimicrobial resistance. In this context, firstly detailed antimicrobial and anti-biofilm activity of four different essential oils (*Thymus sibthorpii*, *Origanum vulgare*, *Salvia fruticosa*, *Crithmum maritimum*) were assessed as Phase I of the project (Chapter 2). Thereafter, optimized collagen type I hydrogels were developed via functionalizing them by six different starPEG crosslinkers with different concentrations (Phase II). Lastly, release profile, release kinetics, and biological activities of developed composite antibacterial collagen hydrogels were evaluated as a content of Phase III.

### 1.4.1. Phase 1 (Chapter 2):

**Overall aim:** To screen the composition and assess antimicrobial and anti-biofilm activity of *Thymus sibthorpii*, *Origanum vulgare*, *Salvia fruticosa*, *Crithmum maritimum* essential oils using Kirby Bauer disc diffusion method, modified broth microdilution assay, and microtiter plate biofilm assay.

**Hypothesis:** Essential oils can be the safer alternative antimicrobial agent candidate substitute for widely used antibiotics in order to combat antimicrobial resistance problem with superior antimicrobial and anti-biofilm activity against various kinds of pathogenic bacteria thanks to their complex chemical structure.

#### Objectives:

- To screen the chemical composition of essential oils.
- To assess antimicrobial activity of essential oils by Kirby Bauer disc diffusion and modified broth microdilution assays.
- To assess anti-biofilm activity of essential oils by microtiter plate biofilm assay.
- To compare the antimicrobial and anti-biofilm activity of essential oils with widely used commercial antibiotics and decide the most effective one as a model agent for the study.
- To screen the antimicrobial and anti-biofilm activity effectiveness of different essential oils.
- To compare the effect of essential oils on methicillin-sensitive, methicillin-resistant, and reference *S. aureus* strains to have insights on their potential to combat antimicrobial resistance problem.

### 1.4.2. Phase 2 (Chapter 3):

**Overall aim:** To develop optimally functionalized collagen type I hydrogels via various starPEG molecules with five different concentrations.

**Hypothesis:** starPEG molecules can effectively crosslink collagen type I hydrogels via covalent bonding with amine group hence enhance the stability of hydrogels.

#### Objectives:

- To optimize the fabrication of collagen type I hydrogels.
- To assess the free amine reduction of functionalized collagen type I hydrogels via TNBSA assay.
- To assess the resistance of developed functionalized hydrogels against collagenase enzyme via collagenase assay.
- To screen the effective concentration plateau for each starPEG crosslinker at 0.5, 1, 2, and 5 mM concentration.
- To investigate the influence of different molecular weight and arm number of starPEG on collagen crosslinking.
- To determine optimal starPEG type and concentration via statistical analysis by using GTA as a positive control.

### 1.4.3. Phase 3 (Chapter 3):

**Overall aim:** To fabricate the functionalized antibacterial collagen type I hydrogels loaded with the selected most efficient essential oil and assess the release profile and release kinetics of the agent from hydrogel network as well as the antimicrobial activity and *in vitro* cytotoxicity of composite systems.

**Hypothesis:** The essential oil incorporated antibacterial collagen type I hydrogels can demonstrate sustained release of the loaded essential oil, Fickian diffusion mechanism, superior antibacterial activity against widely inhabited pathogenic bacteria on the infected tissue area, and no toxic effect on fibroblasts.

#### **Objectives:**

- To fabricate *Thymus sibthorpii* essential oil loaded antibacterial collagen type I hydrogels.
- To investigate the release profile of *Thymus sibthorpii* essential oil from hydrogel network.
- To examine the release kinetics of *Thymus sibthorpii* essential using five different mathematical models.
- To assess antimicrobial activity of antibacterial hydrogels against gram-positive *S. aureus* and gram-negative *E.coli*.
- To assess the metabolic activity and proliferation of NIH-3T3 fibroblasts seeded on the hydrogels.

## 1.5. References

- [1] Vera, D.M.A.; Haynes, M.H.; Ball, A.R.; Dai, T.; Astrakas, C.; Kelso, M.J.; Hamblin, M.R.; Tegos, G.P. Strategies to potentiate antimicrobial photoinactivation by overcoming resistant phenotypes. *Photochem. Photobiol.* 2012, 88, 499–511.
- [2] Cai, J.; Liu, R. Introduction to Antibacterial Biomaterials. *Biomater. Sci.* 2020, 8, 6812–6813.
- [3] Voidarou, C.; Bezirtzoglou, E.; Alexopoulos, A.; Plessas, S.; Stefanis, C.; Papadopoulos, I.; Vavias, S.; Stavropoulou, E.; Fotou, K.; Tzora, A. Occurrence of *Clostridium perfringens* from different cultivated soils. *Anaerobe* 2011, 17, 320–324.
- [4] Tan, S.Y.; Tatsumura, Y. Alexander Fleming (1881–1955): Discoverer of penicillin. *Singap. Med. J.* 2015, 56, 366.
- [5] Nelli, A.; Voidarou, C.; Venardou, B.; Fotou, K.; Tsinas, A.; Bonos, E.; Fthenakis, G.C.; Skoufos, I.; Tzora, A. Antimicrobial and Methicillin Resistance Pattern of Potential Mastitis-Inducing *Staphylococcus aureus* and Coagulase-Negative *Staphylococci* Isolates from the Mammary Secretion of Dairy Goats. *Biology* 2022, 11, 1591.
- [6] Organisation for Economic Cooperation and Development; European Union. Health at a Glance: Europe 2018: State of Health in the EU Cycle; OECD Publishing, Paris/European Union: Brussels, Belgium, 2018.
- [7] Suetens, C.; Latour, K.; Kärki, T.; Ricchizzi, E.; Kinross, P.; Moro, M.L.; Jans, B.; Hopkins, S.; Hansen, S.; Lyytikäinen, O. Prevalence of healthcare-associated infections, estimated incidence and composite antimicrobial resistance index in acute care hospitals and long-term care facilities: Results from two European point prevalence surveys, 2016 to 2017. *Eurosurveillance* 2018, 23, 1800516.
- [8] Cassini, A.; Plachouras, D.; Eckmanns, T.; Abu Sin, M.; Blank, H.-P.; Ducomble, T.; Haller, S.; Harder, T.; Klingeberg, A.; Sixtensson, M. Burden of six healthcare-associated infections on European population health: Estimating incidence-based disability-adjusted life years through a population prevalence-based modelling study. *PLoS Med.* 2016, 13, e1002150.
- [9] U.S. Centers for Disease Control and Prevention. Antibiotic Resistance Threats in the United State; Department of Health and Human Services, CDC: Atlanta, GA, USA, 2019.
- [10] Organisation for Economic Cooperation and Development; European Union. Tackling Wasteful Spending on Health; OECD Publishing: Paris, France, 2017.

- [11] Prestinaci, F.; Pezzotti, P.; Pantosti, A. Antimicrobial resistance: A global multifaceted phenomenon. *Pathog. Glob. Health* 2015, 109, 309–318.
- [12] Dadgostar, P. Antimicrobial resistance: Implications and costs. *Infect. Drug Resist.* 2019, 12, 3903.
- [13] Murugaiyan, J.; Kumar, P.A.; Rao, G.S.; Iskandar, K.; Hawser, S.; Hays, J.P.; Mohsen, Y.; Adukkadukkam, S.; Awuah, W.A.; Jose, R.A.M. Progress in alternative strategies to combat antimicrobial resistance: Focus on antibiotics. *Antibiotics* 2022, 11, 200.
- [14] Majumder, M.A.A.; Rahman, S.; Cohall, D.; Bharatha, A.; Singh, K.; Haque, M.; Gittens-St Hilaire, M. Antimicrobial stewardship: Fighting antimicrobial resistance and protecting global public health. *Infect. Drug Resist.* 2020, 13, 4713–4738.
- [15] Tarín-Pelló, A.; Suay-García, B.; Pérez-Gracia, M.-T. Antibiotic resistant bacteria: Current situation and treatment options to accelerate the development of a new antimicrobial arsenal. *Expert Rev. Anti-Infect. Ther.* 2022, 20, 1095–1108.
- [16] Ricard-Blum, S. The collagen family. *Cold Spring Harb. Perspect. Biol.* 2011, 3, a004978.
- [17] Ferreira, A.M.; Gentile, P.; Chiono, V.; Ciardelli, G. Collagen for bone tissue regeneration. *Acta Biomater.* 2012, 8, 3191–3200.
- [18] Stark, Y.; Suck, K.; Kasper, C.; Wieland, M.; van Griensven, M.; Scheper, T. Application of collagen matrices for cartilage tissue engineering. *Exp. Toxicol. Pathol.* 2006, 57, 305–311.
- [19] Zhang, G.; Young, B.; Ezura, Y.; Favata, M.; Soslowsky, L.; Chakravarti, S.; Birk, D.E. Development of tendon structure and function: Regulation of collagen fibrillogenesis. *J. Musculoskelet Neuronal Interact.* 2005, 5, 5–21.
- [20] Priya, S.G.; Jungvid, H.; Kumar, A. Skin tissue engineering for tissue repair and regeneration. *Tissue Eng. Part B Rev.* 2008, 14, 105–118.
- [21] Kalic, T.; Kamath, S.D.; Ruethers, T.; Taki, A.C.; Nugraha, R.; Le, T.T.; Humeniuk, P.; Williamson, N.A.; Hira, D.; Rolland, J.M. Collagen—An important fish allergen for improved diagnosis. *J. Allergy Clin. Immunol. Pract.* 2020, 8, 3084–3092.e3010.
- [22] Sorushanova, A.; Delgado, L.M.; Wu, Z.; Shologu, N.; Kshirsagar, A.; Raghunath, R.; Mullen, A.M.; Bayon, Y.; Pandit, A.; Raghunath, M.; et al. The collagen suprafamily: From biosynthesis to advanced biomaterial development. *Adv. Mater.* 2019, 31, 1801651.
- [23] Rezvani Ghomi, E.; Nourbakhsh, N.; Akbari Kenari, M.; Zare, M.; Ramakrishna, S. Collagen-based biomaterials for biomedical applications. *J. Biomed. Mater. Res.* 2021, 109, 1986–1999.

- [24] David, G. Collagen-based 3D structures—Versatile, efficient materials for biomedical applications. In *Biopolymer-Based Formulations*, 1st ed.; Elsevier: Amsterdam, The Netherlands, 2020; pp. 881–906.
- [25] Lee, C.H.; Singla, A.; Lee, Y. Biomedical applications of collagen. *Int. J. Pharm.* 2001, 221, 1–22.
- [26] Sundar, G.; Joseph, J.; John, A.; Abraham, A. Natural collagen bioscaffolds for skin tissue engineering strategies in burns: A critical review. *Int. J. Polym. Mater.* 2021, 70, 593–604.
- [27.] Singh, O.; Gupta, S.S.; Soni, M.; Moses, S.; Shukla, S.; Mathur, R.K. Collagen dressing versus conventional dressings in burn and chronic wounds: A retrospective study. *J. Cutan. Aesthetic Surg.* 2011, 4, 12.
- [28] Avila Rodríguez, M.I.; Rodríguez Barroso, L.G.; Sánchez, M.L. Collagen: A review on its sources and potential cosmetic applications. *J. Cosmet. Dermatol.* 2018, 17, 20–26.
- [29] Ge, X. Antimicrobial biomaterials with non-antibiotic strategy. *Biosurf. Biotribol.* 2019, 5, 71–82.
- [30] Li, S.; Dong, S.; Xu, W.; Tu, S.; Yan, L.; Zhao, C.; Ding, J.; Chen, X. Antibacterial hydrogels. *Adv. Sci.* 2018, 5, 1700527.
- [31] 3M™ Promogran Prisma™ Matrix. Available online: [https://www.3m.com/3M/en\\_US/p/d/b5005265080/](https://www.3m.com/3M/en_US/p/d/b5005265080/) (accessed on 23 June 2024).
- [32] ColActive®Plus Powder Ag. Available online: <https://www.woundsource.com/product/colactive-plus-powder-ag> (accessed on 23 June 2024).
- [33] Septocoll®E—Biomet. Available online: <https://www.yumpu.com/en/document/view/42479805/septocollar-e-biomet> (accessed on 23 June 2024).
- [34] DermaCol™CollagenMatrix Dressing. Available online: <https://dermarite.com/product/dermacol/> (accessed on 23 June 2024).
- [35] DermaCol/Ag™CollagenMatrix Dressing with Silver. Available online: <https://dermarite.com/product/dermacolag/> (accessed on 23 June 2024).
- [36] SilvaKollagen®Gel Silver CollagenWound Gel. Available online: <https://dermarite.com/product/silvakollagen-gel/> (accessed on 23 June 2024).
- [37] Puracol Plus AG+ Collagen Wound Dressings with Silver. Available online: <https://punchout.medline.com/product/Puracol-Plus-AG-Collagen-Wound-Dressings-with>

Silver/Collagen-Dressings/Z05-PF00137?question=&index=P1&indexCount=1 (accessed on 23 June 2024).

[38] SEESKIN P—Collagen Particle Dressing. Available online: <https://www.synerheal.com/product-page/seeskin-p-collagenparticle-dressing> (accessed on 23 June 2024).

[39] CollaSorb. Available online: <https://www.vitalitymedical.com/collasorb.html> (accessed on 23 June 2024).

[40] GENTA-COLL ®Resorb Collagen Gentamicin Sponge. Available online: <https://resorba.com/region/row/product/biosurgicals/genta-coll-resorb/> (accessed on 23 June 2024).

[41] COLLAMYCIN (Gentamicin Collagen Gel). Available online: <https://www.synerheal.com/product-page/collamycin-gentamicin-collagen-gel> (accessed on 23 June 2024).

[42] Gencoll Gel. Available online: <https://www.cologenesis.net/medicated-gencoll-gel.htm> (accessed on 23 June 2024).

[43] Colloskin-M. Available online: <https://www.cologenesis.net/colloskin-m.htm> (accessed on 23 June 2024).

[44] Collofiber-MM Medicated. Available online: <https://www.cologenesis.net/collofiber-mm-medicated.htm> (accessed on 23 June 2024).

[45] Coloplug. Available online: <https://www.cologenesis.net/coloplug-collagen-sponge.htm> (accessed on 23 June 2024).

[46] Diacoll-S. Available online: <https://www.cologenesis.net/diacoll-s-sterile-collagen-sheet.htm> (accessed on 23 June 2024).

[47] Irastorza, A.; Zarandona, I.; Andonegi, M.; Guerrero, P.; de la Caba, K. The versatility of collagen and chitosan: From food to biomedical applications. *Food Hydrocoll.* 2021, 116, 106633.

[48] Yuan, H.; Chen, L.; Hong, F.F. A biodegradable antibacterial nanocomposite based on oxidized bacterial nanocellulose for rapid hemostasis and wound healing. *ACS Appl. Mater. Interfaces* 2019, 12, 3382–3392.

[49] Ramadass, S.K.; Perumal, S.; Gopinath, A.; Nisal, A.; Subramanian, S.; Madhan, B. Sol-gel assisted fabrication of collagen hydrolysate composite scaffold: A novel therapeutic alternative to the traditional collagen scaffold. *ACS Appl. Mater. Interfaces* 2014, 6, 15015–15025.

- [50] Mahmoudifard, M. Graphene family in cancer therapy: Recent progress in Cancer Gene/Drug delivery applications. *J. Mater. Chem. B* 2023, 11, 2568–2613.
- [51] Oladele, I.; Agbabiaka, O.; Olasunkanmi, O.; Balogun, A.; Popoola, M. Non-synthetic sources for the development of hydroxyapatite. *J. Appl. Biotechnol. Bioeng* 2018, 5, 88–95.
- [52] Zhou, T.; Sui, B.; Mo, X.; Sun, J. Multifunctional and biomimetic fish collagen/bioactive glass nanofibers: Fabrication, antibacterial activity and inducing skin regeneration in vitro and in vivo. *Int. J. Nanomed.* 2017, 12, 3495.
- [53] Dolete, G.; Tihăuan, B.M.; Tutunaru, O.; Mocanu, I.-C.; Balaş, C.; Lavinia, I.; Ardelean, D.S.D.; Kamerzan, C.M.; Maier, S.S. Development and sequential analysis of a collagen-chitosan wound management biomaterial. *Rom. Biotechnol. Lett.* 2019, 24, 108–117.
- [54] ISO 20743:2007; Textiles—Determination of Antibacterial Activity of Antibacterial Finished Products. International Organization for Standardization: Geneva, Switzerland, 2007.
- [55] Gilarska, A.; Lewandowska-Łańcucka, J.; Guzdek-Zajac, K.; Karewicz, A.; Horak, W.; Lach, R.; Wójcik, K.; Nowakowska, M. Bioactive yet antimicrobial structurally stable collagen/chitosan/lysine functionalized hyaluronic acid-based injectable hydrogels for potential bone tissue engineering applications. *Int. J. Biol. Macromol.* 2020, 155, 938–950.
- [56] Valenzuela-Rojo, R.D.; López-Cervantes, J.; Sánchez-Machado, D.I.; Escárcega-Galaz, A.A.; del Rosario Martínez-Macias, M. Antibacterial, mechanical and physical properties of collagen-chitosan sponges from aquatic source. *Sustain. Chem. Pharm.* 2020, 15, 100218.
- [57] Rajasree, S.R.; Gobalakrishnan, M.; Aranganathan, L.; Karthih, M. Fabrication and characterization of chitosan based collagen/gelatin composite scaffolds from big eye snapper *Priacanthus hamrur* skin for antimicrobial and antioxidant applications. *Mater. Sci. Eng. C* 2020, 107, 110270.
- [58] Bian, T.; Pang, N.; Xing, H. Preparation and antibacterial evaluation of a beta-tricalcium phosphate/collagen nanofiber biomimetic composite scaffold. *Mater. Chem. Phys.* 2021, 273, 125059.
- [59] Gao, Y.; Kang, Y.; Wang, T.; Li, C.; Shen, S.; Qu, C.; Gong, S.; Liu, P.; Yang, L.; Liu, J. Alginate microspheres-collagen hydrogel, as a novel 3D culture system, enhanced skin wound healing of hUCMSCs in rats model. *Colloids Surf. B* 2022, 219, 112799.
- [60] Dantas, G.; Sommer, M.O.; Oluwasegun, R.D.; Church, G.M. Bacteria subsisting on antibiotics. *Science* 2008, 320, 100–103.

- [61] Michalska-Sionkowska, M.; Kaczmarek, B.; Walczak, M.; Sionkowska, A. Antimicrobial activity of new materials based on the blends of collagen/chitosan/hyaluronic acid with gentamicin sulfate addition. *Mater. Sci. Eng. C* 2018, 86, 103–108.
- [62] Suchý, T.; Šupová, M.; Klapková, E.; Adamková, V.; Závora, J.; Žaloudková, M.; Rýglová, Š.; Ballay, R.; Denk, F.; Pokorný, M. The release kinetics, antimicrobial activity and cytocompatibility of differently prepared collagen/hydroxyapatite/vancomycin layers: Microstructure vs. nanostructure. *Eur. J. Pharm. Sci.* 2017, 100, 219–229.
- [63] Zhu, Q.; Teng, J.; Liu, X.; Lan, Y.; Guo, R. Preparation and characterization of gentamycin sulfate-impregnated gelatin microspheres/collagen–cellulose/nanocrystal scaffolds. *Polym. Bull.* 2018, 75, 77–91.
- [64] Liu, Y.; Ren, L.; Long, K.; Wang, L.; Wang, Y. Preparation and characterization of a novel tobramycin-containing antibacterial collagen film for corneal tissue engineering. *Acta Biomater.* 2014, 10, 289–299.
- [65] Ma, S.; Adayi, A.; Liu, Z.; Li, M.; Wu, M.; Xiao, L.; Sun, Y.; Cai, Q.; Yang, X.; Zhang, X. Asymmetric collagen/chitosan membrane containing minocycline-loaded chitosan nanoparticles for guided bone regeneration. *Sci. Rep.* 2016, 6, 31822.
- [66] Martin, V.; Ribeiro, I.A.; Alves, M.M.; Gonçalves, L.; Claudio, R.A.; Grenho, L.; Fernandes, M.H.; Gomes, P.; Santos, C.F.; Bettencourt, A.F. Engineering a multifunctional 3D-printed PLA-collagen-minocycline-nanoHydroxyapatite scaffold with combined antimicrobial and osteogenic effects for bone regeneration. *Mater. Sci. Eng. C* 2019, 101, 15–26.
- [67] Yu, X.; Yuan, Q.; Yang, M.; Liu, R.; Zhu, S.; Li, J.; Zhang, W.; You, J.; Xiong, S.; Hu, Y. Development of biocompatible and antibacterial collagen hydrogels via dialdehyde polysaccharide modification and tetracycline hydrochloride loading. *Macromol. Mater. Eng.* 2019, 304, 1800755.
- [68] Rivadeneira, J.; Di Virgilio, A.; Audisio, M.; Boccaccini, A.; Gorustovich, A. Evaluation of antibacterial and cytotoxic effects of nano-sized bioactive glass/collagen composites releasing tetracycline hydrochloride. *J. Appl. Microbiol.* 2014, 116, 1438–1446.
- [69] Semyari, H.; Salehi, M.; Taleghani, F.; Ehterami, A.; Bastami, F.; Jalayer, T.; Semyari, H.; Hamed Nabavi, M.; Semyari, H. Fabrication and characterization of collagen–hydroxyapatite-based composite scaffolds containing doxycycline via freeze-casting method for bone tissue engineering. *J. Biomater. Appl.* 2018, 33, 501–513.

- [70] Perumal, S.; kumar Ramadass, S.; Madhan, B. Sol–gel processed mupirocin silica microspheres loaded collagen scaffold: A synergistic bio-composite for wound healing. *Eur. J. Pharm. Sci.* 2014, 52, 26–33.
- [71] Hajikhani, M.; Emam-Djomeh, Z.; Askari, G. Fabrication and characterization of mucoadhesive bioplastic patch via coaxial polylactic acid (PLA) based electrospun nanofibers with antimicrobial and wound healing application. *Int. J. Biol. Macromol.* 2021, 172, 143–153.
- [72] Yilmaz Atay, H. Antibacterial activity of chitosan-based systems. In *Functional Chitosan: Drug Delivery and Biomedical Applications*; Springer Nature: Berlin/Heidelberg, Germany, 2019; pp. 457–489.
- [73] Tripathi, S.; Singh, B.N.; Divakar, S.; Kumar, G.; Mallick, S.P.; Srivastava, P. Design and evaluation of ciprofloxacin loaded collagen chitosan oxygenating scaffold for skin tissue engineering. *Biomed. Mater.* 2021, 16, 025021.
- [74] Tsekoura, E.; Helling, A.; Wall, J.; Bayon, Y.; Zeugolis, D. Battling bacterial infection with hexamethylene diisocyanate cross-linked and Cefaclor-loaded collagen scaffolds. *Biomed. Mater.* 2017, 12, 035013.
- [75] Ahmadian, S.; Ghorbani, M.; Mahmoodzadeh, F. Silver sulfadiazine-loaded electrospun ethyl cellulose/polylactic acid/collagen nanofibrous mats with antibacterial properties for wound healing. *Int. J. Biol. Macromol.* 2020, 162, 1555–1565.
- [76] Mahmoud, A.A.; Salama, A.H. Norfloxacin-loaded collagen/chitosan scaffolds for skin reconstruction: Preparation, evaluation and in-vivo wound healing assessment. *Eur. J. Pharm. Sci.* 2016, 83, 155–165.
- [77] Song, Y.; Hu, Q.; Liu, Q.; Liu, S.; Wang, Y.; Zhang, H. Design and fabrication of drug-loaded alginate/hydroxyapatite/collagen composite scaffolds for repairing infected bone defects. *J. Mater. Sci.* 2023, 58, 911–926.
- [78] Feris, K.; Otto, C.; Tinker, J.; Wingett, D.; Punnoose, A.; Thurber, A.; Kongara, M.; Sabetian, M.; Quinn, B.; Hanna, C. Electrostatic interactions affect nanoparticle-mediated toxicity to gram-negative bacterium *Pseudomonas aeruginosa* PAO1. *Langmuir* 2010, 26, 4429–4436.
- [79] Luan, B.; Huynh, T.; Zhou, R. Complete wetting of graphene by biological lipids. *Nanoscale* 2016, 8, 5750–5754.

- [80] Armentano, I.; Arciola, C.R.; Fortunati, E.; Ferrari, D.; Mattioli, S.; Amoroso, C.F.; Rizzo, J.; Kenny, J.M.; Imbriani, M.; Visai, L. The interaction of bacteria with engineered nanostructured polymeric materials: A review. *Sci. World J.* 2014, 2014, 1–18.
- [81] Gao, W.; Thamphiwatana, S.; Angsantikul, P.; Zhang, L. Nanoparticle approaches against bacterial infections. *Wiley Interdiscip. Rev. Nanomed. Nanobiotechnol.* 2014, 6, 532–547.
- [82] Rath, G.; Hussain, T.; Chauhan, G.; Garg, T.; Goyal, A.K. Collagen nanofiber containing silver nanoparticles for improved wound-healing applications. *J. Drug Target.* 2016, 24, 520–529.
- [83] Alarcon, E.I.; Udekwu, K.I.; Noel, C.W.; Gagnon, L.B.-P.; Taylor, P.K.; Vulesevic, B.; Simpson, M.J.; Gkatzis, S.; Islam, M.M.; Lee, C.-J. Safety and efficacy of composite collagen–silver nanoparticle hydrogels as tissue engineering scaffolds. *Nanoscale* 2015, 7, 18789–18798.
- [84] You, C.; Li, Q.; Wang, X.; Wu, P.; Ho, J.K.; Jin, R.; Zhang, L.; Shao, H.; Han, C. Silver nanoparticle loaded collagen/chitosan scaffolds promote wound healing via regulating fibroblast migration and macrophage activation. *Sci. Rep.* 2017, 7, 10489.
- [85] Song, J.; Zhang, P.; Cheng, L.; Liao, Y.; Xu, B.; Bao, R.; Wang, W.; Liu, W. Nano-silver in situ hybridized collagen scaffolds for regeneration of infected full-thickness burn skin. *J. Mater. Chem. B* 2015, 3, 4231–4241.
- [86] Ge, L.G.; Xu, Y.X.; Li, X.; Yuan, L.; Tan, H.; Li, D.; Mu, C. Fabrication of Antibacterial Collagen-Based Composite Wound Dressing. *ACS Sustain. Chem. Eng.* 2018, 6, 9153–9166.
- [87] Li, P.; Ruan, L.; Wang, R.; Liu, T.; Song, G.; Gao, X.; Jiang, G.; Liu, X. Electrospun Scaffold of Collagen and Polycaprolactone Containing ZnO Quantum Dots for Skin Wound Regeneration. *J. Bionic Eng.* 2021, 18, 1378–1390.
- [88] Lei, J.; Sun, L.; Huang, S.; Zhu, C.; Li, P.; He, J.; Mackey, V.; Coy, D.H.; He, Q. The antimicrobial peptides and their potential clinical applications. *Am. J. Transl. Res.* 2019, 11, 3919.
- [89] Lazzaro, B.P.; Zasloff, M.; Rolff, J. Antimicrobial peptides: Application informed by evolution. *Science* 2020, 368, eaau5480.
- [90] Kalelkar, P.P.; Riddick, M.; Garcia, A.J. Biomaterial-based antimicrobial therapies for the treatment of bacterial infections. *Nat. Rev. Mater.* 2021, 7, 39–54.
- [91] Kumar, P.; Kizhakkedathu, J.N.; Straus, S.K. Antimicrobial peptides: Diversity, mechanism of action and strategies to improve the activity and biocompatibility in vivo. *Biomolecules* 2018, 8, 4.

- [92] Ghalei, S.; Handa, H. A review on antibacterial silk fibroin-based biomaterials: Current state and prospects. *Mater. Today Chem.* 2022, 23, 100673.
- [93] Stempel, N.; Strehmel, J.; Overhage, J. Potential application of antimicrobial peptides in the treatment of bacterial biofilm infections. *Curr. Pharm. Des.* 2015, 21, 67–84.
- [94] Bacalum, M.; Radu, M. Cationic antimicrobial peptides cytotoxicity on mammalian cells: An analysis using therapeutic index integrative concept. *Int. J. Pept. Res. Ther.* 2015, 21, 47–55.
- [95] Lin, Z.; Wu, T.; Wang, W.; Li, B.; Wang, M.; Chen, L.; Xia, H.; Zhang, T. Biofunctions of antimicrobial peptide-conjugated alginate/hyaluronic acid/collagen wound dressings promote wound healing of a mixed-bacteria-infected wound. *Int. J. Biol. Macromol.* 2019, 140, 330–342.
- [96] Ye, Z.; Zhu, X.; Mutreja, I.; Boda, S.K.; Fischer, N.G.; Zhang, A.; Lui, C.; Qi, Y.; Aparicio, C. Biomimetic mineralized hybrid scaffolds with antimicrobial peptides. *Bioact. Mater.* 2021, 6, 2250–2260.
- [97] Cassin, M.E.; Ford, A.J.; Orbach, S.M.; Saverot, S.E.; Rajagopalan, P. The design of antimicrobial LL37-modified collagen-hyaluronic acid detachable multilayers. *Acta Biomater.* 2016, 40, 119–129.
- [98] Prakobkarn, J.; Makeudom, A.; Jenvoraphot, T.; Supanchart, C.; Krisanaprakornkit, S.; Punyodom, W.; Daranarong, D. Biphasic nanofibrous scaffolds based on collagen and PLC for controlled release LL-37 in guided bone regeneration. *J. Appl. Polym. Sci.* 2022, 139, 51629.
- [99] Hsu, S. Green tea and the skin. *J. Am. Acad. Dermatol.* 2005, 52, 1049–1059.
- [100] Thangapazham, R.L.; Sharad, S.; Maheshwari, R.K. Phytochemicals in wound healing. *Adv. Wound Care* 2016, 5, 230–241.
- [101] Agarwal, T.; Tan, S.-A.; Onesto, V.; Law, J.X.; Agrawal, G.; Pal, S.; Lim, W.L.; Sharifi, E.; Moghaddam, F.D.; Maiti, T.K. Engineered herbal scaffolds for tissue repair and regeneration: Recent trends and technologies. *Biomed. Eng. Adv.* 2021, 2, 100015.
- [102] Fathi, M.; Ahmadi, N.; Forouhar, A.; Hamzeh Atani, S. Natural Hydrogels, the Interesting Carriers for Herbal Extracts. *Food Rev. Int.* 2021, 38, 713–737.
- [103] Râpă, M.; Gaidau, C.; Mititelu-Tartau, L.; Berechet, M.-D.; Berbecaru, A.C.; Rosca, I.; Chiriac, A.P.; Matei, E.; Predescu, A.-M.; Predescu, C. Bioactive Collagen Hydrolysate-Chitosan/Essential Oil Electrospun Nanofibers Designed for Medical Wound Dressings. *Pharmaceutics* 2021, 13, 1939.

- [104] De Luca, I.; Pedram, P.; Moeini, A.; Cerruti, P.; Peluso, G.; Di Salle, A.; Germann, N. Nanotechnology Development for Formulating Essential Oils in Wound Dressing Materials to Promote the Wound-Healing Process: A Review. *Appl. Sci.* 2021, 11, 1713.
- [105] Ersanli, C.; Tzora, A.; Skoufos, I.; Fotou, K.; Maloupa, E.; Gridoriadou, K.; Voidarou, C.; Zeugolis, D.I. The Assessment of Antimicrobial and Anti-Biofilm Activity of Essential Oils against *Staphylococcus aureus* Strains. *Antibiotics* 2023, 12, 384.
- [106] Vaou, N.; Stavropoulou, E.; Voidarou, C.; Tsigalou, C.; Bezirtzoglou, E. Towards advances in medicinal plant antimicrobial activity: A review study on challenges and future perspectives. *Microorganisms* 2021, 9, 2041.
- [107] Cheirmadurai, K.; Thanikaivelan, P.; Murali, R. Highly biocompatible collagen–Delonix regia seed polysaccharide hybrid scaffolds for antimicrobial wound dressing. *Carbohydr. Polym.* 2016, 137, 584–593.
- [108] Thongtham, N.; Chai-in, P.; Unger, O.; Boonrungsiman, S.; Suwanton, O. Fabrication of chitosan/collagen/hydroxyapatite scaffolds with encapsulated *Cissus quadrangularis* extract. *Polym. Adv. Technol.* 2020, 31, 1496–1507.
- [109] Walczak, M.; Michalska-Sionkowska, M.; Kaczmarek, B.; Sionkowska, A. Surface and antibacterial properties of thin films based on collagen and thymol. *Mater. Today Commun.* 2020, 22, 100949.
- [110] Guo, R.; Lan, Y.; Xue, W.; Cheng, B.; Zhang, Y.; Wang, C.; Ramakrishna, S. Collagen-cellulose nanocrystal scaffolds containing curcumin-loaded microspheres on infected full-thickness burns repair. *J. Tissue Eng. Regen. Med.* 2017, 11, 3544–3555.
- [111] Govindarajan, D.; Durairandy, N.; Srivatsan, K.V.; Lakra, R.; Korapatti, P.S.; Jayavel, R.; Kiran, M.S. Fabrication of hybrid collagen aerogels reinforced with wheat grass bioactives as instructive scaffolds for collagen turnover and angiogenesis for wound healing applications. *ACS Appl. Mater. Interfaces* 2017, 9, 16939–16950.
- [112] Derakhshan, M.A.; Nazeri, N.; Khoshnevisan, K.; Heshmat, R.; Omidfar, K. Three-layered PCL-collagen nanofibers containing melilotus officinalis extract for diabetic ulcer healing in a rat model. *J. Diabetes Metab. Disord.* 2022, 21, 313–321.
- [113] Socrates, R.; Prymak, O.; Loza, K.; Sakthivel, N.; Rajaram, A.; Epple, M.; Kalkura, S.N. Biomimetic fabrication of mineralized composite films of nanosilver loaded native fibrillar collagen and chitosan. *Mater. Sci. Eng. C* 2019, 99, 357–366.

- [114] Craciunescu, O.; Seciu, A.-M.; Zarnescu, O. In vitro and in vivo evaluation of a biomimetic scaffold embedding silver nanoparticles for improved treatment of oral lesions. *Mater. Sci. Eng. C* 2021, 123, 112015.
- [115] Mudhafar, M.; Zainol, I.; Alsailawi, H.; Aiza Jaafar, C. Synthesis and characterization of fish scales of hydroxyapatite/collagen–silver nanoparticles composites for the applications of bone filler. *JKCerS* 2021, 59, 229–239.
- [116] Mandal, A.; Sekar, S.; Meera, K.M.S.; Mukherjee, A.; Sastry, T.P.; Mandal, A.B. Fabrication of collagen scaffolds impregnated with sago starch capped silver nanoparticles suitable for biomedical applications and their physicochemical studies. *Phys. Chem. Chem. Phys.* 2014, 16, 20175–20183.
- [117] Păunica-Panea, G.; Ficai, A.; Marin, M.M.; Marin, Ș.; Albu, M.G.; Constantin, V.D.; Dinu-Pîrvu, C.; Vuluga, Z.; Corobea, M.C.; Ghica, M.V. New collagen-dextran-zinc oxide composites for wound dressing. *J. Nanomater.* 2016, 2016, 34.
- [118] Neacsu, I.-A.; Melente, A.E.; Holban, A.-M.; Ficai, A.; Ditu, L.-M.; Kamerzan, C.-M.; TIHĂUAN, B.M.; Nicoara, A.I.; Bezirtzoglou, E.; CHIFIRIUC, C. Novel hydrogels based on collagen and ZnO nanoparticles with antibacterial activity for improved wound dressings. *Rom. Biotechnol. Lett.* 2019, 24, 317–323.
- [119] Albu, M.G.; Vladkova, T.G.; Ivanova, I.A.; Shalaby, A.S.; Moskova-Doumanova, V.S.; Staneva, A.D.; Dimitriev, Y.B.; Kostadinova, A.S.; Topouzova-Hristova, T.I. Preparation and biological activity of new collagen composites, part I: Collagen/zinc titanate nanocomposites. *Appl. Biochem. Biotechnol.* 2016, 180, 177–193.
- [120] Fan, X.; Chen, K.; He, X.; Li, N.; Huang, J.; Tang, K.; Li, Y.; Wang, F. Nano-TiO<sub>2</sub>/collagen-chitosan porous scaffold for wound repairing. *Int. J. Biol. Macromol.* 2016, 91, 15–22.
- [121] Tiplea, R.E.; Lemnaru, G.-M.; Trușcă, R.D.; Holban, A.; Kaya, M.G.A.; Dragu, L.D.; Ficai, D.; Ficai, A.; Bleotu, C. Antimicrobial films based on chitosan, collagen, and zno for skin tissue regeneration. *Biointerface Res. Appl. Chem* 2021, 11, 11985–11995.
- [122] Alfata, R.; Ramahdita, G.; Yuwono, A.H. The Effect of Additional Zinc Oxide to Antibacterial Property of Chitosan/Collagen-Based Scaffold. *Mater. Sci. Forum* 2020, 1000, 107–114.

- [123] Pasca, P.; Cavalu, S. The influence of propolis nanoparticles on dermal fibroblasts migration: Premises for development of propolis-based collagen dermal patches. *Dig. J. Nanomater. Biostructures*. 2021, 16, 929–938.
- [124] Jiménez, R.A.; Millán, D.; Suesca, E.; Sosnik, A.; Fontanilla, M.R. Controlled release of an extract of *Calendula officinalis* flowers from a system based on the incorporation of gelatin-collagen microparticles into collagen I scaffolds: Design and in vitro performance. *Drug Deliv. Transl. Res.* 2015, 5, 209–218.
- [125] Chen, Z.; Li, Y.; Dai, Y.; Zhou, Z.; Hu, Y.; Liu, H. Fabrication and Characterization of a Novel Berberine-oleanolic Acid Delivery Collagen I scaffold. *J. Phys. Conf. Ser.* 2020, 1637, 012105.
- [126] Laghezza Masci, V.; Taddei, A.R.; Courant, T.; Tezgel, O.; Navarro, F.; Giorgi, F.; Mariolle, D.; Fausto, A.M.; Texier, I. Characterization of collagen/lipid nanoparticle–curcumin cryostructures for wound healing applications. *Macromol. Biosci.* 2019, 19, 1800446.
- [127] Senthilkumar, C.; Kannan, P.R.; Balashanmugam, P.; Raghunandhakumar, S.; Sathiamurthi, P.; Sivakumar, S.; Arockiarajan, A.; Mary, S.A.; Madhan, B. Collagen-*Annona* polysaccharide scaffolds with tetrahydrocurcumin loaded microspheres for antimicrobial wound dressing. *Carbohydr. Polym. Technol. Appl.* 2022, 3, 100204.
- [128] Hasan, M.M.; Shahid, M.A. PVA, Licorice, and Collagen (PLC) Based Hybrid Bio-nano Scaffold for Wound Healing Application. *J. Biomater. Sci. Polym. Ed.* 2022, 1–15. <https://doi.org/10.1080/09205063.2022.2163454>.
- [129] Shaik, M.M.; Dapkekar, A.; Rajwade, J.M.; Jadhav, S.H.; Kowshik, M. Antioxidant-antibacterial containing bi-layer scaffolds as potential candidates for management of oxidative stress and infections in wound healing. *J. Mater. Sci. Mater. Med.* 2019, 30, 1–13.
- [130] Mitra, T.; Manna, P.J.; Raja, S.; Gnanamani, A.; Kundu, P. Curcumin loaded nano graphene oxide reinforced fish scale collagen—a 3D scaffold biomaterial for wound healing applications. *RSC Adv.* 2015, 5, 98653–98665.
- [131] Duraipandy, N.; Lakra, R.; Srivatsan, K.V.; Ramamoorthy, U.; Korrapati, P.S.; Kiran, M.S. Plumbagin caged silver nanoparticle stabilized collagen scaffold for wound dressing. *J. Mater. Chem. B* 2015, 3, 1415–1425.

- [132] Thapa, R.K.; Kiick, K.L.; Sullivan, M.O. Encapsulation of collagen mimetic peptide-tethered vancomycin liposomes in collagen-based scaffolds for infection control in wounds. *Acta Biomater.* 2020, 103, 115–128.
- [133] Nejaddehbashi, F.; Hashemitabar, M.; Bayati, V.; Abbaspour, M.; Moghimipour, E.; Orazizadeh, M. Application of polycaprolactone, chitosan, and collagen composite as a nanofibrous mat loaded with silver sulfadiazine and growth factors for wound dressing. *Artif. Organs* 2019, 43, 413–423.
- [134] He, Y.; Jin, Y.; Ying, X.; Wu, Q.; Yao, S.; Li, Y.; Liu, H.; Ma, G.; Wang, X. Development of an antimicrobial peptide-loaded mineralized collagen bone scaffold for infective bone defect repair. *Regen. Biomater.* 2020, 7, 515–525.
- [135] Antezana, P.E.; Municoy, S.; Pérez, C.J.; Desimone, M.F. Collagen Hydrogels Loaded with Silver Nanoparticles and Cannabis Sativa Oil. *Antibiotics* 2021, 10, 1420.
- [136] Srivatsan, K.V.; Duraipandy, N.; Begum, S.; Lakra, R.; Ramamurthy, U.; Korrapati, P.S.; Kiran, M.S. Effect of curcumin caged silver nanoparticle on collagen stabilization for biomedical applications. *Int. J. Biol. Macromol.* 2015, 75, 306–315.
- [137] Suchý, T.; Šupová, M.; Sauerová, P.; Kalbáčová, M.H.; Klapková, E.; Pokorný, M.; Horný, L.; Závora, J.; Ballay, R.; Denk, F. Evaluation of collagen/hydroxyapatite electrospun layers loaded with vancomycin, gentamicin and their combination: Comparison of release kinetics, antimicrobial activity and cytocompatibility. *Eur. J. Pharm. Biopharm.* 2019, 140, 50–59.
- [138] Muthukumar, T.; Prabu, P.; Ghosh, K.; Sastry, T.P. Fish scale collagen sponge incorporated with *Macrotyloma uniflorum* plant extract as a possible wound/burn dressing material. *Colloids Surf. B* 2014, 113, 207–212.
- [139] Ghorbani, M.; Nezhad-Mokhtari, P.; Ramazani, S. Aloe vera-loaded nanofibrous scaffold based on Zein/Polycaprolactone/Collagen for wound healing. *Int. J. Biol. Macromol.* 2020, 153, 921–930.
- [140] Uzunalan, G.; Ozturk, M.T.; Dincer, S.; Tuzlakoglu, K. A newly designed collagen-based bilayered scaffold for skin tissue regeneration. *J. Compos. Biodegrad. Polym.* 2013, 1, 8–15.
- [141] Pal, P.; Nguyen, Q.C.; Benton, A.H.; Marquart, M.E.; Janorkar, A.V. Drug-Loaded Elastin-Like Polypeptide–Collagen Hydrogels with High Modulus for Bone Tissue Engineering. *Macromol. Biosci.* 2019, 19, 1900142.

- [142] Tihan, G.T.; Rău, I.; Zgârian, R.G.; Ungureanu, C.; Barbaresso, R.C.; Kaya, M.G.A.; Dinu-Pîrvu, C.; Ghica, M.V. Oxytetracycline versus doxycycline collagen sponges designed as potential carrier supports in biomedical applications. *Pharmaceutics* 2019, 11, 363.
- [143] Daza, J.H.U.; Righetto, G.M.; Chaud, M.V.; da Conceição Amaro Martins, V.; Lopes Baratella da Cunha Camargo, I.; Maria de Guzzi Plepis, A. PVA/anionic collagen membranes as drug carriers of ciprofloxacin hydrochloride with sustained antibacterial activity and potential use in the treatment of ulcerative keratitis. *J. Biomater. Appl.* 2020, 35, 301–312.
- [144] Budhiraja, M.; Zafar, S.; Akhter, S.; Alrobaian, M.; Rashid, M.A.; Barkat, M.A.; Beg, S.; Ahmad, F.J. Mupirocin-loaded chitosan microspheres embedded in Piper betle extract containing collagen scaffold accelerate wound healing activity. *AAPS PharmSciTech* 2022, 23, 77.
- [145] Deaconu, M.; Prelipcean, A.-M.; Brezoiu, A.-M.; Mitran, R.-A.; Isopencu, G.; Matei, C.; Berger, D. Novel Collagen-Polyphenols-Loaded Silica Composites for Topical Application. *Pharmaceutics* 2023, 15, 312.

**Chapter 2: Screening of the antimicrobial and anti-biofilm  
activity of different essential oils**

**Sections of this chapter have been published in:**

*The assessment of antimicrobial and anti-biofilm activity of essential oils against Staphylococcus aureus strains, **Ersanli, C.**, Tzora, A., Skoufos, I., Fotou, K., Maloupa, E., Grigoriadou, K., Voidarou, C. and Zeugolis, D.I., Antibiotics, 12(2), 384, 2023.*

## 2.1. Introduction

Increased consumption and misuse of antimicrobial agents in both humans and animals [1,2] have caused the spread of antimicrobial resistance, which seriously threatens public and animal health [3]. Whereas infections due to antimicrobial resistance exhibited by bacteria can be adaptive, intrinsic, and acquired [4], multidrug-resistant bacteria (e.g., methicillin-resistant *Staphylococcus aureus*) cause infections that end up with longer hospitalization periods, remarkable morbidity, and mortality [3,5], as well as high healthcare costs. According to a report from the Organization of Economic Cooperation and Development (OECD), approximately 2.4 million people are expected to die due to this kind of infection in North America, Australia, and Europe over the next three decades, and treatment may cost up to USD 3.5 billion per year [6]. Among the bacteria that pose the greatest threat to world public health is methicillin-resistant *Staphylococcus aureus* (MRSA), where in particular, healthcare costs for a single specific serotype of *S. aureus*-caused infection reached almost EUR 9000 in Germany [7], and more than USD 18,000 in the U.S. [8].

In general, *S. aureus* is one of the major opportunistic human pathogens [9], which has the ability to escape the immune system and can give rise to diversified infections ranging from superficial skin wounds to life-threatening sepsis [10]. Among the wide variety of infections, *S. aureus* is a well-known bacteria associated with wound infections, which generally colonize the outermost layer of wounds [11]. In particular, *S. aureus*-caused wound infections may be evaluated as a potential risk factor for MRSA concern [12], which has brought about the development of alternative antimicrobials substituted for traditional antibiotics. Moreover, *S. aureus* (especially MRSA) has the ability to adhere to living or inert surfaces, secreting an extracellular polymeric substance of proteins, polysaccharides, nucleic acids, and water, known as a biofilm. Subsequently, the biofilm matrix acts as a physical barrier that prevents the permeability of the drug into the bacterial community and helps the microbe resist and minimize the effect of traditional antibiotics [13]. These challenges have given rise to a significant interest in the scientific community in developing herbal-based therapeutics with antimicrobial activity (e.g., essential oils) as a safer, green alternative to antibiotics [14].

Essential oils (EOs) are colored, aroma-rich, complex hydrophobic liquids [15], also known as volatile oils [16]. They are defined as the secondary metabolic product of aromatic plants [17] and

are found in the various parts of plants such as flowers, roots, barks, stems, leaves, and seeds [18]. EOs are potent agents to diminish antimicrobial resistance [19] due to their significant therapeutic properties (i.e., antibacterial, antiseptic, and antioxidant activities) [20,21]. For this reason, EOs from pharmaceutical plants have also been examined as potent antimicrobial agents in animal production systems [22]. The antimicrobial activity of EOs does not only stem from their qualitative chemical composition, but also from the quantitative intensity of every single component that is included in the structure, as well as all plant-based products [23]. Their complex structure is mainly composed of terpenes (generally monoterpenes and sesquiterpenes) and terpenoids [24]. Even though some of these chemicals are water soluble, most of them are hydrophobic, so EOs are defined as hydrophobic [25,26].

Hydrophobicity is one of the most important features of an EO [16], enabling them to penetrate through the phospholipid-bilayer bacterial cell membrane after attaching to the cell surface [27]. As a consequence of the accumulation of EOs, the structure of the cell membrane may be destroyed, which results in an unfavorable change in the cell metabolism and causes the death of the cell [28]. It is also worth mentioning that the mechanism of action of EOs on the inhibition of bacterial growth is attributed to a series of reactions detrimental to bacterial cells that are defined as EO versatility [29]. EOs also exert anti-biofilm activity owing to both hydrophobic and hydrophilic moieties in their composition [30]. Accordingly, the hydrophobic components of EOs permeate the lipid sub-stances of the cell membrane to diminish biofilm formation, while the hydrophilic ones diffuse through the exopolysaccharide matrix of the biofilm [31].

In this chapter, EOs of *Thymus sibthorpii*, *Origanum vulgare*, *Salvia fruticosa*, and *Crithmum maritimum* plants were chosen as the potential antimicrobial agents against various *S. aureus* strains to combat the antimicrobial resistance problem. All these species have already been used for traditional medications. Essential oils extracted from *Thymus* species are extensively used for pharmaceutical and cosmetic purposes with their various biological activities (e.g., antimicrobial and antioxidant activities) [32]. *Origanum vulgare* has been evaluated in preclinical studies for a long time thanks to its anti-inflammatory, antimicrobial, antioxidant, and anti-cancer properties [33]. EO of the *Salvia fruticosa* plant, which is one of the thousand species of the *Salvia* genus, is a traditional remedy for intestinal problems, epidermal problems, and gingivitis since ancient times

[34,35]. *Crithmum maritimum* has not only been preferred for culinary purposes but has also been used for pharmaceutical and cosmetic reasons [36].

Thus, the chemical composition and the antimicrobial and anti-biofilm activity of *Thymus sibthorpii*, *Origanum vulgare*, *Salvia fruticosa*, and *Crithmum maritimum* EOs, extracted from freshly collected plants, were examined to identify potential antimicrobial and anti-biofilm agents (**Figure 2.1**). All EOs were tested against wild-type methicillin-sensitive and methicillin-resistant *S. aureus*, as well *S. aureus* ATCC 29213, bacteria, which have different antimicrobial resistance profiles. We hypothesized that if methicillin-sensitive and -resistant *S. aureus* strains do not differ in EO susceptibility, the selected EOs can be evaluated as alternative and safe players to combat the antimicrobial resistance problem. We strongly believe that with the present study, we filled this gap and made an important proposal since *S. aureus* is a reference species in the frontline of the resistance to antibiotics inquiry.

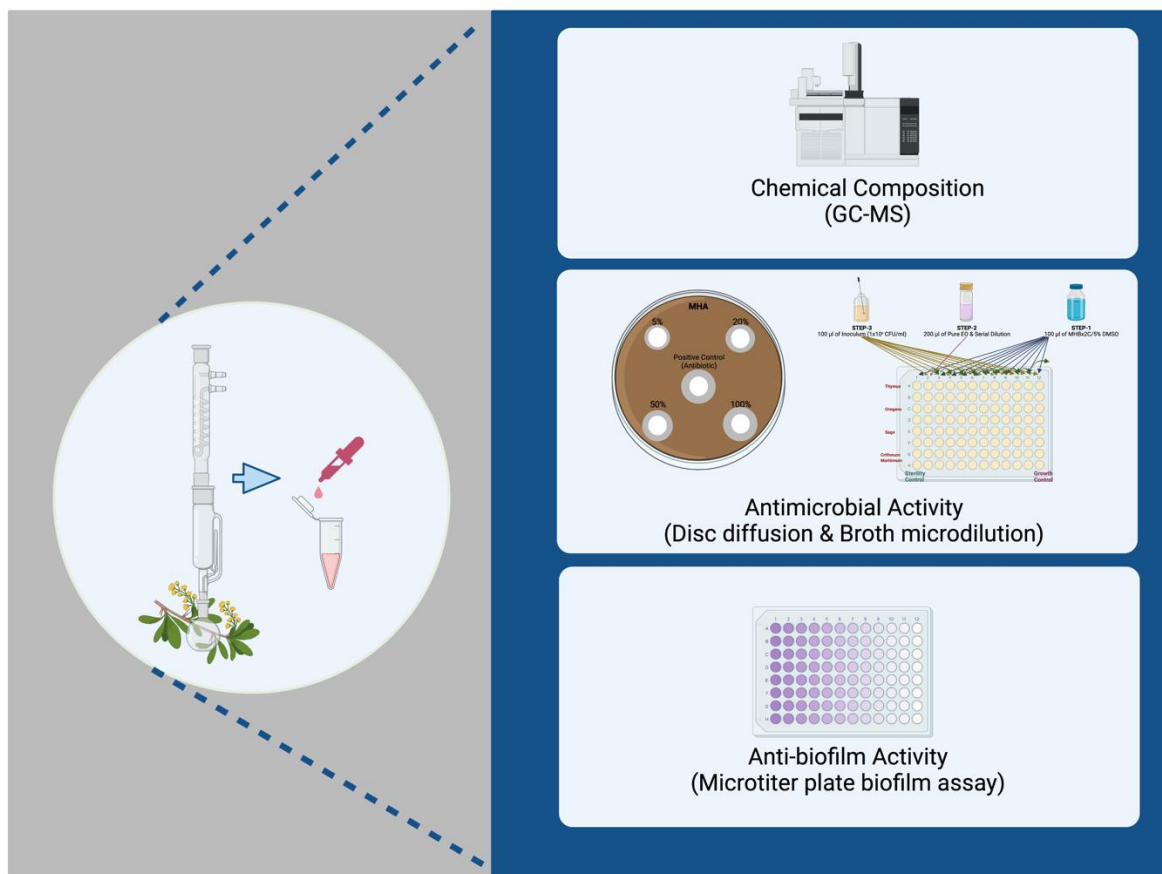


**Figure 2.1.** Experimental summary of chapter 2.

## 2.2. Materials and methods

### 2.2.1. Plant material and extraction of essential oils

Aerial parts from *Thymus sibthorpii*, *Origanum vulgare* sbsp. *hirtum*, *Salvia fruticosa*, and *Crithmum maritimum* were collected during the flowering season in 2021 from the experimental farm of the Laboratory for Protection and Evaluation of Native species of the Institute of Plant Breeding and Genetic Resources (IPB&GR), preserved in Thessaloniki, Greece. The biomass was dried under ambient temperature in shade and subjected to distillation for 1.5 h for *Origanum vulgare* sbsp. *hirtum* and 1 h for the three other species, using a 50 L pilot-scale steam distillatory unit under steam pressure of 1.2 atm. The essential oils were collected and separated in a Florentine flask, dried over anhydrous sodium sulfate, and stored at 4–6 °C until further analysis [37]. Living mother plants and herbarium specimens of the species used for the production of EOs for experimentation are maintained at the collection of the Balkan Botanic Garden of Kroussia, Institute of Plant Breeding and Genetic Resources, Hellenic Agricultural Organization (ELGO)—DIMITRA, with the following unique IPEN (International Plant Exchange Network) accession numbers: *Thymus sibthorpii* GR-1-BBGK-01,1796, *Origanum vulgare* sbsp. *hirtum* GR-1-BBGK-03,2107, *Salvia fruticosa* GR-1-BBGK-04,2411, and *Crithmum maritimum* GR-1-BBGK-97,719. The specific density of each fresh EO was measured by using a 10 mL pycnometer at 25 °C [38].

### 2.2.2. Identification of the chemical composition of essential oils

The essential oils were analyzed by gas chromatography–mass spectroscopy (GC-MS) on a capillary HP-5MS column (Agilent, Santa Clara, CA, USA), using a gas chromatograph 17A Ver. 3 interfaced with a mass spectrometer Shimadzu QP-5050A supported by the GC/MS Solution Ver. 1.21 software, using the method described previously [39]. The conditions of analysis were as follows: injection temperature, 260 °C; interface heating, 300 °C; ion source heating, 200 °C; EI mode, 70 eV; scan range, 41–450 amu; and scan time, 0.50 s. Oven temperature programs: (a) 55–120 °C (3 °C/min), 120–200 °C (4 °C/min), 200–220 °C (6 °C/min), and 220 °C for 5 min; and (b) 60–240 °C at 3 °C/min; carrier gas He, 54.8 kPa, split ratio 1:30. The relative content of each compound was calculated as percent of the total chromatographic area. The identification of the compounds was based on a comparison of their retention indices (RI) relative to n-alkanes (C7-

C22) with corresponding literature data, and by matching their spectra with those of MS libraries (NIST 98, Wiley, Hoboken, NJ, USA) [40].

### 2.2.3. Antimicrobial susceptibility test and bacterial strains

The antimicrobial activity of *Thymus sibthorpii*, *Origanum vulgare*, *Salvia fruticosa*, and *Crithmum maritimum* EOs were screened against MSSA, MRSA, and *S. aureus* ATCC 29213 by the Kirby–Bauer disc diffusion and broth microdilution methods. The modified microtiter plate biofilm assay was also performed to assess the biofilm formation ability of tested strains, and the anti-biofilm activity of EOs, as well as reference antimicrobials. *Staphylococcus epidermidis* (*S. epidermidis*) ATCC 12228 and *S. epidermidis* 35984 were used as negative and positive quality control strains, respectively, for this bioassay. The wild-type MSSA and MRSA were previously derived from goat milk in our laboratory [41], and the other strains were purchased from American Type Culture Collection (ATCC).

#### 2.2.3.1. Antimicrobial activity

##### *Disc diffusion method*

The CLSI M02-A11 document [42] was followed for the disc diffusion test, as schematically described in **Figure 2.2 (a)**. Penicillin, enrofloxacin, gentamicin sulfate, tetracycline hydrochloride, and cefaclor (Oxoid, Hampshire, UK) were examined as reference antimicrobials. Briefly, the bacterial cells were grown in blood agar media overnight at 37 °C. Then, the inoculum was prepared in a sterile saline solution (bioMérieux, Marcy-l'Étoile, France) by adjusting the McFarland unit to 0.5 ( $\sim 1 \times 10^8$  CFU/mL) with fresh colonies. Afterward, the prepared inoculum was immediately spread out on dried Mueller–Hinton agar (Oxoid, Hampshire, UK) plates. The 6 mm diameter sterile Whatman paper N.1 discs were placed with 5, 20, 50, and 100% (v/v) of each EO diluted in 5% (v/v) dimethyl sulfoxide, DMSO (Honeywell, Charlotte, NC, USA), as well commercial antibiotic discs. EOs on paper discs were air-dried for half an hour, and plates were incubated at 37 °C overnight. At the end of the incubation period, images of each plate were taken, and inhibition zone diameters were evaluated using ImageJ software (version 2.0.0) by measuring the zone diameter of each disc a minimum of ten times from different points. Each condition was tested with three independent experiments.

***The modified broth microdilution method***

The broth microdilution method was studied according to the CLSI M07-Ed11 document with slight modifications [43] to assess the minimum inhibitory concentration (MIC) of each EO and the reference antimicrobials (gentamicin sulfate, tetracycline hydrochloride, and cefaclor). We used 5% (v/v) DMSO diluted in double-strength Mueller–Hinton broth (Fluka-Honeywell, Charlotte, NC, USA) as growth media for cells. Firstly, cells were grown on blood agar (Fluka-Honeywell, US) media and adjusted to a final concentration of  $5 \times 10^5$  CFU/mL utilizing sterile saline solution to prepare the inoculum. In a related row of 96-well plates, the first and last wells were defined as sterility and growth control, respectively. Serial dilution was performed by transferring 100  $\mu$ L of well-mixed EO suspension to the other, and 100  $\mu$ L of freshly prepared inoculum was added to the wells, except for the sterility control group. The concentration range was between 100% and 0.0488% (v/v) for EOs and between 128 and 0.000488  $\mu$ g/mL for reference antibiotics. The 96-well plates were incubated in a horizontally shaking incubator at 37 °C and 75 rpm for 20 h, then re-incubated for 2 h after 1% (w/v) triphenyl tetrazolium chloride, TTC (Merk, Rahway, New Jersey, US), Gram stain transferring to each well. The red color indicated the living cells in the relevant well, and MIC was recorded as the concentration of the well just before the first red-colored well. Each test was repeated by three independent experiments. The experimental procedure is schematically described in **Figure 2.2 (b)**.

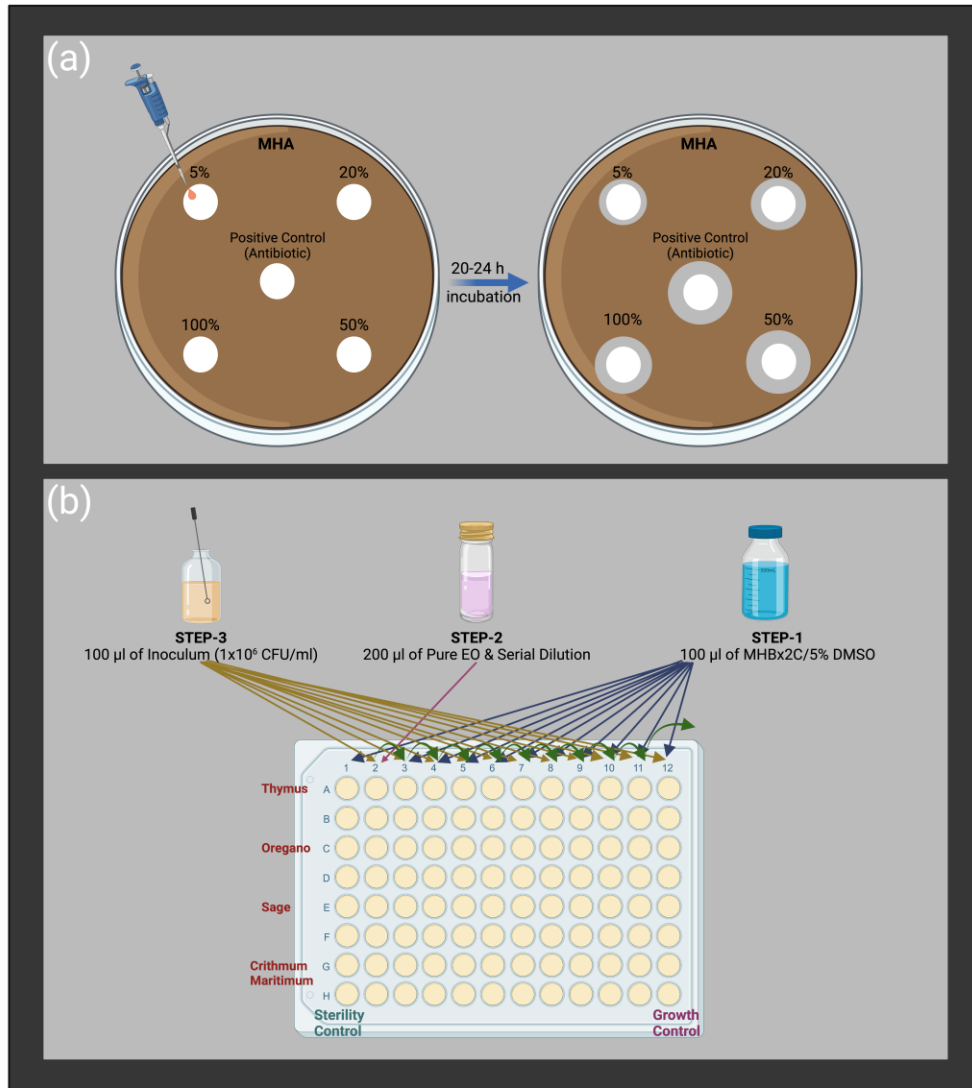


**Figure 2.2.** Schematic illustration of the experimental procedure of (a) disc diffusion and (b) broth microdilution methods.

### 2.2.3.2. Anti-biofilm activity

#### *Modified microtiter plate biofilm formation assay*

The biofilm formation ability of three *S. aureus* strains and the anti-biofilm activity of EOs and reference antimicrobials were assessed by microtiter plate biofilm formation assay [44,45] with some modifications. A flat-bottom 96-well microtiter plate (Sarstedt, Nümbrecht, Germany) was utilized for the analysis.

We mixed 100  $\mu\text{L}$  of tryptic soy broth (Millipore Sigma, Burlington, UK) supplemented with 1% (w/v) glucose (TSBG) with 100  $\mu\text{L}$  of inoculum, which was adjusted to a final concentration of  $5 \times 10^5$  CFU/mL, with fresh colonies grown on blood agar overnight at 37 °C by utilizing sterile saline solution. We used 100  $\mu\text{L}$  of adjusted concentration of EO instead of TSBG to screen the anti-biofilm activity of antimicrobials. Then, plates were incubated at 37 °C for 20–24 h without agitation, which allows the cells to adhere to the surface of the well, followed by dumping out the cells by turning the plate over. Afterward, wells were washed with 250  $\mu\text{L}$  of sterile water twice to remove planktonic bacteria, and the attached cells were fixed with 200  $\mu\text{L}$  of pure methanol (Honeywell, Charlotte, NC, USA) for 15 min. Next, fixed cells were stained with 200  $\mu\text{L}$  of 0.4% (w/v) gentian violet, also called crystal violet (Sigma-Aldrich, Dorset, UK) for 5 min, and the excess stain was rinsed off by placing the plates under gently running tap water. Stained cells in air-dried plates were resolubilized by 160  $\mu\text{L}$  of 33% (v/v) glacial acetic acid (Honeywell, Charlotte, NC, USA). Each well was mixed thoroughly to ensure re-solubilization of the attached cells; then, 100  $\mu\text{L}$  of suspension was transferred to a new sterile plate, and the optical density (OD) was read at 630 nm. The biofilm inhibition percentage of each antimicrobial was evaluated as shown in the following equation. Three independent experiments were performed for each treatment.

$$\text{Biofilm Inhibition \%} = \left[ \frac{\text{OD}_{\text{Positive Control}} - \text{OD}_{\text{Experimental}}}{\text{OD}_{\text{Positive Control}}} \right] \times 100$$

#### **2.2.4. Statistical analysis**

Antimicrobial analyses were carried out with three independent experiments for each treatment. The data were presented as the mean  $\pm$  standard deviation and subjected to the one-way analysis of variance (ANOVA) followed by Tukey's HSD (honestly significant difference) test at  $p < 0.05$ . All statistical analyses were performed in SPSS Statistics 20 (IBM SPSS Statistics, Version 20.0. Armonk, NY, USA, IBM Corp).

### 2.3. Results

The chemical composition of EOs was examined by GC-MS on a capillary column, and results are listed in **Table 2.1** by their percentage of total presence. Twenty-eight, twenty-seven, thirty, and twenty-four compounds were identified in the *Thymus sibthorpii*, *Origanum vulgare*, *Salvia fruticosa*, and *Crithmum maritimum* EOs, respectively. The main chemical classes for EOs were monoterpene hydrocarbons, oxygenated monoterpenes, sesquiterpenes, and small amounts of alcohol, acetone, and quinone.

Carvacrol was detected as the major compound in *Thymus sibthorpii* and *Origanum vulgare* EOs with 52.62 and 78.72% of presence, while 1,8-cineol (39.70%) and  $\beta$ -phellandrene (28.01%) were the major substances in *Salvia fruticosa* and *Crithmum maritimum* EOs, respectively. Furthermore, the specific density of *Thymus sibthorpii*, *Origanum vulgare*, *Salvia fruticosa*, and *Crithmum maritimum* EOs was measured as 0.931, 0.932, 0.913, and 0.903 g/mL, respectively.

**Table 2.1.** The essential oil composition of *Thymus sibthorpii*, *Origanum vulgare*, *Salvia fruticosa*, and *Crithmum maritimum* isolated during the flowering period, including the percentage of components and the experimental (RI) and literature-based (RIL) retention indices.

<i>Thymus sibthorpii</i>				<i>Origanum vulgare</i>				<i>Salvia fruticosa</i>				<i>Crithmum maritimum</i>			
Compound	RI	RIL	%	Compound	RI	RIL	%	Compound	RI	RIL	%	Compound	RI	RIL	%
Carvacrol	1309	1298	52.62	Carvacrol	1309	1298	78.72	1,8-cineol	1036	1033	39.70	$\beta$ -phellandrene	1034	1031	28.01
<i>p</i> -cymene	1029	1026	18.75	<i>p</i> -cymene	1029	1026	8.19	Camphor	1150	1143	12.39	Sabinene	975	976	20.96
Thymoquinone	1247	1249	6.71	$\gamma$ -terpinene	1061	1062	2.11	$\beta$ -thujone	1116	1114	7.54	$\gamma$ -terpinene	1061	1062	18.69
$\beta$ -caryophyllene	1413	1418	3.70	Myrcene	991	991	1.64	$\alpha$ -pinene	936	939	7.03	1,8-cineol	1036	1033	9.53
Thymol	1295	1290	2.15	$\beta$ -caryophyllene	1413	1418	1.27	$\alpha$ -terpinyl acetate	1345	1346	6.72	Thymol methyl ether	1236	1235	4.07
Carvacrol methyl ether	1242	1244	1.98	$\alpha$ -terpinene	1020	1018	1.01	<i>p</i> -cymene	1029	1026	4.31	cis- $\beta$ -ocimene	1040	1040	3.68
cis-sabinene hydrate	1062	1065	1.85	$\alpha$ -pinene	936	939	0.98	Camphene	953	953	4.11	<i>p</i> -cymene	1029	1026	3.55
$\beta$ -bisabolene	1507	1509	1.74	cis-sabinene hydrate	1062	1065	0.62	3-octanone	988	986	3.26	Terpinen-4-ol	1183	1177	2.66
Thymoquinone	1558	1553	1.36	Terpinen-4-ol	1183	1177	0.55	$\beta$ -pinene	980	980	2.35	$\alpha$ -pinene	936	939	2.42
Caryophyllene oxide	1593	1581	1.03	$\alpha$ -thujene	929	931	0.48	Limonene	1032	1031	2.27	$\alpha$ -terpinene	1020	1018	1.64
$\alpha$ -thujene	929	931	0.86	Borneol	1175	1165	0.42	$\alpha$ -terpineol	1187	1189	2.00	Myrcene	991	991	1.44
$\alpha$ -terpinene	1020	1018	0.74	1-octen-3-ol	985	978	0.38	$\alpha$ -thujone	1105	1102	1.27	$\alpha$ -terpinolene	1086	1088	0.91
1,8-cineol	1036	1033	0.57	$\alpha$ -humulene	1452	1452	0.30	Borneol	1175	1165	0.80	$\alpha$ -thujene	929	931	0.48
$\alpha$ -humulene	1452	1452	0.42	Thymol	1295	1290	0.28	$\beta$ -caryophyllene	1420	1418	0.74	$\alpha$ -phellandrene	1008	1005	0.44
$\alpha$ -pinene	936	939	0.36	Limonene	1032	1031	0.27	Terpinen-4-ol	1183	1177	0.64	trans- $\beta$ -ocimene	1050	1050	0.24

trans-sabinene hydrate	1103	1098	0.32	Camphene	953	953	0.25	Linalyl acetate	1257	1257	0.52	Allo-ocimene	1132	1129	0.23
Terpinen-4-ol	1183	1177	0.29	Caryophyllene oxide	1593	1581	0.24	$\delta$ -terpineol	1161	1162	0.47	$\beta$ -pinene	980	980	0.20
Limonene	1032	1031	0.27	$\beta$ -phellandrene	1034	1031	0.23	trans-pinocamphone	1159	1160	0.32	Bicyclgermacrene	1492	1494	0.14
1-octen-3-ol	985	978	0.22	$\alpha$ -phellandrene	1008	1005	0.18	Linalool	1104	1098	0.31	cis-2- <i>p</i> -menthen-1-ol	1120	1117	0.11
$\beta$ -pinene	980	980	0.17	$\beta$ -pinene	980	980	0.16	Caryophyllene oxide	1593	1581	0.18	$\alpha$ -terpineol	1187	1189	0.08
$\beta$ -phellandrene	1034	1031	0.16	$\alpha$ -terpinolene	1086	1088	0.15	Viridiflorol	1590	1590	0.18	$\beta$ -caryophyllene	1420	1418	0.08
trans- $\beta$ -farnesene	1456	1458	0.12	$\delta$ -cadinene	1517	1524	0.13	Tricyclene	925	926	0.13	Camphene	953	953	0.07
Germacrene D	1478	1480	0.11	$\delta$ -3-carene	1010	1011	0.10	$\alpha$ -thujene	929	931	0.13	cis-sabinene hydrate	1062	1065	0.07
$\delta$ -cadinene	1517	1524	0.11	trans- $\beta$ -farnesene	1456	1458	0.10	Aromadendrene	1434	1419	0.11	Caryophyllene oxide	1593	1581	0.02
Borneol	1175	1165	0.07	$\beta$ -bisabolene	1507	1509	0.10	Viridiflorene	1491	1493	0.08				
Camphene	953	953	0.06	Germacrene D	1478	1480	0.08	cis-sabinene hydrate	1062	1065	0.07				
$\delta$ -3-carene	1010	1011	0.05	1,8-cineol	1036	1033	0.07	$\alpha$ -terpinene	1020	1018	0.06				
Spathulenol	1580	1576	0.05					1-octen-3-ol	985	978	0.05				
								$\gamma$ -terpinene	1061	1062	0.05				
								$\beta$ -bisabolene	1507	1509	0.05				

Following the disc diffusion test, the inhibition zone diameters of varying concentrations of EOs and reference antibiotics are presented in **Table 2.2**. Among all tested antimicrobials, *Thymus sibthorpii* was found to be the strongest EO on all strains. **Figure 2.3** shows the inhibition zone of each antimicrobial on each strain qualitatively. It can easily be seen that *Thymus sibthorpii* caused full inhibition on Mueller–Hinton agar plates for all microbial strains.

**Table 2.2** demonstrates the MIC of the EOs, and reference antimicrobials used on *S. aureus* strains. *Thymus sibthorpii* showed the lowest MIC for MSSA, whereas it has the same MIC as *Origanum vulgare* on MRSA and *S. aureus* ATCC 29213 strains. Contrary to this, the remaining EOs could not show lower MIC against all strains.

**Table 2.2.** Inhibition zone diameter and minimum inhibition concentration of essential oils and reference antibiotics on treating microorganisms. A 6 mm inhibition zone diameter indicates no activity, and ND means not determined. Each value represents the mean of triplicate experiments with standard deviations. Different superscripts (a-m) in the row differ significantly for each strain (Tukey,  $p < 0.05$ ).

Treatment	Disc content	Methicillin-Sensitive <i>S. aureus</i>		Methicillin-Resistant <i>S. aureus</i>		<i>S. aureus</i> ATCC 29213	
		Zone Diameter (mm)	MIC (mg/mL)	Zone Diameter (mm)	MIC (mg/mL)	Zone Diameter (mm)	MIC (mg/mL)
<i>Thymus sibthorpii</i>	5%	13.968 ± 0.679 <sup>c,d</sup>	0.091	15.527 ± 0.698 <sup>b</sup>	0.091	32.415 ± 1.992 <sup>g</sup>	0.091
	20%	61.645 ± 1.923 <sup>k</sup>		68.970 ± 4.667 <sup>d</sup>		60.908 ± 0.298 <sup>h</sup>	
	50%	70.765 ± 6.283 <sup>l</sup>		68.983 ± 2.340 <sup>d</sup>		61.380 ± 0.490 <sup>h</sup>	
	100%	78.913 ± 2.897 <sup>m</sup>		70.128 ± 5.797 <sup>d</sup>		69.353 ± 2.581 <sup>i</sup>	
<i>Origanum vulgare</i>	5%	7.039 ± 0.388 <sup>a,b</sup>	0.182	6.310 ± 0.046 <sup>a</sup>	0.091	6.000 ± 0.000 <sup>a</sup>	0.091
	20%	17.811 ± 0.342 <sup>d,e</sup>		14.005 ± 0.260 <sup>b</sup>		11.137 ± 0.093 <sup>c</sup>	
	50%	24.960 ± 0.149 <sup>f,g</sup>		22.778 ± 0.293 <sup>c</sup>		17.122 ± 0.171 <sup>d</sup>	
	100%	25.089 ± 0.253 <sup>f,g</sup>		23.569 ± 0.318 <sup>c</sup>		17.552 ± 0.080 <sup>d</sup>	
<i>Salvia fruticosa</i>	5%	6.000 ± 0.000 <sup>a</sup>	2.853	6.000 ± 0.000 <sup>a</sup>	2.853	6.000 ± 0.000 <sup>a</sup>	2.853
	20%	13.643 ± 0.494 <sup>c,d</sup>		6.000 ± 0.000 <sup>a</sup>		6.000 ± 0.000 <sup>a</sup>	
	50%	14.289 ± 0.534 <sup>c,d</sup>		8.213 ± 0.249 <sup>a</sup>		7.149 ± 0.103 <sup>a,b</sup>	
	100%	17.464 ± 0.253 <sup>d,e</sup>		11.184 ± 0.209 <sup>a,b</sup>		9.399 ± 0.148 <sup>b,c</sup>	
<i>Crithmum maritimum</i>	5%	6.000 ± 0.000 <sup>a</sup>	5.644	6.000 ± 0.000 <sup>a</sup>	5.644	6.000 ± 0.000 <sup>a</sup>	5.644
	20%	6.000 ± 0.000 <sup>a</sup>		6.000 ± 0.000 <sup>a</sup>		6.000 ± 0.000 <sup>a</sup>	
	50%	9.407 ± 0.138 <sup>a,b,c</sup>		6.471 ± 0.066 <sup>a</sup>		7.011 ± 0.164 <sup>a</sup>	
	100%	11.128 ± 0.201 <sup>b,c</sup>		7.689 ± 0.236 <sup>a</sup>		7.527 ± 0.133 <sup>a,b</sup>	
Gentamicin	10 µg	30.348 ± 0.149 <sup>h</sup>	0.00025	22.914 ± 0.134 <sup>c</sup>	0.0005	20.948 ± 0.022 <sup>e</sup>	0.00025
Tetracycline	30 µg	41.125 ± 0.220 <sup>j</sup>	0.002	10.426 ± 0.187 <sup>a,b</sup>	0.032	26.897 ± 0.188 <sup>f</sup>	0.001
Cefaclor	30 µg	28.120 ± 0.052 <sup>g,h</sup>	0.002	6.693 ± 0.097 <sup>a</sup>	0.016	20.826 ± 0.048 <sup>e</sup>	0.002
Penicillin	10 units	22.355 ± 0.129 <sup>e</sup>	ND	8.476 ± 0.038 <sup>a</sup>	ND	18.719 ± 0.113 <sup>d,e</sup>	ND
Enrofloxacin	5 µg	36.118 ± 0.091 <sup>i</sup>	ND	25.059 ± 0.091 <sup>c</sup>	ND	24.690 ± 0.132 <sup>f</sup>	ND

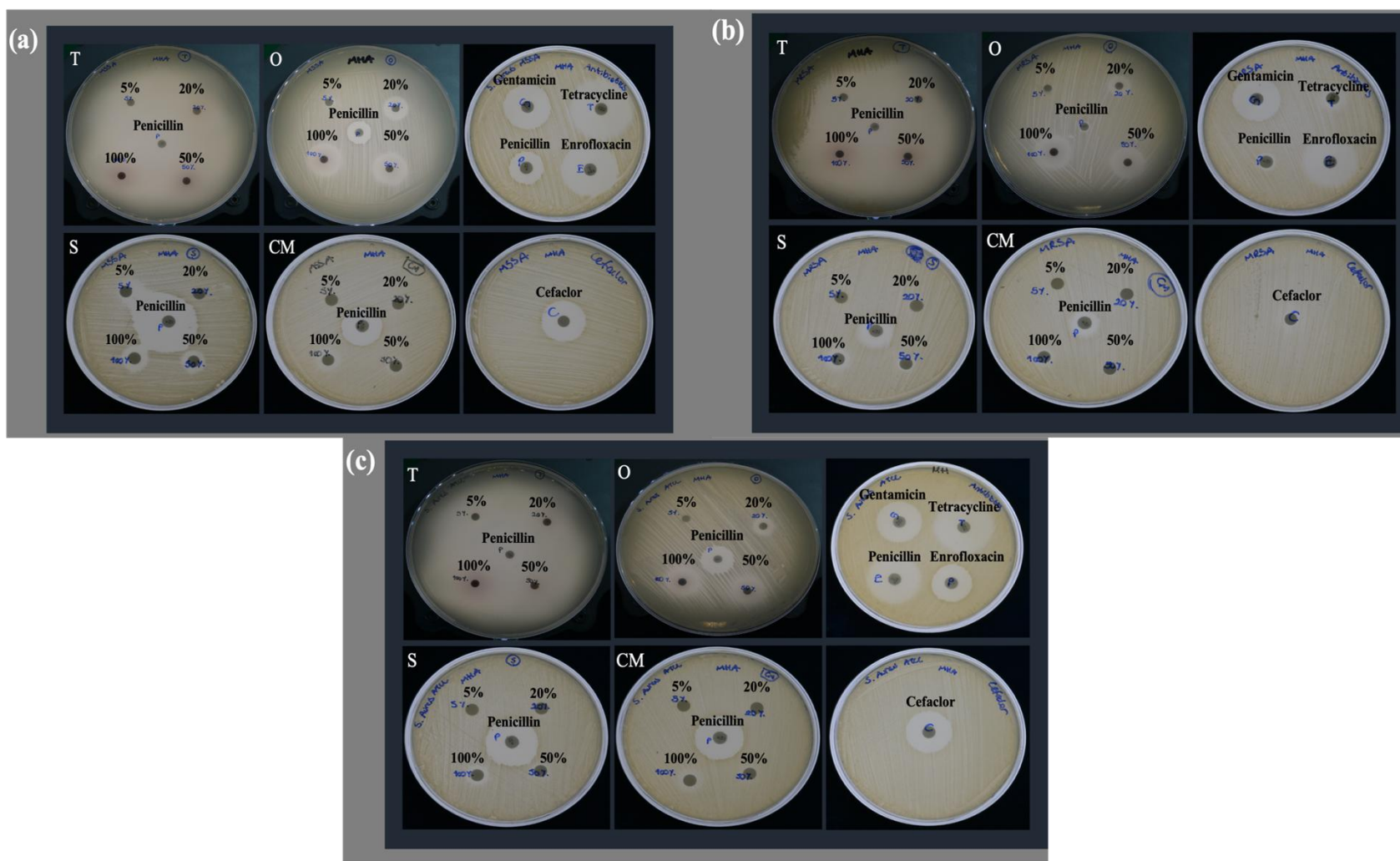


**Figure 2.3.** Qualitative illustration of inhibition zone diameters arising from testing EOs with different concentrations and reference antibiotics against (a) MSSA, (b) MRSA, and (c) *S. aureus* ATCC 29213.

In the scope of the assessment of the inhibitory effect of antimicrobials on the biofilm formed by *S. aureus* cells, the biofilm formation capacity of these strains was examined. **Figure 2.4** illustrates a comparison of the optical density of strains at 630 nm by modified microtiter plate biofilm formation assay. According to the results, while *S. epidermidis* ATCC 35984 showed the highest biofilm formation as expected, all tested *S. aureus* strains significantly produced biofilm.

All tested EOs inhibited the biofilm formed by *S. aureus* cells by about 95%, even at their half MIC. Gentamicin sulfate, which is the commonly used antimicrobial in the formulation of commercial antimicrobial and/or wound dressing products, could not show sufficient anti-biofilm activity at its MIC on testing strains (**Table 2.3**).

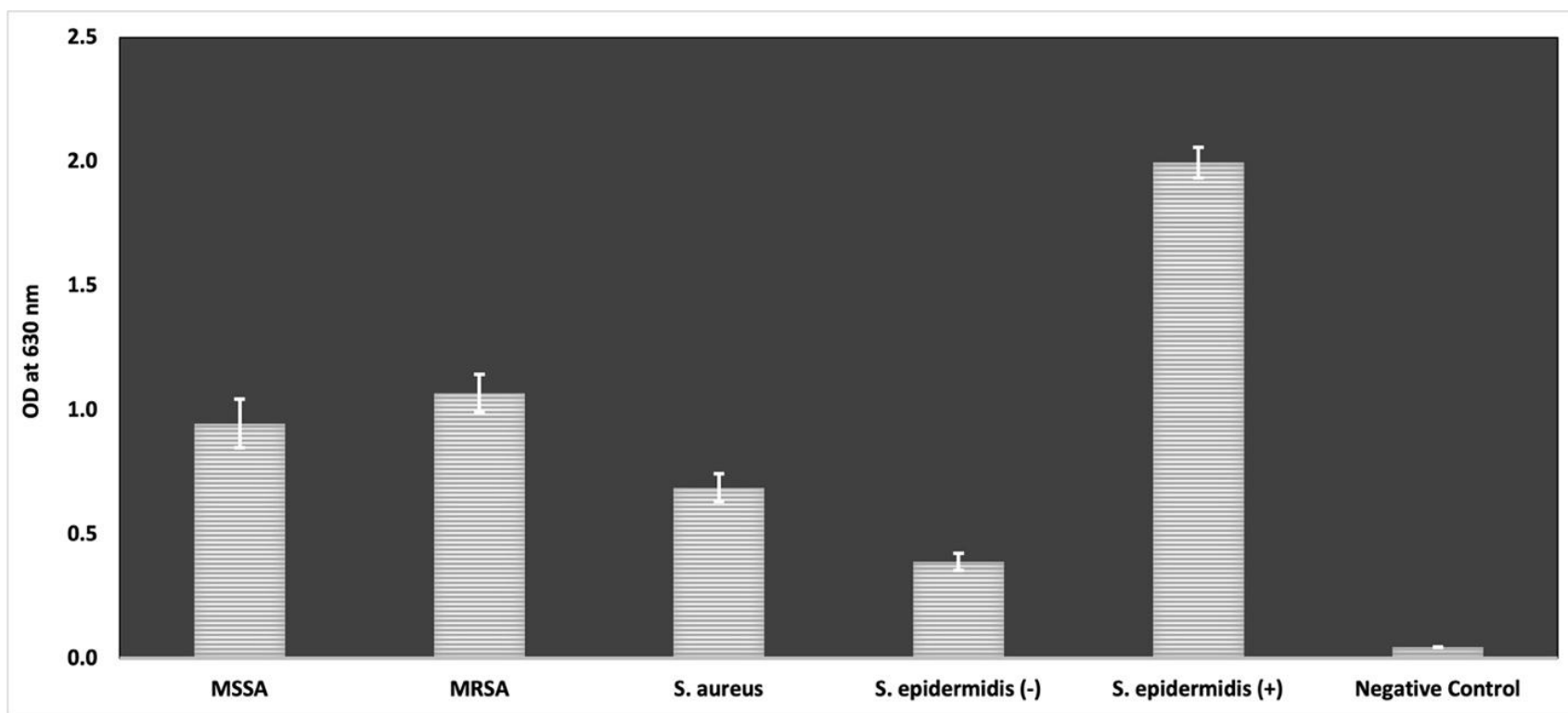


**Figure 2.4.** Comparison of biofilm formation ability of MSSA, MRSA, *S. aureus* ATCC 29213 (*S. aureus*), *S. epidermidis* ATCC 12228 (*S. epidermidis* (-)), and *S. epidermidis* ATCC 35984 (*S. epidermidis* (+)) regarding their OD values with negative control (TSBG medium only). Each value represents the mean of triplicate experiments with standard deviations (Tukey,  $p < 0.05$ ).

**Table 2.3.** Biofilm formation inhibition percentages of different concentrations of essential oils and different concentrations of reference antibiotics on treating microorganisms. Each value represents the mean of triplicate experiments with standard deviations. Different superscripts (a-c) in the row differ significantly for each strain (Tukey,  $p < 0.05$ ).

Treatment	Concentration	Methicillin-Sensitive <i>S. aureus</i>	Methicillin-Resistant <i>S. aureus</i>	<i>S. aureus</i> ATCC 29213
<i>Thymus sibthorpii</i>	x4 MIC	95.134 ± 0.053 <sup>c</sup>	95.817 ± 0.097 <sup>c</sup>	93.528 ± 0.073 <sup>b</sup>
	x2 MIC	95.293 ± 0.053 <sup>c</sup>	95.817 ± 0.097 <sup>c</sup>	93.577 ± 0.042 <sup>b</sup>
	MIC	95.275 ± 0.061 <sup>c</sup>	95.786 ± 0.081 <sup>c</sup>	93.359 ± 0.042 <sup>b</sup>
	x1/2 MIC	95.364 ± 0.081 <sup>c</sup>	95.364 ± 0.609 <sup>c</sup>	93.577 ± 0.042 <sup>b</sup>
<i>Origanum vulgare</i>	x4 MIC	94.306 ± 0.239 <sup>c</sup>	95.786 ± 0.047 <sup>c</sup>	93.528 ± 0.126 <sup>b</sup>
	x2 MIC	95.170 ± 0.214 <sup>c</sup>	95.770 ± 0.054 <sup>c</sup>	93.455 ± 0.073 <sup>b</sup>
	MIC	95.205 ± 0.110 <sup>c</sup>	95.708 ± 0.027 <sup>c</sup>	93.334 ± 0.183 <sup>b</sup>
	x1/2 MIC	94.993 ± 0.152 <sup>c</sup>	93.772 ± 1.001 <sup>c</sup>	93.068 ± 0.373 <sup>b</sup>
<i>Salvia fruticosa</i>	x2 MIC	94.253 ± 0.583 <sup>c</sup>	95.380 ± 0.311 <sup>c</sup>	93.140 ± 0.414 <sup>b</sup>
	MIC	94.905 ± 0.186 <sup>c</sup>	95.427 ± 0.027 <sup>c</sup>	93.189 ± 0.168 <sup>b</sup>
	x1/2 MIC	85.985 ± 12.555 <sup>c</sup>	95.068 ± 0.241 <sup>c</sup>	93.262 ± 0.374 <sup>b</sup>
<i>Crithmum maritimum</i>	x2 MIC	95.081 ± 0.242 <sup>c</sup>	95.583 ± 0.241 <sup>c</sup>	93.043 ± 0.484 <sup>b</sup>
	MIC	94.658 ± 0.692 <sup>c</sup>	95.551 ± 0.124 <sup>c</sup>	93.031 ± 0.364 <sup>b</sup>
	x1/2 MIC	83.799 ± 7.710 <sup>c</sup>	95.349 ± 0.216 <sup>c</sup>	91.521 ± 1.505 <sup>b</sup>
Gentamicin	x4 MIC	95.275 ± 0.162 <sup>c</sup>	95.458 ± 0.540 <sup>c</sup>	93.261 ± 0.183 <sup>b</sup>
	x2 MIC	58.342 ± 13.212 <sup>b</sup>	81.598 ± 1.935 <sup>b</sup>	48.201 ± 16.185 <sup>a</sup>
	MIC	32.198 ± 20.528 <sup>a</sup>	77.899 ± 2.234 <sup>b</sup>	57.994 ± 10.493 <sup>a</sup>
	x1/2 MIC	43.957 ± 20.026 <sup>a,b</sup>	69.860 ± 7.767 <sup>a</sup>	58.745 ± 16.368 <sup>a</sup>
Tetracycline	x4 MIC	95.240 ± 0.242 <sup>c</sup>	95.833 ± 0.000 <sup>c</sup>	93.552 ± 0.042 <sup>b</sup>
	x2 MIC	95.187 ± 0.092 <sup>c</sup>	95.754 ± 0.118 <sup>c</sup>	93.504 ± 0.042 <sup>b</sup>
	MIC	95.169 ± 0.061 <sup>c</sup>	95.848 ± 0.071 <sup>c</sup>	93.528 ± 0.192 <sup>b</sup>
	x1/2 MIC	95.223 ± 0.170 <sup>c</sup>	95.520 ± 0.450 <sup>c</sup>	93.553 ± 0.151 <sup>b</sup>
Cefaclor	x4 MIC	95.152 ± 0.061 <sup>c</sup>	95.630 ± 0.275 <sup>c</sup>	93.407 ± 0.210 <sup>b</sup>
	x2 MIC	95.117 ± 0.200 <sup>c</sup>	95.567 ± 0.282 <sup>c</sup>	93.189 ± 0.294 <sup>b</sup>
	MIC	95.205 ± 0.110 <sup>c</sup>	95.770 ± 0.177 <sup>c</sup>	92.462 ± 0.965 <sup>b</sup>
	x1/2 MIC	92.508 ± 4.779 <sup>c</sup>	95.817 ± 0.135 <sup>c</sup>	83.106 ± 3.567 <sup>b</sup>

## 2.4. Discussion

There has been a remarkable interest in EOs as alternative antimicrobial agents to overcome microbial resistance issues in both humans and animals [46–49], which directly threaten public health [50]. Thus, the scientific community has shown substantial interest in antimicrobial activity screening methods [51]. The antimicrobial activity of EOs is examined by a variety of bioassays, such as Kirby–Bauer disc diffusion, agar well diffusion, bioautographic, agar dilution, and broth macro- and micro-dilution methods.

In the present study, *Thymus sibthorpii*, *Origanum vulgare*, *Salvia fruticosa*, and *Crithmum maritimum* EOs were assessed for their in vitro antimicrobial and anti-biofilm efficacy, as well as their chemical compositions. Their activities were also compared with the commonly used antimicrobials gentamicin sulfate [52], tetracycline hydrochloride [53], cefaclor [54], penicillin [55], and enrofloxacin [56]. Regarding the potency, according to the GC-MS results, the main bioactive component found is carvacrol for *Thymus sibthorpii* and *Origanum vulgare*. Eucalyptol and  $\beta$ -phellandrene were observed as the main compounds of *Salvia fruticosa* and *Crithmum maritimum* EOs, respectively.

Among the antimicrobial susceptibility tests, disc diffusion is a widely used method for the antimicrobial screening of plant-derived materials (e.g., EOs) [57], with its cost efficiency and convenience for evaluating a wide range of antimicrobials and microbes. In our study, *Thymus sibthorpii* was proven as the most effective EO against all tested methicillin-sensitive and -resistant *S. aureus* strains, followed by *Origanum vulgare*, which showed higher bacterial growth inhibition, against the same strains, than *Salvia fruticosa* and *Crithmum maritimum*, even at their lower concentrations (**Table 2.2, Figure 2.3**). Remarkably, 20% (v/v) of *Thymus sibthorpii* exhibited higher inhibition than all tested concentrations of other EOs and reference antibiotics on three of the tested *S. aureus* strains. However, *Salvia fruticosa* and *Crithmum maritimum* did not demonstrate a significant effect on the inhibition of *S. aureus* strains, a finding similar to previous findings in the literature [34,58]. This effect might be due to there being less of the active components present in these plants compared to *Thymus sibthorpii* and *Origanum vulgare* EOs. Houta et al. (2015) likewise reported that *Crithmum maritimum* EOs that were extracted from different plant parts did not present sufficient antimicrobial activity [58]. However, there were some

differences between our results and some other studies. In one study, the antimicrobial activity of *Origanum vulgare* EO was screened against different *S. aureus* isolates by evaluating inhibition zone diameters and MIC values [59]. While zone diameters were generally higher than our results, the MIC of this EO as revealed in our work is significantly lower than the reported MIC values. This can be explained by differences in the composition of EOs even from the same plant species due to several factors affecting the chemical composition of EOs, such as harvesting season, climate, type of soil, and plant age [60]. Therefore, the antimicrobial activity of the same EOs may vary in different studies. To the best of our knowledge, the antimicrobial activity of *Thymus sibthorpii* EO has not been reported in the literature. However, the antimicrobial activity of crude extracts of *Thymus sibthorpii* was studied against the *S. aureus* bacterium, and the inhibition zone diameters were reported to be in the range of 9–15 mm [61], which was found to be higher for the EO in the present study.

According to the breakpoints of antibiotics reported by CLSI, penicillin, tetracycline [62], and cefaclor [63], MRSA appears resistant to them. For instance, if the zone diameter of tetracycline is equal to or larger than 19 mm on *Staphylococcus* species, then this microorganism can be evaluated as sensitive since its inhibition zone was evaluated as 10.426 mm in our work. Moreover, all tested *S. aureus* strains presented resistance against penicillin. Even though resistance was observed for most antibiotics, both methicillin-sensitive and -resistant *S. aureus* strains did not differ in their susceptibility to *Thymus sibthorpii*, which may indicate its power to combat microbial resistance.

Despite its several advantages, disc diffusion is not a suitable method to examine the MIC of antimicrobials since it is a qualitative assay and does not allow for evaluating the number of penetrated antimicrobials into the agar media. Thus, the broth microdilution method was performed to assess the MIC of each EO and the reference antibiotics. The lowest concentration of an antimicrobial that can fully inhibit the growth of a microbial in microwells/tubes is defined as the MIC [64]. The MIC of *Thymus sibthorpii* for each strain was found to be 0.091 mg/mL, which is the same as the MIC of *Origanum vulgare* for MRSA and *S. aureus* ATCC 29213, whereas its MIC is 0.182 mg/mL for MSSA. This indicates the antimicrobial strength of these two EOs in lower concentrations. Surprisingly, while *Origanum vulgare* did not inhibit bacterial growth as

effectively as *Thymus sibthorpii* in the disc diffusion method, they both showed similar MICs according to the broth microdilution method, which may be related to the qualitative nature of the disc diffusion method.

*Salvia fruticosa* exhibited 2.853 mg/mL MIC for all strains, which is two-fold lower than the MIC value of *Crithmum maritimum* for each strain. In other words, it can be said that a higher concentration of *Crithmum maritimum* is needed to complete bacterial growth inhibition towards *Salvia fruticosa*. In contrast to our findings, Kulaksiz and their team revealed that pure *Origanum vulgare* and *Salvia fruticosa* EOs presented more than 50% (v/v) MIC values against *S. aureus* ATCC 25923 [65].

The resistance of MRSA to reference antibiotics may be observed by comparing their MIC with the methicillin-sensitive strain, as in the disc diffusion method. According to CLSI breakpoints, tetracycline and cefaclor were determined to be resistant and intermediate antimicrobials, respectively [62,63]. Even though these antibiotics did not demonstrate susceptibility for MRSA, as opposed to MSSA and *S. aureus* ATCC 29213 strains, which is consistent with CLSI documents, all the EOs exhibited the same level of activity for all strains. This outcome may also reveal the potency of EOs as a possible solution to microbial resistance.

It is believed that the substantial antimicrobial activity of the *Thymus sibthorpii* and *Origanum vulgare* EOs results from their main active ingredients, carvacrol and p-cymene, as well the contribution and synergism of other constituents. The major compounds of these EOs are carvacrol and p-cymene in different percentages of their content (**Table 2.1**). The phenolic monoterpene carvacrol is one of the most studied active compounds for antimicrobial activity [23]. It leads to an increase in bacterial cell membrane permeability and fluidity by damaging the cell membrane both functionally and structurally [66,67]. Moreover, it was reported that carvacrol may give rise to changes in the fatty acid composition [68] and transportation of cytoplasmic membrane ions, releasing of lipo-polysaccharides [69,70], and alteration on cell membrane proteins and periplasmic enzymes [71,72]. On the other hand, the carvacrol precursor p-cymene was observed to increase the antimicrobial activity of single compounds present in EOs, such as carvacrol [23,73]. Although p-cymene cannot alter the membrane permeability and fluidity, it may cause a

reduction in the melting point and enthalpy of the cell membrane [74], which can increase the impurity of the membrane.

*S. aureus* strains tested in our work exhibited strong biofilm formation (**Figure 2.4**). All tested EOs indicated a remarkable level of biofilm inhibition at their half MIC values against all three strains. Moreover, for *Salvia fruticosa* and *Crithmum maritimum*, which did not show higher growth inhibition like *Thymus sibthorpii*, their half MIC provided a sufficient level of biofilm inhibition. It was stated that both hydrophobic and hydrophilic components of EO are effective to exert anti-biofilm activity, while hydrophobic constituents are the main ones for inhibiting the growth of bacterial cells [30,75]. Therefore, the higher effectivity of testing EOs on the inhibition of biofilm formation compared to their antimicrobial activity might be explained by this phenomenon. In another respect, gentamicin was not found as an antimicrobial agent to inhibit the formation of biofilm by *S. aureus* cells, perhaps due to the antimicrobial resistance of the testing strains to gentamicin. For instance, gentamicin presented about 95% anti-biofilm activity on MRSA, which is a higher concentration, equivalent to a concentration of 1 mg/l. As a consequence, all EOs exerted good anti-biofilm activity on all *S. aureus*-formed biofilms at relatively low concentrations.

## 2.5. Conclusion

Essential oils are prominent antimicrobial and anti-biofilm agents due to the presence of various active components in their composition. Alongside their antimicrobial activity, they have great potency to overcome microbial resistance. In the present study, *Thymus sibthorpii* and *Origanum vulgare* EOs demonstrated great activity in the inhibition of the growth of different *S. aureus* strains, as well as in the inhibition of biofilm formation of these strains. We believed that the strength of these two EOs stems from the high amount of carvacrol and *p*-cymene in their structure. Even though *Salvia fruticosa* and *Crithmum maritimum* did not show sufficient antimicrobial activity, they could inhibit the biofilm formation by almost 95% with their half MIC values. From another perspective, the tested EOs show great anti-biofilm activity, while gentamicin sulfate could not inhibit biofilm even at its double MIC. This study clearly elucidates the in vitro effectiveness of different EOs on different *S. aureus* strains and reveals the adaptation of safer alternatives to overcome the incremental microbial resistance problem.

## 2.6. References

- [1] Harbarth, S.; Balkhy, H.H.; Goossens, H.; Jarlier, V.; Kluytmans, J.; Laxminarayan, R.; Saam, M.; Van Belkum, A.; Pittet, D. Antimicrobial resistance: One world, one fight! *Antimicrob. Resist. Infect. Control.* 2015, 49.
- [2] Rozos, G.; Skoufos, I.; Fotou, K.; Alexopoulos, A.; Tsinas, A.; Bezirtzoglou, E.; Tzora, A.; Voidarou, C. Safety Issues Regarding the Detection of Antibiotics Residues, Microbial Indicators and Somatic Cell Counts in Ewes' and Goats' Milk Reared in Two Different Farming Systems. *Appl. Sci.* 2022, 12, 1009.
- [3] Christaki, E.; Marcou, M.; Tofarides, A. Antimicrobial resistance in bacteria: Mechanisms, evolution, and persistence. *J. Mol. Evol.* 2020, 88, 26–40.
- [4] Lee, J.-H. Perspectives towards antibiotic resistance: From molecules to population. *J. Microbiol.* 2019, 57, 181–184.
- [5] Liu, W.; Yang, C.; Gao, R.; Zhang, C.; Ou-Yang, W.; Feng, Z.; Zhang, C.; Pan, X.; Huang, P.; Kong, D. Polymer Composite Sponges with Inherent Antibacterial, Hemostatic, Inflammation-Modulating and Proregenerative Performances for Methicillin-Resistant *Staphylococcus aureus*-Infected Wound Healing. *Adv. Healthc. Mater.* 2021, 10, 2101247.
- [6] Hofer, U. The cost of antimicrobial resistance. *Nat. Rev. Microbiol.* 2019, 17, 3.
- [7] Hübner, C.; Hübner, N.-O.; Hopert, K.; Maletzki, S.; Flessa, S. Analysis of MRSA-attributed costs of hospitalized patients in Germany. *Eur. J. Clin. Microbiol.* 2014, 33, 1817–1822.
- [8] Filice, G.A.; Nyman, J.A.; Lexau, C.; Lees, C.H.; Bockstedt, L.A.; Como-Sabetti, K.; Leshner, L.J.; Lynfield, R. Excess costs and utilization associated with methicillin resistance for patients with *Staphylococcus aureus* infection. *Infect. Control Hosp. Epidemiol.* 2010, 31, 365–373.
- [9] Ke, Y.; Ye, L.; Zhu, P.; Zhu, Z.J.F.i.M. The clinical characteristics and microbiological investigation of pediatric burn patients with wound infections in a tertiary hospital in Ningbo, China: A ten-year retrospective study. *Front. Microbiol.* 2022, 13, 5238.
- [10] Pollitt, E.J.; Szkuta, P.T.; Burns, N.; Foster, S.J. *Staphylococcus aureus* infection dynamics. *PLoS Pathog.* 2018, 14, e1007112.
- [11] Serra, R.; Grande, R.; Butrico, L.; Rossi, A.; Settimio, U.F.; Caroleo, B.; Amato, B.; Gallelli, L.; De Franciscis, S. Chronic wound infections: The role of *Pseudomonas aeruginosa* and *Staphylococcus aureus*. *Expert Rev. Anti-Infect. Ther.* 2015, 13, 605–613.

- [12] Almeida, G.C.M.; dos Santos, M.M.; Lima, N.G.M.; Cidral, T.A.; Melo, M.C.N.; Lima, K.C. Prevalence and factors associated with wound colonization by *Staphylococcus* spp. and *Staphylococcus aureus* in hospitalized patients in inland northeastern Brazil: A cross-sectional study. *BMC Infect.* 2014, 14, 328.
- [13] Idrees, M.; Sawant, S.; Karodia, N.; Rahman, A.; Health, P. *Staphylococcus aureus* biofilm: Morphology, genetics, pathogenesis and treatment strategies. *Int. J. Environ. Res.* 2021, 18, 7602.
- [14] Taiwo, M.; Adebayo, O. Plant essential oil: An alternative to emerging multidrug resistant pathogens. *JMEN* 2017, 5, 00163.
- [15] Mishra, A.P.; Devkota, H.P.; Nigam, M.; Adetunji, C.O.; Srivastava, N.; Saklani, S.; Shukla, I.; Azmi, L.; Shariati, M.A.; Coutinho, H.D.M. Combination of essential oils in dairy products: A review of their functions and potential benefits. *LWT* 2020, 133, 110116.
- [16] Chouhan, S.; Sharma, K.; Guleria, S. Antimicrobial activity of some essential oils—Present status and future perspectives. *Medicines* 2017, 4, 58.
- [17] Ni, Z.-J.; Wang, X.; Shen, Y.; Thakur, K.; Han, J.; Zhang, J.-G.; Hu, F.; Wei, Z.-J. Recent updates on the chemistry, bioactivities, mode of action, and industrial applications of plant essential oils. *Trends Food Sci. Technol.* 2021, 110, 78–89.
- [18] Maurya, A.; Prasad, J.; Das, S.; Dwivedy, A.K. Essential oils and their application in food safety. *Front. Sustain. Food Syst.* 2021, 5, 653420.
- [19] Stefanakis, M.K.; Touloupakis, E.; Anastasopoulos, E.; Ghanotakis, D.; Katerinopoulos, H.E.; Makridis, P. Antibacterial activity of essential oils from plants of the genus *Origanum*. *Food Control* 2013, 34, 539–546.
- [20] Cimino, C.; Maurel, O.M.; Musumeci, T.; Bonaccorso, A.; Drago, F.; Souto, E.M.B.; Pignatello, R.; Carbone, C. Essential oils: Pharmaceutical applications and encapsulation strategies into lipid-based delivery systems. *Pharmaceutics* 2021, 13, 327.
- [21] Saad, N.Y.; Muller, C.D.; Lobstein, A. Major bioactivities and mechanism of action of essential oils and their components. *Flavour Fragr. J.* 2013, 28, 269–279.
- [22] Tzora, A.; Giannenas, I.; Karamoutsios, A.; Papaioannou, N.; Papanastasiou, D.; Bonos, E.; Skoufos, S.; Bartzanas, T.; Skoufos, I. Effects of oregano, attapulgate, benzoic acid and their blend on chicken performance, intestinal microbiology and intestinal morphology. *Poult. Sci. J.* 2017, 54, 218–227.

- [23] Nazzaro, F.; Fratianni, F.; De Martino, L.; Coppola, R.; De Feo, V. Effect of essential oils on pathogenic bacteria. *Pharmaceuti-cals* 2013, 6, 1451–1474.
- [24] Masyita, A.; Sari, R.M.; Astuti, A.D.; Yasir, B.; Rumata, N.R.; Emran, T.B.; Nainu, F.; Simal-Gandara, J. Terpenes and terpe-noids as main bioactive compounds of essential oils, their roles in human health and potential application as natural food preservatives. *Food Chem. X* 2022, 13, 100217.
- [25] Man, A.; Santacroce, L.; Iacob, R.; Mare, A.; Man, L. Antimicrobial activity of six essential oils against a group of human pathogens: A comparative study. *Pathogens* 2019, 8, 15.
- [26] Martins, M.A.; Silva, L.P.; Ferreira, O.; Schröder, B.; Coutinho, J.A.; Pinho, S.P. Terpenes solubility in water and their envi-ronmental distribution. *J. Mol. Liq.* 2017, 241, 996–1002.
- [27] da Silva, B.D.; Bernardes, P.C.; Pinheiro, P.F.; Fantuzzi, E.; Roberto, C.D. Chemical composition, extraction sources and action mechanisms of essential oils: Natural preservative and limitations of use in meat products. *Meat Sci.* 2021, 176, 108463.
- [28] Bhavaniramya, S.; Vishnupriya, S.; Al-Aboody, M.S.; Vijayakumar, R.; Baskaran, D. Role of essential oils in food safety: An-timicrobial and antioxidant applications. *GOST* 2019, 2, 49–55.
- [29] Burt, S. Essential oils: Their antibacterial properties and potential applications in foods—A review. *Int. J. Food Microbiol.* 2004, 94, 223–253.
- [30] Rossi, C.; Chaves-López, C.; Serio, A.; Casaccia, M.; Maggio, F.; Paparella, A. Effectiveness and mechanisms of essential oils for biofilm control on food-contact surfaces: An updated review. *Crit. Rev. Food Sci. Nutr.* 2022, 62, 2172–2191.
- [31] Kostoglou, D.; Protopappas, I.; Giaouris, E. Common plant-derived terpenoids present increased anti-biofilm potential against *Staphylococcus* bacteria compared to a quaternary ammonium biocide. *Foods* 2020, 9, 697.
- [32] Amiri, H. Essential oils composition and antioxidant properties of three thymus species. *eCAM* 2012, 2012, 728065.
- [33] Pezzani, R.; Vitalini, S.; Iriti, M. Bioactivities of *Origanum vulgare* L.: An update. *Phytochem. Rev.* 2017, 16, 1253–1268.
- [34] Bahadirli, N.P. Comparison of Chemical Composition and Antimicrobial Activity of *Salvia fruticosa* Mill. and *S. aramiensis* Rech. Fill. (Lamiaceae). *J. Essent. Oil-Bear. Plants* 2022, 25, 716–727.

- [35] Karousou, R.; Vokou, D.; Kokkini, S. Variation of *Salvia fruticosa* essential oils on the island of Crete (Greece). *Bot. Acta* 1998, 111, 250–254.
- [36] Senatore, F.; Napolitano, F.; Ozcan, M. Composition and antibacterial activity of the essential oil from *Crithmum maritimum* L.(Apiaceae) growing wild in Turkey. *Flavour Fragr. J.* 2000, 15, 186–189.
- [37] Maloupa, E.; Krigas, N. The Balkan Botanic Garden of Kroussia, Northern Greece. *Sibbaldia Int. J. Bot. Gard. Hortic.* 2008, 6, 9–27.
- [38] Simirgiotis, M.J.; Burton, D.; Parra, F.; López, J.; Muñoz, P.; Escobar, H.; Parra, C. Antioxidant and antibacterial capacities of *Origanum vulgare* L. essential oil from the arid Andean Region of Chile and its chemical characterization by GC-MS. *Metabolites* 2020, 10, 414.
- [39] Sarrou, E.; Tselika, N.; Chatzopoulou, P.; Tsakalidis, G.; Menexes, G.; Mavromatis, A. Conventional breeding of Greek oregano (*Origanum vulgare* ssp. *hirtum*) and development of improved cultivars for yield potential and essential oil quality. *Euphytica* 2017, 213, 104.
- [40] Adams, R.P. Identification of essential oil components by gas chromatography/mass spectrometry. In *Quadrupole Mass Spectroscopy*; Allured Publishing Corporation: Carol Stream, IL, USA, 2007; Volume 456.
- [41] Fotou, K.; Tzora, A.; Voidarou, C.; Alexopoulos, A.; Plessas, S.; Avgeris, I.; Bezirtzoglou, E.; Akrida-Demertzi, K.; Demertzis, P. Isolation of microbial pathogens of subclinical mastitis from raw sheep's milk of Epirus (Greece) and their role in its hygiene. *Anaerobe* 2011, 17, 315–319.
- [42] CLSI. Performance Standards for Antimicrobial Disk Susceptibility Tests: Approved Standard—CLSI Document M02-A11; Clinical & Laboratory Standards Institute: Wayne, PA, USA, 2015.
- [43] CLSI. Methods for Dilution Antimicrobial Susceptibility Tests for Bacteria That Grow Aerobically: Approved Standard—Eighth Edition—CLSI Document M07-A7; Clinical & Laboratory Standards Institute: Wayne, PA, USA, 2006.
- [44] Stepanović, S.; Vuković, D.; Dakić, I.; Savić, B.; Švabić-Vlahović, M. A modified microtiter-plate test for quantification of staphylococcal biofilm formation. *J. Microbiol. Methods* 2000, 40, 175–179.
- [45] Borges, S.; Silva, J.; Teixeira, P. Survival and biofilm formation by Group B streptococci in simulated vaginal fluid at different pHs. *ALJMAO* 2012, 101, 677–682.

- [46] Battisti, M.A.; Caon, T.; de Campos, A.M. A short review on the antimicrobial micro-and nanoparticles loaded with *Melaleuca alternifolia* essential oil. *J. Drug Deliv. Sci. Technol.* 2021, 63, 102283.
- [47] Aljeldah, M.M. Antioxidant and antimicrobial potencies of chemically-profiled essential oil from *asteriscus graveolens* against clinically-important pathogenic microbial strains. *Molecules* 2022, 27, 3539.
- [48] Jaradat, N. Phytochemical profile and in vitro antioxidant, antimicrobial, vital physiological enzymes inhibitory and cyto-toxic effects of *artemisia jordanica* leaves essential oil from Palestine. *Molecules* 2021, 26, 2831.
- [49] Chávez-González, M.; Rodríguez-Herrera, R.; Aguilar, C. Essential oils: A natural alternative to combat antibiotics resistance. In *Antibiotic Resistance. Mechanisms and New Antimicrobial Approaches*; Rai, K.K.M., Ed.; Elsevier: Amsterdam, The Netherlands, 2016; pp. 227–223.
- [50] Martin, I.; Sawatzky, P.; Liu, G.; Mulvey, M. STIs and sexual health awareness month: Antimicrobial resistance to *Neisseria gonorrhoeae* in Canada: 2009–2013. *CCDR* 2015, 41, 35.
- [51] Balouiri, M.; Sadiki, M.; Ibnsouda, S.K. Methods for in vitro evaluating antimicrobial activity: A review. *JPA* 2016, 6, 71–79.
- [52] Zain, K.J.; Brad, B.A.; Al Kurdi, S.B.; Jumaa, M.M.G.; Alkhouli, M. Evaluation of Antimicrobial Activity of  $\beta$ -tricalcium Phosphate/Calcium Sulfate Mixed-up with Gentamicin: In-Vitro Study. *Int. J. Dent. Oral Sci.* 2021, 8, 4753–4757.
- [53] Kulshreshtha, G.; Critchley, A.; Rathgeber, B.; Stratton, G.; Banskota, A.H.; Hafting, J.; Prithiviraj, B. Antimicrobial effects of selected, cultivated red seaweeds and their components in combination with tetracycline, against poultry pathogen *Salmonella enteritidis*. *J. Mar. Sci. Eng.* 2020, 8, 511.
- [54] Tsekoura, E.; Helling, A.; Wall, J.; Bayon, Y.; Zeugolis, D. Battling bacterial infection with hexamethylene diisocyanate cross-linked and Cefaclor-loaded collagen scaffolds. *Biomed. Mater.* 2017, 12, 035013.
- [55] Górnjak, I.; Bartoszewski, R.; Króliczewski, J. Comprehensive review of antimicrobial activities of plant flavonoids. *Phyto-chem. Rev.* 2019, 18, 241–272.
- [56] Chokejaroenrat, C.; Sakulthaew, C.; Satchasataporn, K.; Snow, D.D.; Ali, T.E.; Assiri, M.A.; Watcharenwong, A.; Imman, S.; Suriyachai, N.; Kreetachat, T. Enrofloxacin and Sulfamethoxazole

Sorption on Carbonized Leonardite: Kinetics, Isotherms, Influential Effects, and Antibacterial Activity toward *S. aureus* ATCC 25923. *Antibiotics* 2022, 11, 1261.

[57] Das, K.; Tiwari, R.; Shrivastava, D. Techniques for evaluation of medicinal plant products as antimicrobial agent: Current methods and future trends. *J. Med. Plant Res.* 2010, 4, 104–111.

[58] Houta, O.; Akrou, A.; Najja, H.; Neffati, M.; Amri, H.J.J.o.E.O.B.P. Chemical composition, antioxidant and antimicrobial activities of essential oil from *Crithmum maritimum* cultivated in Tunisia. *J. Essent. Oil Bear. Plants* 2015, 18, 1459–1466.

[59] de Lima Marques, J.; Volção, L.M.; Funck, G.D.; Kroning, I.S.; da Silva, W.P.; Fiorentini, Â.M.; Ribeiro, G.A. Antimicrobial activity of essential oils of *Origanum vulgare* L. and *Origanum majorana* L. against *Staphylococcus aureus* isolated from poultry meat. *Ind. Crops Prod.* 2015, 77, 444–450.

[60] Chan, W.-K.; Tan, L.T.-H.; Chan, K.-G.; Lee, L.-H.; Goh, B.-H. Nerolidol: A sesquiterpene alcohol with multi-faceted pharmacological and biological activities. *Molecules* 2016, 21, 529.

[61] Kunduhoglu, B.; Pilatin, S.; Caliskan, F. Antimicrobial screening of some medicinal plants collected from Eskisehir, Turkey. *Fresenius Environ. Bull.* 2011, 20, 945–952.

[62] CLSI. Performance Standards for Antimicrobial Susceptibility Testing: Twenty-fifth Informational Supplement—CLSI Document M100-S25; Clinical & Laboratory Standards Institute: Wayne, PA, USA, 2012.

[63] CLSI. Performance Standards for Antimicrobial Susceptibility Testing: Twenty-second Informational Supplement—CLSI Document M100-S22; Clinical & Laboratory Standards Institute: Wayne, PA, USA, 2012.

[64] CLSI. Methods for Dilution Antimicrobial Susceptibility Tests for Bacteria That Grow Aerobically: Approved Standard—Ninth Edition—CLSI Document M07-A9; Clinical & Laboratory Standards Institute: Wayne, PA, USA, 2018.

[65] Kulaksiz, B.; Sevda, E.; Üstündağ-Okur, N.; Saltan-İşcan, G. Investigation of antimicrobial activities of some herbs containing essential oils and their mouthwash formulations. *Turk. J. Pharm. Sci.* 2018, 15, 370.

[66] Sikkema, J.; de Bont, J.A.; Poolman, B. Mechanisms of membrane toxicity of hydrocarbons. *Microbiol. Rev.* 1995, 59, 201–222.

- [67] Sharifi-Rad, M.; Varoni, E.M.; Iriti, M.; Martorell, M.; Setzer, W.N.; del Mar Contreras, M.; Salehi, B.; Soltani-Nejad, A.; Ra-jabi, S.; Tajbakhsh, M. Carvacrol and human health: A comprehensive review. *Phytother. Res.* 2018, 32, 1675–1687.
- [68] Di Pasqua, R.; Betts, G.; Hoskins, N.; Edwards, M.; Ercolini, D.; Mauriello, G. Membrane toxicity of antimicrobial compounds from essential oils. *J. Agric. Food Chem.* 2007, 55, 4863–4870.
- [69] Helander, I.M.; Alakomi, H.-L.; Latva-Kala, K.; Mattila-Sandholm, T.; Pol, I.; Smid, E.J.; Gorris, L.G.; von Wright, A. Characterization of the action of selected essential oil components on Gram-negative bacteria. *J. Agric. Food Chem.* 1998, 46, 3590–3595.
- [70] Kachur, K.; Suntres, Z. The antibacterial properties of phenolic isomers, carvacrol and thymol. *Crit. Rev. Food Sci. Nutr.* 2020, 60, 3042–3053.
- [71] Juven, B.; Kanner, J.; Schved, F.; Weisslowicz, H. Factors that interact with the antibacterial action of thyme essential oil and its active constituents. *J. Appl. Bacteriol.* 1994, 76, 626–631.
- [72] Churklam, W.; Chaturongakul, S.; Ngamwongsatit, B.; Aunpad, R. The mechanisms of action of carvacrol and its synergism with nisin against *Listeria monocytogenes* on sliced bologna sausage. *Food Control* 2020, 108, 106864.
- [73] Rattanachaikunsopon, P.; Phumkhachorn, P. Assessment of factors influencing antimicrobial activity of carvacrol and cymene against *Vibrio cholerae* in food. *JBB* 2010, 110, 614–619.
- [74] Cristani, M.; D'Arrigo, M.; Mandalari, G.; Castelli, F.; Sarpietro, M.G.; Micieli, D.; Venuti, V.; Bisignano, G.; Saija, A.; Trom-betta, D. Interaction of four monoterpenes contained in essential oils with model membranes: Implications for their antibacterial activity. *J. Agric. Food Chem.* 2007, 55, 6300–6308.
- [75] Shahabi, N.; Tajik, H.; Moradi, M.; Forough, M.; Ezati, P. Physical, antimicrobial and antibiofilm properties of *Zataria multiflora* Boiss essential oil nanoemulsion. *Int. J. Food Sci. Technol.* 2017, 52, 1645–1652.

**Chapter 3: Optimization and development of *Thymus sibthorpii* EO-loaded  
collagen hydrogels**

**Sections of this chapter have been published in:**

*Release profile and antibacterial activity of Thymus sibthorpii essential oil-incorporated, optimally stabilized type I collagen hydrogels*, **Ersanli, C.**, Skoufos, I., Fotou, K., Tzora, A., Bayon, Y., Mari, D., Sarafi, E., Nikolaou, K., Zeugolis, D.I., *Bioengineering*, 12(1), 89, 2025.

### 3.1. Introduction

Antibiotics have generally been first line treatment for microbial infections due to their low toxicity and great bactericidal features [1-4]. Despite their superior biological efficacies, overuse and misuse of antibiotics have contributed to the promotion of microbes' antimicrobial resistance which has emerged as one of the major global health concerns according to the World Health Organization (WHO) [5]. In 2019, it was reported that annually 33,000 and 35,000 deaths were caused due to antibiotic-resistant infections in the European Union countries [6], and the United States [7], respectively. On the other hand, high concentrations of antibiotics may be required to treat infections caused by biofilm-forming bacteria, since lower concentrations of antibiotics have led to the enhancement of drug resistance [8-10]. However, high doses of antibiotic utilization may cause several adverse effects to the host, such as toxicity in the non-target area and allergies [11-14]. In consequence, safer and innovative antimicrobial treatment approaches [15] utilizing natural alternatives, such as essential oils, have garnered significant attention.

Essential oils (EOs) are plants' secondary metabolites obtained from various parts (e.g., stem, root, flower) [16-18]. They are colored, volatile, aromatic liquids [19,20] with a characteristic strong odor, demonstrating complex chemical compositions that offer a broad spectrum of antimicrobial activity [21], making them promising candidates in the battle to combat antimicrobial resistance. *Thymus sibthorpii* EO is derived from the *Thymus sibthorpii* plant, a species of the genus *Thymus* that belongs to the family Lamiaceae, which mainly inhabits southeastern Europe. *Thymus sibthorpii* EO has a complex chemical composition mainly consisted of carvacrol, thymol, and p-cymene [22]. Although in literature its superior antimicrobial, anti-biofilm [22], and antioxidant [23] activities have already been described due to its high volatility and sensitivity, it would be more effective within a biomaterial system [24]. In this context, it is crucial to develop a cytocompatible scaffold as a carrier of the EO, which should also present controlled EO release features. To our best knowledge, *Thymus sibthorpii* EO has not been introduced yet within medical devices in the field of tissue engineering applications according to the literature.

Collagen, a fibrous, non-soluble protein is one of the most prominent polymers for the development of antimicrobial biomaterials, attributable to its superior biocompatibility, excellent biodegradability, hydrophilic nature, reduced cytotoxicity, and high cell attachment affinity [25-

30]. Nevertheless, the fabricated forms of collagen need to be functionalized via in situ crosslinking due to a lack of stability [31,32]. Since physical and biological crosslinking mechanisms have generally resulted in low crosslinking efficacy, carboxyl, and amine terminal crosslinking strategies are favored in research, as arises in literature [33]. Among the above, since carbodiimide and glutaraldehyde often cause cytotoxicity [34,35], alternative crosslinkers such as multi-arm, star-shaped poly(ethylene glycol) succinimidyl glutarate (starPEG) have emerged as the subject of research [33,36-39]. For instance, Collin et al. have indicated that collagen-based hydrogels crosslinked with 4-arm starPEG molecules showed no toxicity for adipose-derived stem cells [39].

In this study, at first, collagen type I hydrogels crosslinked with six different starPEG molecules were developed and optimized. Accordingly, the optimally starPEG-crosslinked collagen hydrogels were loaded with several concentrations of *Thymus sibthorpii* EO and the release profile and kinetics of the EO were investigated. Finally, the antimicrobial activity of the developed composite hydrogels was assessed against *Staphylococcus aureus* (*S. aureus*), and *Escherichia coli* (*E. coli*), whilst their cytocompatibility was examined on NIH-3T3 fibroblast cell line.

## 3.2. Materials and methods

### 3.2.1. Materials

Porcine dermis pepsinized collagen type I with a purity over 99% was provided by Medtronic (France). *S. aureus* (ATCC<sup>®</sup> 29213) and *E. coli* (ATCC<sup>®</sup> 25922) were purchased from the American Type Culture Collection (USA). NIH-3T3 mouse fibroblast cell line (ATCC, CRL-1658) was provided by the Department of Biological Applications and Technology, School of Health Sciences, University of Ioannina (Greece). 4arm PEG Succinimidyl Glutarate, pentaerythritol (10 and 20 kDa), 8arm PEG Succinimidyl Glutarate, hexaglycerol (10 and 20 kDa), and 8arm PEG Succinimidyl Glutarate, tripentaerythritol (10 and 20 kDa) were purchased from JenKem Technology USA (Allen, TX). Phosphate buffered saline (PBS, P4417), sodium hydroxide (NaOH, S8045), sodium bicarbonate (NaHCO<sub>3</sub>, S5761), calcium chloride (CaCl<sub>2</sub>, C1016), Dulbecco's Modified Eagle Medium-high glucose (DMEM, D6429), fetal bovine serum (FBS, F7524), penicillin-streptomycin (P/S, P4333), trypan blue (T8154), and Dulbecco's Phosphate Buffered Saline (DPBS, D1408) were obtained from Sigma Aldrich (Athens, Greece). 2,4,6-Trinitrobenzene sulfonic acid (TNBSA, 28997), glutaraldehyde (GTA, 119980010), sodium dodecyl sulfate (SDS, S/P530/53), glycine white crystals (BP381), collagenase type II from *Clostridium histolyticum* (Gibco<sup>™</sup>, 17101-15), tris-base (BP152), Pierce<sup>™</sup> BCA protein assay kit (23227), trypsin-EDTA (0.25%, 25200-056), alamarBlue<sup>™</sup> assay kit (Invitrogen<sup>™</sup>, DAL1100), and Quant-iT<sup>™</sup> PicoGreen<sup>™</sup> dsDNA assay kit (Invitrogen<sup>™</sup>, P11496) were purchased from Thermo Fisher Scientific (Athens, Greece). Acetic acid (33209), and hydrochloric acid (HCL, 30721) were ordered from Honeywell, Fluka<sup>™</sup> (Germany). All tissue culture plasticware was purchased from Sarstedt (Nümbrecht, Germany).

### 3.2.2. Fabrication and crosslinking of collagen type I hydrogels

Collagen type I hydrogels were prepared at a volume of 300  $\mu$ L. For this reason, type I collagen was dissolved in 0.05 M acetic acid at a final concentration of 5 mg/mL. The pH of the solution was adjusted between 7.1 and 7.4 using 1 N NaOH and 10x Phosphate Buffer Saline (PBS). Then stock crosslinker solution was added to the mixture at a desired final concentration. The final

mixture was incubated at 37 °C for 1 h for complete gelation. Several types of multi-arm, star-shaped PEG succinimidyl glutarate molecules (**Table 3.1**) with different functional groups were used as crosslinking agents at concentrations of 0.5 mM, 1 mM, 2 mM, and 5 mM. Glutaraldehyde (GTA) at a concentration of 0.625% w/v was used as a positive control [40], whilst non-crosslinked (NCL) hydrogels were determined as a negative control.

**Table 3.1.** Six different PEG succinimidyl glutarate crosslinkers used in the study.

Full name	Abbreviation	Code	Arm number	Functional group	MW (kDa)	Concentration (mM)
4arm PEG Succinimidyl Glutarate, pentaerythritol, 10 kDa	4SP,pentaerythritol,10 kDa	SP1	4	pentaerythritol	10	0, 0.5, 1, 2, 5
4arm PEG Succinimidyl Glutarate, pentaerythritol, 20 kDa	4SP,pentaerythritol,20 kDa	SP2	4	pentaerythritol	20	0, 0.5, 1, 2, 5
8arm PEG Succinimidyl Glutarate, hexaglycerol, 10 kDa	8SP,hexaglycerol,10 kDa	SP3	8	hexaglycerol	10	0, 0.5, 1, 2, 5
8arm PEG Succinimidyl Glutarate, hexaglycerol, 20 kDa	8SP,hexaglycerol,20 kDa	SP4	8	hexaglycerol	20	0, 0.5, 1, 2, 5
8arm PEG Succinimidyl Glutarate, tripentaerythritol, 10 kDa	8SP,tripentaerythritol,10 kDa	SP5	8	tripentaerythritol	10	0, 0.5, 1, 2, 5
8arm PEG Succinimidyl Glutarate, tripentaerythritol, 20 kDa	8SP,tripentaerythritol,20 kDa	SP6	8	tripentaerythritol	20	0, 0.5, 1, 2, 5

### **3.2.3. Screening of the crosslinking efficacy of starPEG crosslinkers on collagen type I hydrogels**

#### **3.2.3.1. Quantification of the free-amine groups**

The remaining primary free amines of the collagen type I hydrogels were quantified by using TNBSA assay as previously described [41]. The linear standard curve was prepared by using known concentrations of glycine. The fabricated hydrogels were incubated in 0.1 M of sodium bicarbonate at pH 8.5. Then, 0.01% w/v of TNBSA was added which was diluted in 0.1 M sodium bicarbonate and samples were incubated for 2 h in a 37 °C incubator. Just after that, the reaction was stopped by adding 10% w/v of SDS and 1 M of HCl. The absorbance of each sample was assessed at 335 nm by microplate reader (BioTek Synergy HT, BioTek Instruments Inc., Winooski, Vermont, USA) and free amine groups were quantified by using the linear standard curve to find the concentration that corresponds to their absorbance.

#### **3.2.3.2. Enzymatic degradation analysis**

The resistance of fabricated hydrogels to proteolytic degradation was examined using collagenase assay, as has been described previously [41] with slight modifications. Briefly, hydrogels were placed into microcentrifuge tubes for each experimental group and each time point (0, 2, 4, 8, 24 h). Then, 0.1 M Tris-HCl buffer at pH 7.4, and 50 Units/mL degradation buffer prepared from collagenase type II extracted from *Clostridium histolyticum* were added to the samples in equal volumes. All samples were incubated at 37 °C on the horizontal orbital shaking incubator at 150 rpm. At each defined time point, the supernatant was collected and transferred into a new microcentrifuge tube. The amount of dissolved collagen was assessed using Pierce™ BCA protein assay, as per manufacturer's protocol.

#### **3.2.4. Essential oil-loading and release kinetics analysis**

*Thymus sibthorpii* EO was chosen as an antimicrobial agent based on the detailed antimicrobial and anti-biofilm activity assessment of various EOs in our previous study [22]. Following the screening of various starPEG crosslinkers with different concentrations regarding hydrogel stability, EO was loaded into hydrogels crosslinked with 0.5 mM of 4SP, pentaerythritol, 10 kDa, 4SP, pentaerythritol, 20 kDa, and 8SP, hexaglycerol, 20 kDa. Hydrogels were fabricated as described in section 2.2. In order to incorporate EO into hydrogels, EO was added to the hydrogel

preparation solution with a final concentration of 0.5, 1, and 2% v/v, and the solution was thoroughly mixed using a benchtop vortex. Then, the final mixture containing the added EO was incubated at 37 °C for 1 h for complete gelation.

The release profile of EO was analyzed, as has been described previously [42] with slight modifications. The fabricated EO-loaded hydrogels were soaked into 1 mL of 1x PBS (pH 7.4) at 37 °C using a horizontal shaker incubator. At each defined time point (0, 0.5, 1, 1.5, 2, 2.5, 3, 3.5, 4, 24, and 48 h), 100 µL of sample was removed and replaced by 100 µL fresh 1x PBS. The linear calibration curve was prepared with different concentrations of *Thymus sibthorpii* EO using 70% v/v ethanol, which was used as a solvent. Then, the absorbance of the supernatant was measured at 365 nm and the concentration of the released *Thymus sibthorpii* EO was determined by using the standard curve to find where their concentration corresponds. After spectrophotometric evaluation, the cumulative release percentage of EO was estimated according to equation (1), where  $M_t$  is the released amount of EO at time  $t$ , and  $M_0$  is the initial EO amount.

$$\text{Cumulative Release \%} = \sum_{t:0}^t \frac{M_t}{M_0} \times 100 \quad (1)$$

Besides the cumulative release percentages, we studied the release kinetics according to the release profile of *Thymus sibthorpii* EO. Hence, the zero-order, first-order, Higuchi, Korsmeyer-Peppas, and Hixon-Crowell release kinetics models have been applied to post-burst-release data with the equations 2-6 that follow [43-47], where  $M_\infty$  indicates the amount of EO at the final time of the measurements,  $K$  is the release constant, and  $n$  is the release exponent.

$$\text{Zero – order model: } \frac{M_t}{M_\infty} = Kt \quad (2)$$

$$\text{First – order model: } \ln \left( 1 - \frac{M_t}{M_\infty} \right) = -Kt \quad (3)$$

$$\text{Higuchi model: } \frac{M_t}{M_\infty} = Kt^{1/2} \quad (4)$$

$$\text{Korsmeyer – Peppas model: } \frac{M_t}{M_\infty} = Kt^n \quad (5)$$

$$\text{Hixson – Crowell model: } M_0^{1/3} - M_t^{1/3} = Kt \quad (6)$$

### 3.2.5. Biological activity of essential oil-loaded hydrogels

#### 3.2.5.1. Microbiological activity analysis

The antimicrobial activity of *Thymus sibthorpii* EO-loaded collagen type I hydrogels was assessed by Kirby-Bauer disc diffusion method against gram-positive *S. aureus* ATCC 29213, and gram-negative *E. coli* ATCC 25922 [48]. Penicillin (10 units) and enrofloxacin (5 µg) discs were used as control antimicrobials. On the other hand, the antimicrobial activity of 0.5, 1, and 2% v/v *Thymus sibthorpii* EO was studied as a positive control. All solutions required to fabricate hydrogels were exposed to UV light for 15 min, in order to be sterilized prior to the fabrication. The fabricated EO-loaded collagen type I hydrogels were sterilized by UV irradiation for 1 h before their antimicrobial activity assessment.

Briefly, *S. aureus* and *E. coli* were cultured overnight at a 37 °C incubator on blood agar and MacConkey agar, respectively. Then, the bacteria inoculum was prepared with  $1 \times 10^8$  CFU/mL concentration for each strain separately and spread on the Muller-Hinton agar plates. Afterwards, sterilized EO-loaded collagen type I hydrogels were placed on the Muller-Hinton agar plates. For each experimental group, three replicates were used. Thereafter, Muller-Hinton agar plates with the microbial inoculum and the hydrogels were incubated overnight at 37 °C. The inhibition zone diameters were measured for the quantitative evaluation, whilst the images of plates were taken for the qualitative evaluation.

### 3.2.5.2. Cytocompatibility analysis

Since 0.5% v/v *Thymus sibthorpii* EO loaded collagen type I hydrogels showed no significant difference compared to penicillin, the study was moved forward with 0.5% v/v *Thymus sibthorpii* EO loaded hydrogels for the *in vitro* cytocompatibility assessments. The cytocompatibility test of developed hydrogels was conducted, as has been described previously [49,50], with slight modifications. The EO-loaded hydrogels were placed into 24-well tissue culture plates and sterilized using ultraviolet irradiation for 1 h before cell culture experiments' initiation. NIH-3T3 fibroblasts were expanded and grown in a culture medium containing high glucose (4500 mg/L) DMEM, 10% FBS, and 1% penicillin/streptomycin. Subsequently, 50,000 cells were seeded per hydrogel and were maintained at 37 °C in a humidified atmosphere containing 5% CO<sub>2</sub>. Fibroblasts were allowed to grow for 1, 3, and 5 days, which were the time points of the measurements. The cell metabolic activity was conducted using alamarBlue™ assay according to the manufacturer's protocol and results were expressed consistent with the reduction percentage of the alamarBlue solution at each readout day (Day 1, 3, 5). The proliferation of the NIH-3T3 fibroblasts was carried out by Quant-iT™ PicoGreen™ dsDNA assay in accordance with the instructions provided by the supplier. The DNA content (ng/mL) of each sample was quantified by interpolating values from a linear standard curve.

### 3.2.6. Statistical analysis

In this chapter, all experiments were triplicated, and data were represented as mean ± standard deviation. One-way analysis of variance (ANOVA) was performed using GraphPad Prism®, Version 9.0 (La Jolla, California, USA), after confirmation of the assumptions of parametric analysis. Statistical significance was accepted at  $p < 0.05$ . The symbols \* and # denote a statistically significant difference among different experimental groups and a statistically significant difference in an individual group compared to positive control GTA, respectively. The levels of statistically significant difference were indicated as follows: \* or # for  $p < 0.05$ , \*\* or ## for  $p < 0.01$ , \*\*\* or ### for  $p < 0.001$ , and \*\*\*\* or #### for  $p < 0.0001$ .

### 3.3. Results

#### 3.3.1. Determination of optimal starPEG type and concentration on hydrogel stability

TNBSA assay was performed to assess the free amine content of the fabricated hydrogels functionalized with various starPEG crosslinkers with 0.5, 1, 2 and 5 mM concentrations (Table 1). starPEG-crosslinked hydrogels presented significantly decreased free amine content for all types of crosslinkers with all tested concentrations compared to NCL hydrogels (**Figure 3.1**) ( $p < 0.05$ ). An effective plateau was observed between 0.5 and 2 mM, and no statistical difference was noted among 0.5 mM, 1 mM, and 2 mM crosslinked hydrogels ( $p < 0.05$ ). In this plateau, the free amine reduction percentage was between 44.82% and 58.57%. The resistance of the hydrogels against enzymatic degradation was evaluated by bacterial collagenase assay followed by Pierce™ BCA protein assay (**Figure 3.2**). Non-crosslinked hydrogels were completely degraded within a couple of hours. In general perspective, scaffolds showed higher resistance to degradation when crosslinked with GTA, that was used as a positive control. However, hydrogels crosslinked with 0.5 mM of 4SP, pentaerythritol, 10 kDa showed no statistical difference compared to GTA crosslinked hydrogels, whilst 0.5 mM of 4SP, pentaerythritol, 20 kDa, and 8SP, hexaglycerol, 20 kDa displayed the lowest significant difference than all other groups ( $p < 0.05$ ). Therefore, 0.5 mM of the above three crosslinkers were deemed to be optimal conditions for functionalizing collagen hydrogels.

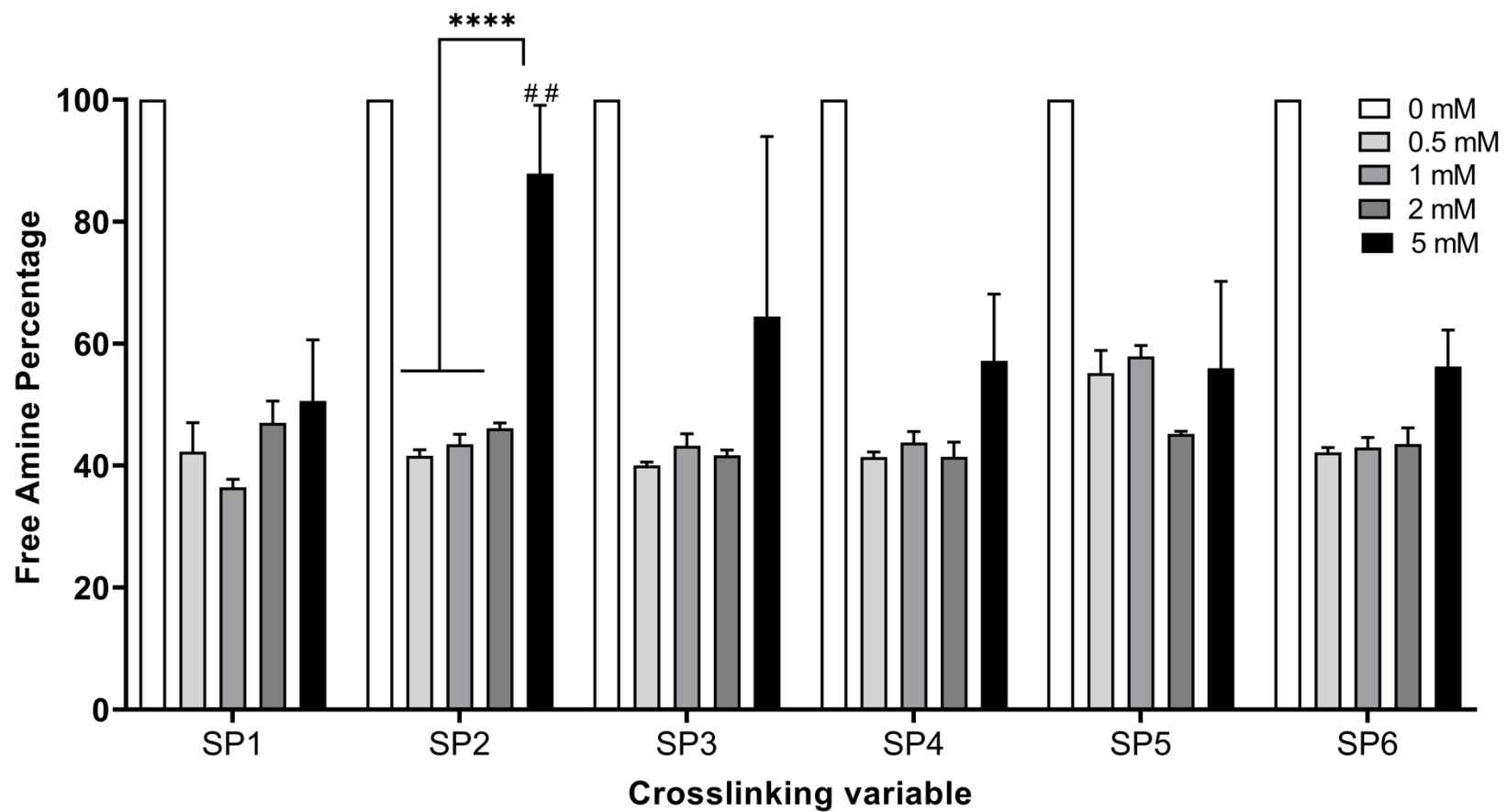


**Figure 3.1.** Free amine content of non-crosslinked (NCL) and various starPEG crosslinked collagen type I hydrogels (n=3, one-way ANOVA,  $p < 0.05$ ). Glutaraldehyde (GTA) was used as a positive control.

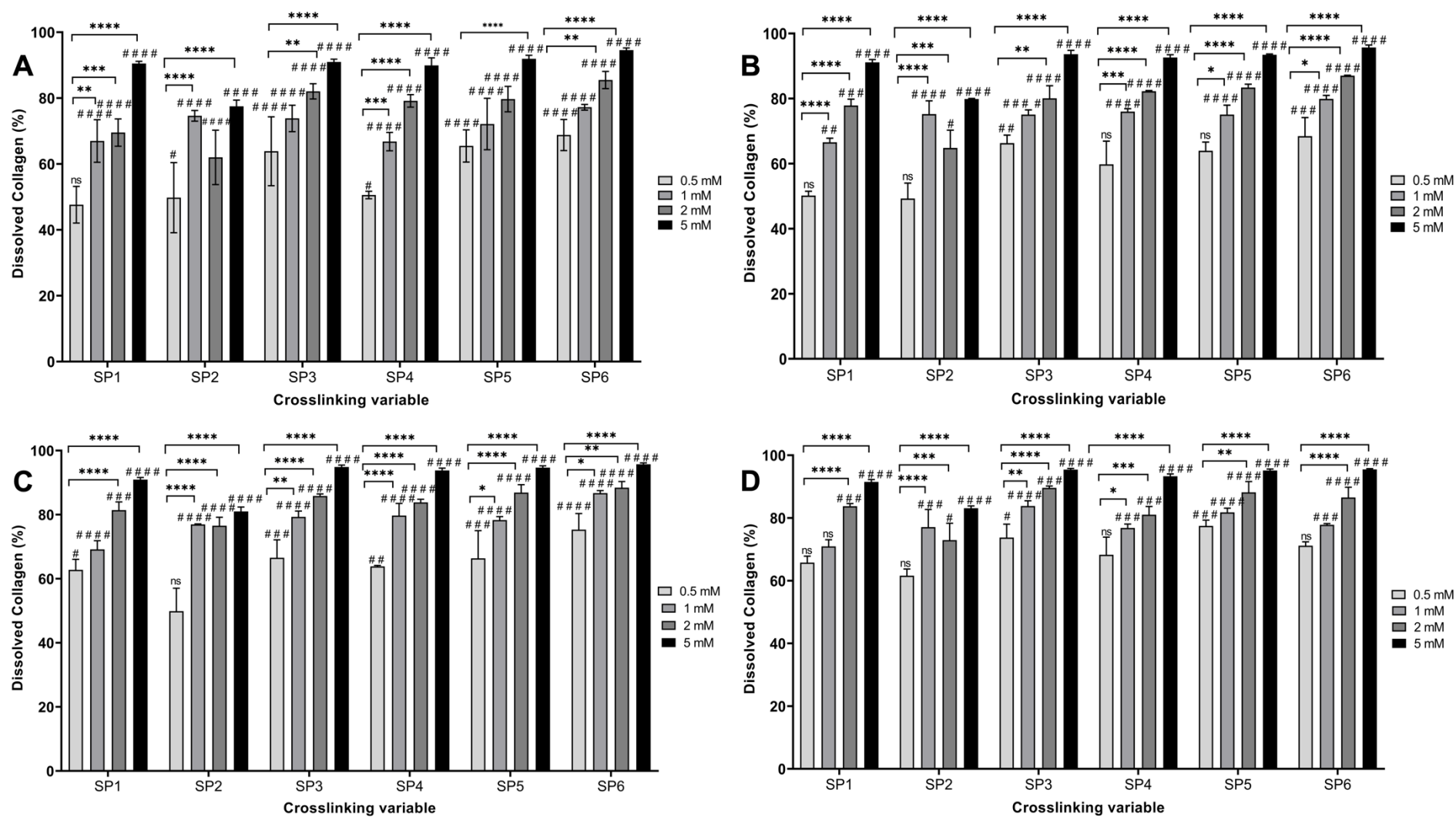


**Figure 3.2.** The mass of dissolved collagen of various starPEG crosslinked collagen type I hydrogels after (A) 2 h, (B) 4 h, (C) 8 h, (D) 24 h of collagenase digestion (n=3, one-way ANOVA,  $p < 0.05$ ).

### 3.3.2. EO release profile and release kinetics

*Thymus sibthorpii* EO was loaded at 0.5, 1, and 2% v/v into optimized collagen hydrogels, and their release profile was assessed spectrophotometrically (**Figure 3.3**). The non-crosslinked hydrogels demonstrated burst release and completely released EO within a couple of hours was observed. Although GTA crosslinked scaffolds released almost all loaded quantity of the EO at 0.5% v/v from the polymeric network, the chosen optimized hydrogels crosslinked with 0.5 mM of 4SP, pentaerythritol, 10 kDa, 4SP, pentaerythritol, 20 kDa and 8SP, hexaglycerol, 20 kDa, released  $63.92 \pm 3.31\%$ ,  $75.85 \pm 9.00\%$  and  $57.82 \pm 4.08\%$  of the EO loaded at the same concentration after 48 h. Moreover, the release kinetics was studied by applying five different mathematical models. Hixson-Crowell model did not fit any of the experimental groups, whilst the other four models fitted to different experimental groups. Moreover, the release exponent (n) values evaluated by the Korsmeyer-Peppas model indicated that the release mechanism of EO from crosslinked hydrogels obeyed the Fickian diffusion.

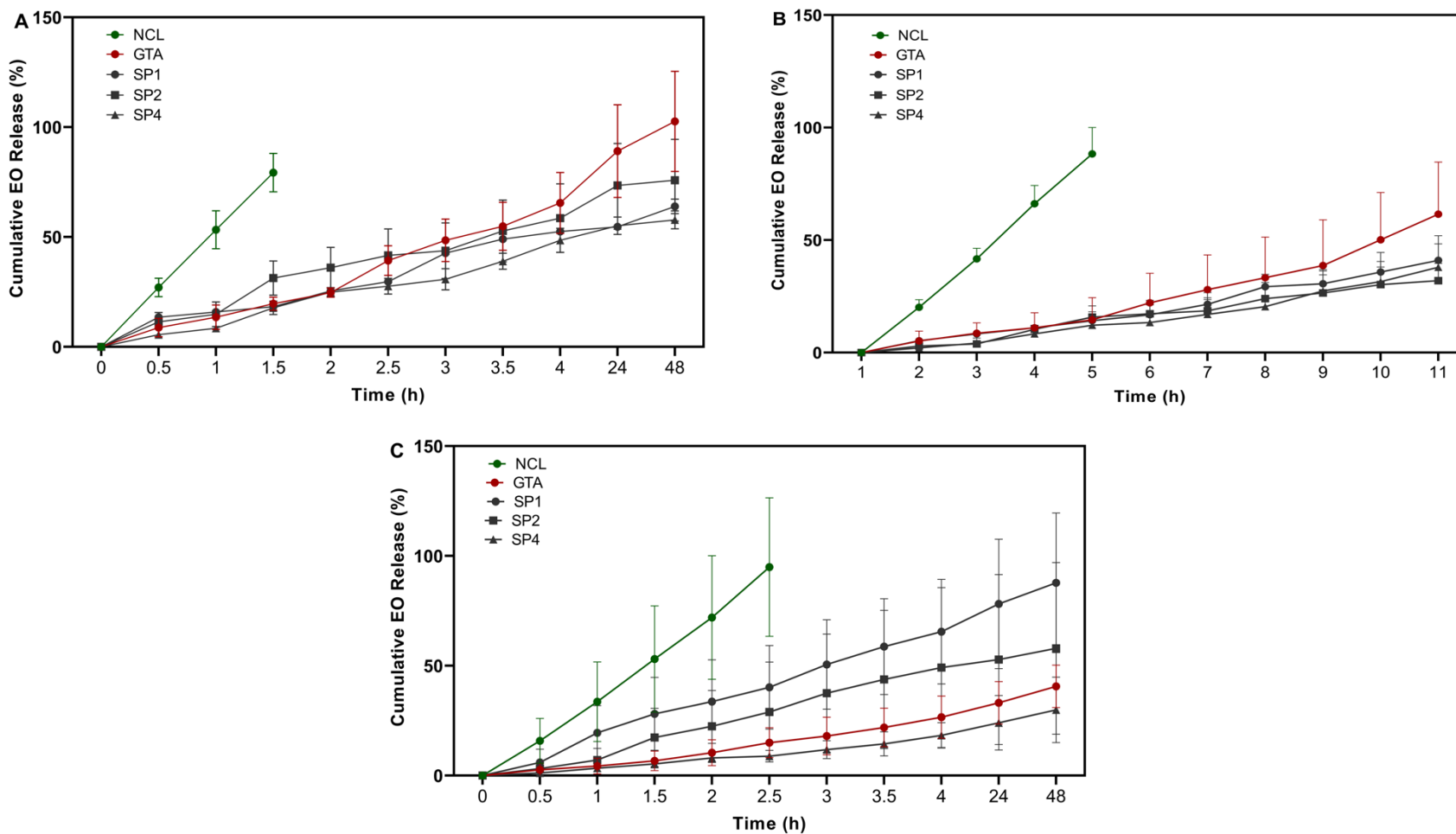


**Figure 3.3.** The cumulative release profile of (A) 0.5 v%, (B) 1 v%, and (C) 2 v% of *Thymus sibthorpii* essential oil from optimally crosslinked collagen type I hydrogels in 1x PBS at 37 °C.

**Table 3.2.** Regression coefficients ( $R^2$ ) of the five different release kinetic models fitted to the release of three different concentrations of *Thymus sibthorpii* EO from starPEG-crosslinked collagen type I hydrogels. T0.5, T1, and T2 represent the 0.5, 1, and 2 v% of *Thymus sibthorpii* essential oil within hydrogels.

Model	Zero-order	First-order	Higuchi	Korsmeyer-Peppas		Hixson-Crowell
	$R^2$	$R^2$	$R^2$	$R^2$	n	$R^2$
NCL-T0.5	0.9996	0.9538	0.9294	1.0000	0.9789	0.4040
NCL-T1	0.9991	0.9050	0.8987	0.9996	1.0720	0.5536
NCL-T2	0.9972	0.8101	0.8821	0.9997	1.1065	0.6183
GTA-T0.5	0.9574	1.0000	0.9971	0.9985	0.1789	0.0235
GTA-T1	0.9973	0.9998	0.9897	0.9666	0.1779	0.7033
GTA-T2	0.9998	0.9997	0.9806	0.9494	0.1613	0.9434
4SP, pentaerythritol, 10 kDa-T0.5	0.9153	0.9039	0.8113	0.6980	0.0677	0.6412
4SP, pentaerythritol, 10 kDa-T1	0.9973	0.9991	0.9897	0.9573	0.1111	0.7033
4SP, pentaerythritol, 10 kDa-T2	0.9829	0.9997	0.9995	0.9830	0.1140	0.1856
4SP, pentaerythritol, 20 kDa-T0.5	0.8124	0.8400	0.9196	0.9747	0.1082	0.0953
4SP, pentaerythritol, 20 kDa-T1	0.9336	0.9382	0.9887	0.9996	0.0747	0.1965
4SP, pentaerythritol, 20 kDa-T2	0.9981	0.9952	0.9615	0.8993	0.0607	0.0152

8SP, hexaglycerol, 20 kDa-T0.5	0.9155	0.9277	0.9802	0.9999	0.0706	0.9991
8SP, hexaglycerol, 20 kDa-T1	0.9949	0.9916	0.9502	0.8958	0.1197	0.0280
8SP, hexaglycerol, 20 kDa-T2	0.9982	0.9996	0.9876	0.9645	0.1882	0.7830

---

### 3.3.3. Biological analyses of the EO-loaded hydrogels

The antimicrobial activity of EO-loaded hydrogels was investigated against gram-positive *S. aureus* and gram-negative *E. coli* using the Kirby-Bauer disc diffusion assay. The results were presented qualitatively (**Figure 3.4**) and quantitatively (**Figure 3.5**). Composite antibacterial hydrogels were less effective against gram-negative *E. coli*. More specifically, hydrogels crosslinked with 0.5 mM 4SP, pentaerythritol, 10 kDa and loaded with 0.5 v% EO demonstrated  $2.83 \pm 0.47$  cm, and  $1.23 \pm 0.15$  cm inhibition zone diameter against *S. aureus*, and *E. coli*, respectively. Moreover, hydrogels containing 0.5% v/v of EO, which was the minor concentration, did not show a statistical difference regarding their antimicrobial activity compared to positive control penicillin (for gram-positive bacteria), and enrofloxacin (for gram-negative bacteria) ( $p < 0.05$ ). Hence, 0.5% v/v concentration of *Thymus sibthorpii* EO was chosen as the optimal concentration to incorporate into collagen scaffolds. Thereafter, cytocompatibility of 0.5% v/v EO incorporated hydrogels was assessed on NIH-3T3 fibroblast cell line (**Figure 3.6**). According to cell metabolic activity and proliferation studies, none of the fabricated hydrogels showed any toxicity on fibroblasts ( $p < 0.05$ ).

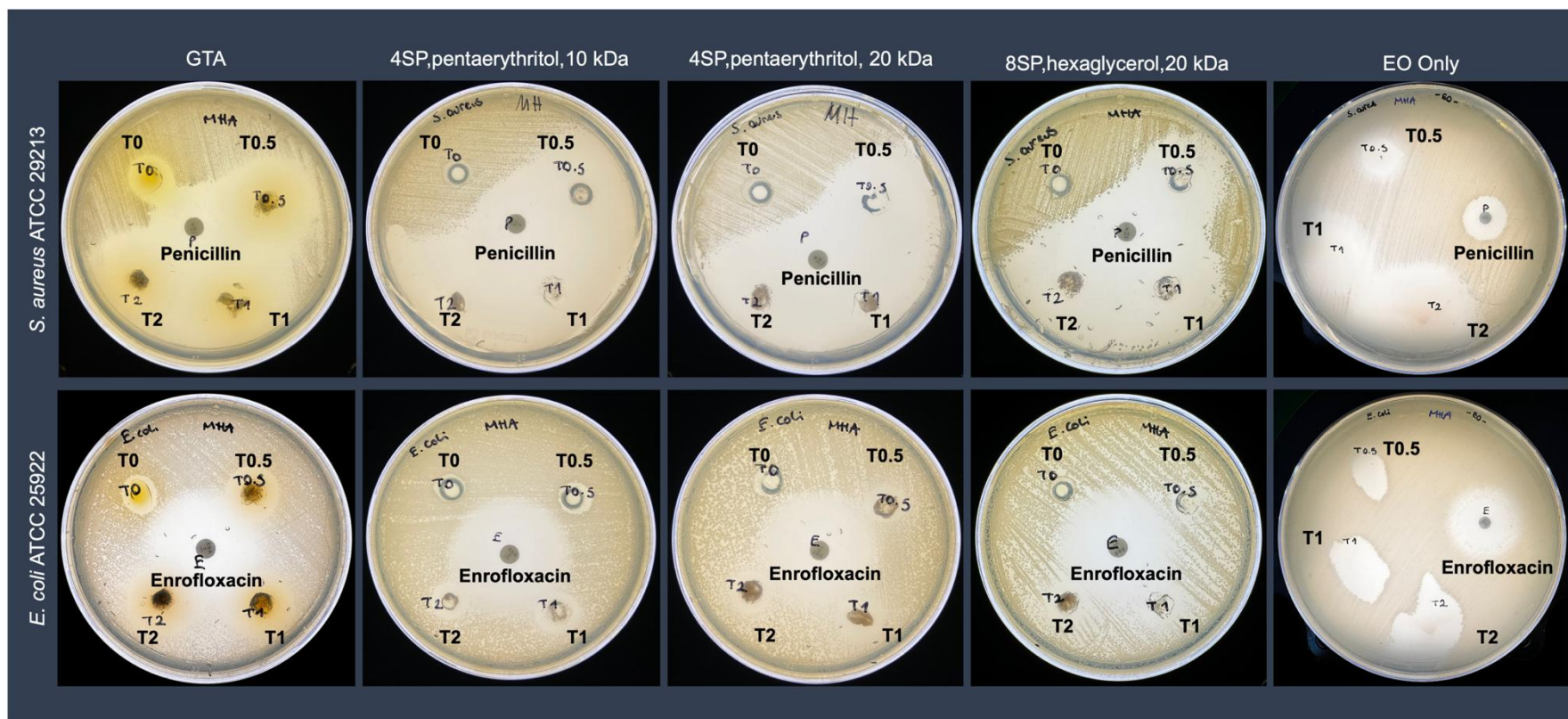


**Figure 3.4.** The qualitative analysis of the antibacterial effect of 0.5 v% (T0.5), 1 v% (T1), and 2 v% (T2) *Thymus sibthorpii* essential loaded optimally crosslinked collagen type I hydrogels against *S. aureus* ATCC 29213, and *E. coli* ATCC 25922. Penicillin and enrofloxacin were used as positive control for *S. aureus*, and *E. coli* strains, respectively.

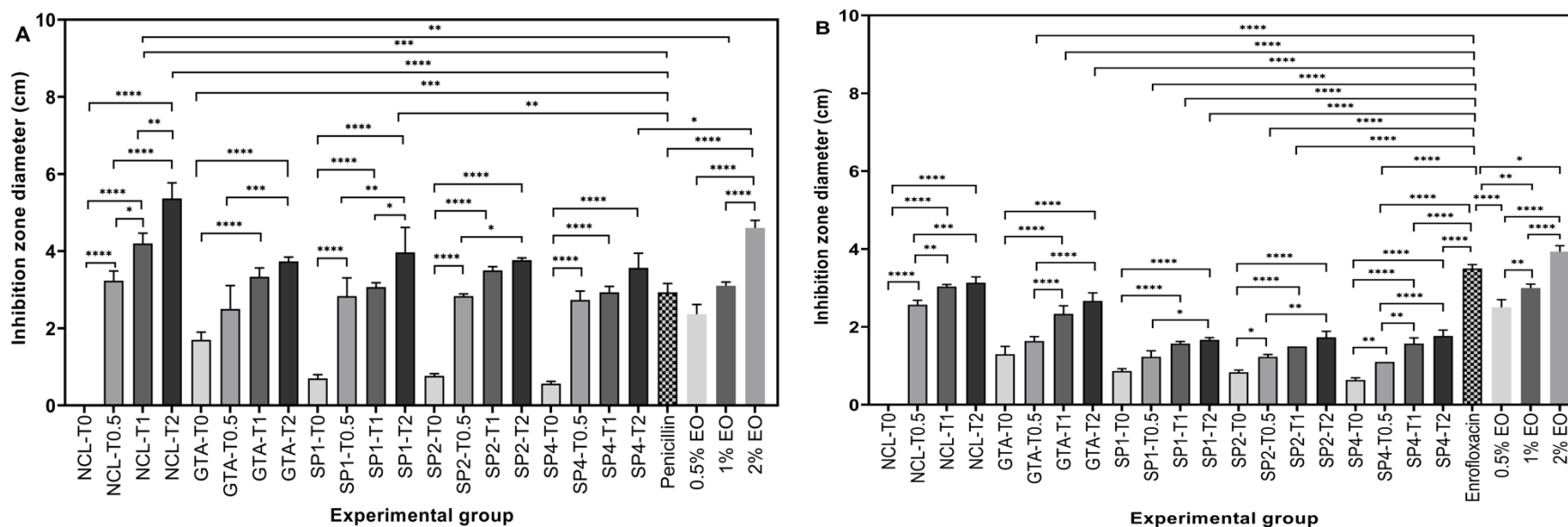


**Figure 3.5.** Inhibitions zone diameters of 0.5 v% (T0.5), 1 v% (T1), and 2 v% (T2) *Thymus sibthorpii* essential loaded optimally crosslinked collagen type I hydrogels against **(A)** *S. aureus* ATCC 29213, and **(B)** *E. coli* ATCC 25922 (n=3, one-way ANOVA,  $p < 0.05$ ). Penicillin and enrofloxacin were used as positive control for *S. aureus*, and *E. coli* strains, respectively.

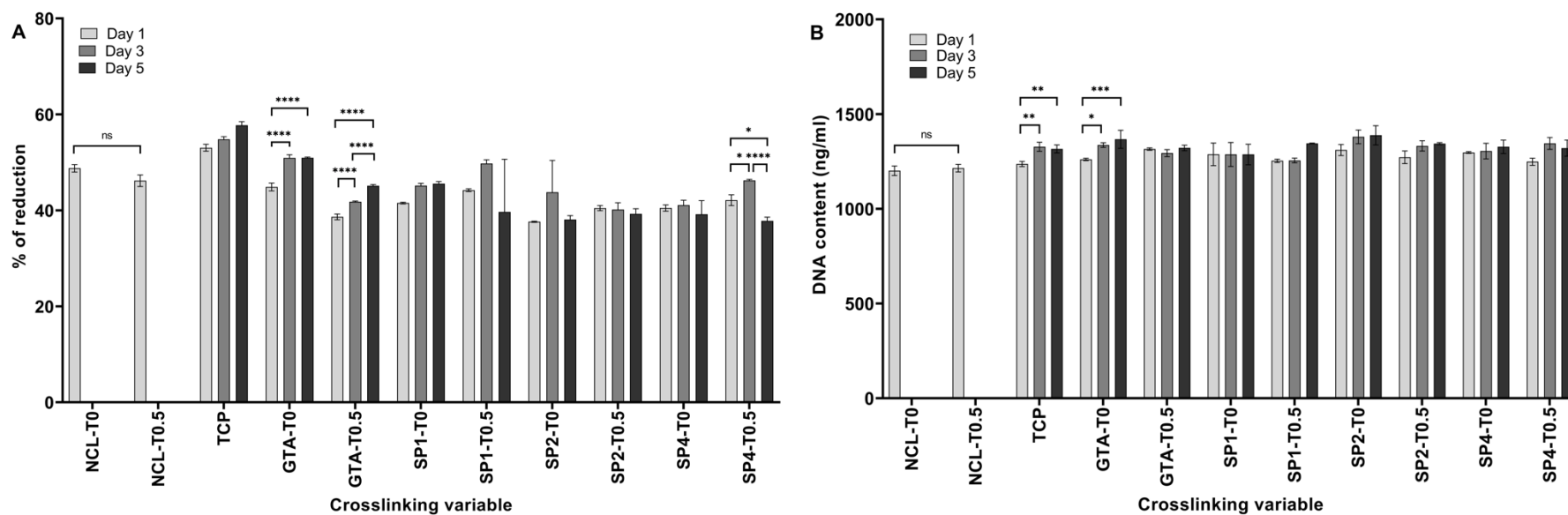


**Figure 3.6.** The in vitro (A) metabolic activity, and (B) DNA content of NIH-3T3 fibroblasts seed on the 0.5 v% *Thymus sibthorpii* essential loaded optimally crosslinked collagen type I hydrogels (n=3, one-way ANOVA,  $p < 0.05$ ).

### 3.4. Discussion

Antimicrobial resistance has been stated as one of the three critical public health threats by the World Health Organization (WHO) [5]. On the other hand, infections caused by antimicrobial-resistant microorganisms have been reported as the third major disease after cardiovascular diseases [51]. According to the report published by the Centers for Disease Control and Prevention (CDC), antimicrobial-resistant infections have led to the death of over twenty-three thousand people among the more than two million people who got infected [52]. It is expected that ten million people are going to get infected by antimicrobial-resistant microbes by 2050 according to a study published in January 2023 [53]. Therefore, the need for alternative treatments substitutes for antibiotic-based treatments to combat antimicrobial resistance has significantly gained attention. In this context, essential oils have emerged as promising alternatives with superior antimicrobial activities [54-56]. Although EOs have shown spectacular biological activities, they need to be incorporated in a carrier due to their high volatility, and sensitivity [24]. In this study, firstly, we screened the crosslinking efficacy of six different starPEG molecules with their various concentrations to stabilize collagen type I hydrogels via *in situ* crosslinking. Subsequently, the optimally starPEG-crosslinked collagen hydrogels were loaded with various concentrations of *Thymus sibthorpii* EO, and the release profile and release kinetics of the EO were examined. Finally, the antimicrobial activity and cytocompatibility of the developed hydrogels were assessed.

Collagen-type I-based medical devices (e.g., hydrogels, sponges, nanofibers) have customarily been used for tissue engineering applications thanks to outstanding properties of collagen such as bioactivity, biocompatibility, versatility, and ability to mimic natural extracellular matrix [25,33,57,58]. However, to enhance the stability, control the biodegradation rate and release profile of loaded drugs, collagen devices are needed to be introduced by crosslinking [59]. Even though enzymatic [60] and physical [61] crosslinking approaches have been studied, chemical crosslinking is generally needed for higher resistance against (bio)degradation which creates a covalently bonded polymeric network [62,63]. Among the most studied crosslinking agents, glutaraldehyde and carbodiimide may often show some drawbacks such as poor cell attachment, growth and proliferation, and cytotoxicity. As the literature reveals, 4-arm starPEG molecules have been studied as a crosslinking agent and indicated the enhanced stability of collagen-based hydrogels [39,64]. Herein, we assessed the influence of diverse concentrations (0.5, 1, 2, 5 mM)

of the six different starPEG crosslinkers which have different arm numbers (4, 8), molecular weight (10, 20 kDa), and functional groups (**Table 3.1**) on the stability of the collagen hydrogels. starPEG has a pegylated structure which shows multi-arm N-hydroxy succinimidyl (NHS) groups. The reactive NHS groups are expected to react with the free amine groups in the collagen backbone, consequently improving the stability of the three-dimensional collagen network. All six kinds of starPEG crosslinkers significantly decreased the free amine groups compared to non-crosslinked collagen type I hydrogels ( $p \leq 0.05$ ) and showed an effective plateau between 0.5 and 2 mM according to free amine analysis (**Figure 3.1**). It is believed that 5 mM exceeds the effective concentration range for starPEG crosslinkers. In other words, the increase in the concentration to the 5 mM led to the higher free amine groups, which indicated the lower crosslinking efficacy. While the proven optimal concentration of GTA [40] decreased the free amine content of the collagen hydrogels approximately by 41%, 0.5, 1, and 2 mM of studied starPEG crosslinkers showed a higher decrease with all concentrations. Besides, 0.5 mM of all crosslinkers except 8SP, triptaerythritol, 10 kDa approximately showed a 60% reduction in the free amine groups. Moreover, neither molecular weight nor arm number of starPEG molecules show a significant effect on the hydrogel stability. According to the collagenase assay, the non-crosslinked hydrogels completely degraded within 4 hours due to their low stability, whilst starPEG crosslinked hydrogels were not degraded even after 24 hours (**Figure 3.2**). Similar to free amine quantification results, 5 mM concentration of each starPEG crosslinkers showed lower efficacy than the 0.5, 1, and 2 mM of crosslinkers. The lower resistance of 5 mM starPEG crosslinked collagen hydrogels may also be explained by the self-assembly behavior of star-shaped PEG molecules. Likewise, Collin et al. have revealed that the increased concentration of 4-arm starPEG crosslinker displayed a detrimental effect on the collagen type II hydrogel stability [39]. Since 0.5 mM starPEG concentration did not show any significant difference compared to 1 and 2 mM concentrations, it was deemed optimal. Furthermore, among the screened starPEG molecules, 4SP-pentaerythritol, 10 kDa, 4SP-pentaerythritol, 20 kDa, and 8SP-hexaglycerol, 20 kDa were chosen as the optimal crosslinkers according to the hydrogel stability outcomes.

The release profile of *Thymus sibthorpii* EO from starPEG-crosslinked hydrogels was assessed by UV-vis spectroscopy. 0.5, 1, and 2% v/v of the EO according to the total hydrogel volume (300  $\mu$ L) was loaded into collagen hydrogels. The release behavior was examined for 0.5 h to 48 h at

37 °C. During the defined period of time, *Thymus sibthorpii* EO-loaded collagen hydrogels displayed a constant release profile (**Figure 3.3**). Since the crosslinking density and chemical composition are the key parameters for a hydrogel [65] network that can directly influence the release profile, non-crosslinked hydrogels showed burst release within a few hours, as expected. We suppose that after crosslinking, collagen hydrogels became denser which slowed down the EO release because of the reduced pore size and limited diffusion pathways [66]. On the other hand, the initial loading capacity of an antimicrobial agent into a polymeric network may lead to prolonged release [67]. For instance, hydrogels crosslinked with 4SP, pentaerythritol, 10 kDa approximately released 60% and 40% of the 0.5% v/v and 1% v/v loaded EO, respectively at the end of the 12 h. In this context, it is important to understand the EO release mechanism of the hydrogel-based polymeric network. Therefore, zero-order [43], first-order [44], Higuchi [45], Korsmeyer-Peppas [46], and Hixson-Crowell [47] release kinetics models have been applied to release data. According to the regression coefficient of the applied mathematical models (**Table 3.2**), the Hixson-Crowell model did not fit the EO-loaded various collagen systems. It was an expected outcome since the Hixson-Crowell model mainly describes the release of a drug from the systems where the change in surface area is an important parameter. On the other hand, release exponent ( $n$ ) assessed using the Korsmeyer-Peppas model is a key parameter to examine the diffusion way of a drug from the polymeric networks. According to this model, for a spherical matrix, the cases  $n \leq 0.45$ ,  $0.45 < n < 0.89$ , and  $n \geq 0.89$  indicate the Fickian diffusion, non-Fickian diffusion, and Case-II transport, respectively. In our study, except for non-crosslinked hydrogel systems, all developed EO-loaded hydrogel systems represented Fickian diffusion which means there are no boundaries for the release of the drug from the polymeric network. In other words, if a system obeys the Fickian diffusion, a drug within the system can dissolve from any part of the polymeric matrix. Similarly, in a study, Unalan et al. loaded clove EO into the alginate/xanthan gum hydrogels, and revealed that the release of the incorporated EO showed Fickian diffusion [66].

In our previous study, *Thymus sibthorpii* EO showed extraordinary antimicrobial activity against both antibiotic-resistant and non-resistant *S. aureus* strains [22]. Therefore, it was used as an antimicrobial agent in this work. On the other hand, *S. aureus* and *E. coli* are two of the most inhabited Gram-positive, and Gram-negative bacteria on the infected tissue area [68-70]. Hence,

the antimicrobial activity of the developed composite hydrogels was assessed against *S. aureus* and *E. coli* using the disc diffusion method. Although pristine collagen hydrogels showed antimicrobial activity, EO-loaded hydrogels presented significantly higher activity against both gram-positive and gram-negative bacteria (**Figure 3.4, Figure 3.5**). This outcome may be explained by the antibacterial action mechanism of *Thymus sibthorpii* EO. The EO might damage the bacterial cell membrane which become permeable and the diffusion through the membrane leads to cell death [71,72]. Gram-negative bacteria have been considered more resistant to an antimicrobial agent compared to gram-positive bacteria since their double-layered cell membrane is denser than the single-layered cell membrane of gram-positive bacteria [73]. Accordingly, the developed antibacterial hydrogels exhibited higher antimicrobial activity against gram-positive *S. aureus*. Additionally, some of the essential oils could diffuse through the lipophilic cell wall of gram-negative bacteria (e.g., *E. coli*) due to the diverse chemical composition of essential oils, which could explain the observed antimicrobial action of composite collagen hydrogels. For instance, Aras et al. [74] developed *Nigella sativa* EO-incorporated polyurethane-based nanofibrous mats. The developed wound dressings showed higher antibacterial activity on *E.coli* than on *S. aureus* [74]. We used penicillin and enrofloxacin as a control antimicrobial agent for the comparison of the efficacy of *Thymus sibthorpii* EO on *S. aureus* and *E. coli*, respectively. The hydrogels crosslinked with all three different starPEG and loaded with 0.5% v/v EO did not show any significant difference compared to control antimicrobials. For this reason, 0.5% v/v *Thymus sibthorpii* EO concentration was deemed optimal to incorporate into collagen type I antibacterial hydrogels. We believe that since even the lowest concentration of *Thymus sibthorpii* EO can be used instead of penicillin, *Thymus sibthorpii* EO can be presented as an alternative and effective antimicrobial agent to overcome the antimicrobial resistance problem raised by misuse and long-term use of antibiotics.

Collagen-based medical devices are widely used for tissue engineering applications because they show advanced biocompatibility with mammalian cells in addition to other outstanding features [58,75]. Among the collagen-based scaffolds, collagen hydrogels demonstrate cell attachment, proliferation, and metabolic activity due to their porous and fibrillar network [76,77]. The optimized, 0.5% v/v *Thymus sibthorpii* EO loaded collagen hydrogels crosslinked with 4SP-pentaerythritol,10 kDa, 4SP-pentaerythritol,20 kDa, and 8SP- hexaglycerol,20 kDa were

examined by alamarBlue™, and Quant-iT™ PicoGreen™ dsDNA assays for metabolic activity, and the proliferation of the seeded NIH-3T3 fibroblasts, respectively. The experimental outcomes indicate that all of the developed composite hydrogels were found cytocompatible with fibroblasts (**Figure 3.6**). Moreover, it can be concluded that 0.5 v% concentration of *Thymus sibthorpii* EO has no toxic effect on the NIH-3T3 fibroblasts.

### 3.5. Conclusion

Antimicrobial resistance is an emerging global health threat that causes drastically increasing mortality and economic burden every year. Consequently, alternative safer antibacterial therapy strategies need to be taken into consideration to combat this threat. In the quest for alternative antibacterial therapies, herein, we developed collagen type I hydrogel systems optimally crosslinked and loaded with *Thymus sibthorpii* essential oil. The proposed antimicrobial agent incorporated into the collagen type I scaffolds showed strong activity against *S. aureus*, demonstrated a sustained release profile, and had no toxicity on fibroblasts. The outcomes of this work make this developed composite antibacterial medical devices a promising candidate for infected tissue engineering applications.

### 3.6. References

- [1] Kyriacou, H.; Kamaraj, A.; Khan, W.S. Developments in antibiotic-eluting scaffolds for the treatment of osteomyelitis. *Appl. Sci.* **2020**, *10*, 2244.
- [2] Kalhapure, R.S.; Suleman, N.; Mocktar, C.; Seedat, N.; Govender, T. Nanoengineered drug delivery systems for enhancing antibiotic therapy. *J. Pharm. Sci.* **2015**, *104*, 872-905.
- [3] Gosselin, R.A.; Roberts, I.; Gillespie, W.J. Antibiotics for preventing infection in open limb fractures. *Cochrane Database Syst. Rev.* **2004**, *1*.
- [4] Vallet-Regí, M.; Lozano, D.; González, B.; Izquierdo-Barba, I. Biomaterials against bone infection. *Adv. Healthc. Mater.* **2020**, *9*, 2000310.
- [5] Salam, M.A.; Al-Amin, M.Y.; Salam, M.T.; Pawar, J.S.; Akhter, N.; Rabaan, A.A.; Alqumber, M.A. Antimicrobial resistance: a growing serious threat for global public health. *Healthcare.* **2023**, *11*, 1946.
- [6] Organization for Economic Cooperation and Development; European Union. Antimicrobial Resistance-Tackling the Burden in the European Union; OECD Publishing: Paris, France, **2019**.
- [7] U.S. Centers for Disease Control and Prevention. Antibiotic Resistance Threats in the United States; U.S. Department of Health and Human Services, CDC: Atlanta, GA, USA, **2019**.
- [8] Singh, A.; Amod, A.; Pandey, P.; Bose, P.; Pingali, M.S.; Shivalkar, S.; Varadwaj, P.K.; Sahoo, A.K.; Samanta, S.K. Bacterial biofilm infections, their resistance to antibiotics therapy and current treatment strategies. *Biomed. Mater.* **2022**, *17*, 022003.
- [9] Ciofu, O.; Rojo-Molinero, E.; Macià, M.D.; Oliver, A. Antibiotic treatment of biofilm infections. *Apmis.* **2017**, *125*, 304-319.
- [10] Fragkou, I.A.; Skoufos, J.; Cripps, P.J.; Kyriazakis, I.; Papaioannou, N.; Boscós, C.M.; Tzora, A.; Fthenakis, G.C. Differences in susceptibility to *Mannheimia haemolytica*-associated mastitis between two breeds of dairy sheep. *J. Dairy Res.* **2007**, *74*, 349-355.
- [11] Kalelkar, P.P.; Riddick, M.; Garcia, A.J. Biomaterial-based antimicrobial therapies for the treatment of bacterial infections. *Nat. Rev. Mater.* **2021**, 1-16.
- [12] Langdon, A.; Crook, N.; Dantas, G. The effects of antibiotics on the microbiome throughout development and alternative approaches for therapeutic modulation. *Genome Med.* **2016**, *8*, 1-16.
- [13] Levin-Reisman, I.; Ronin, I.; Gefen, O.; Braniss, I.; Shores, N.; Balaban, N.Q. Antibiotic tolerance facilitates the evolution of resistance. *Science.* **2017**, *355*, 826-830.

- [14] Rigas, D.; Grivas, N.; Nelli, A.; Gouva, E.; Skoufos, I.; Kormas, K.; Tzora, A.; Lagkouvardos, I. Persistent Dysbiosis, Parasite Rise and Growth Impairment in Aquacultured European Seabass after Oxytetracycline Treatment. *Microorganisms*. **2023**, *11*, 2302.
- [15] Álvarez-Martínez, F.J.; Barrajon-Catalán, E.; Micol, V. Tackling antibiotic resistance with compounds of natural origin: A comprehensive review. *Biomedicines*. **2020**, *8*, 405.
- [16] Baptista-Silva, S.; Borges, S.; Ramos, O.L.; Pintado, M.; Sarmiento, B. The progress of essential oils as potential therapeutic agents: A review. *J. Essent. Oil Res.* **2020**, *32*, 279-295.
- [17] Ni, Z.-J.; Wang, X.; Shen, Y.; Thakur, K.; Han, J.; Zhang, J.-G.; Hu, F.; Wei, Z.-J. Recent updates on the chemistry, bioactivities, mode of action, and industrial applications of plant essential oils. *Trends Food Sci. Technol.* **2021**, *110*, 78-89.
- [18] Maurya, A.; Prasad, J.; Das, S.; Dwivedy, A.K. Essential oils and their application in food safety. *Front. Sustain. Food Syst.* **2021**, *5*, 653420.
- [19] Sadgrove, N.J.; Padilla-González, G.F.; Phumthum, M. Fundamental chemistry of essential oils and volatile organic compounds, methods of analysis and authentication. *Plants*. **2022**, *11*, 789.
- [20] Benkhoud, H.; M'Rabet, Y.; Gara Ali, M.; Mezni, M.; Hosni, K. Essential oils as flavoring and preservative agents: Impact on volatile profile, sensory attributes, and the oxidative stability of flavored extra virgin olive oil. *J. Food Process. Pres.* **2022**, *46*, e15379.
- [21] Falleh, H.; Jemaa, M.B.; Saada, M.; Ksouri, R. Essential oils: A promising eco-friendly food preservative. *Food Chem.* **2020**, *330*, 127268.
- [22] Ersanli, C.; Tzora, A.; Skoufos, I.; Fotou, K.; Maloupa, E.; Gridoriadou, K.; Voidarou, C.; Zeugolis, D.I. The Assessment of Antimicrobial and Anti-Biofilm Activity of Essential Oils against *Staphylococcus aureus* Strains. *Antibiotics* **2023**, *12*, 384.
- [23] Kontogiorgis, C.; Ntella, M.; Mpompou, L.; Karallaki, F.; Athanasios, P.; Hadjipavlou-Litina, D.; Lazari, D. Study of the antioxidant activity of *Thymus sibthorpii* Bentham (Lamiaceae). *J. Enzyme Inhib. Med. Chem.* **2016**, *31*, 154-159.
- [24] Unalan, I.; Endlein, S.J.; Slavik, B.; Buettner, A.; Goldmann, W.H.; Detsch, R.; Boccaccini, A.R. Evaluation of electrospun poly ( $\epsilon$ -caprolactone)/gelatin nanofiber mats containing clove essential oil for antibacterial wound dressing. *Pharmaceutics* **2019**, *11*, 570.
- [25] Rezvani Ghomi, E.; Nourbakhsh, N.; Akbari Kenari, M.; Zare, M.; Ramakrishna, S. Collagen-based biomaterials for biomedical applications. *J. Biomed. Mater. Res.* **2021**, *109*, 1986-1999.

- [26] David, G. Collagen-based 3D structures-versatile, efficient materials for biomedical applications. In *Biopolymer-Based Formulations*, 1st ed.; Elsevier: Amsterdam, The Netherlands, **2020**; pp. 881-906.
- [27] Miyata, T.; Taira, T.; Noishiki, Y. Collagen engineering for biomaterial use. *Clin. Mater.* **1992**, *9*, 139-148.8.
- [28] Lee, C.H.; Singla, A.; Lee, Y. Biomedical applications of collagen. *Int. J. Pharm.* **2001**, *221*, 1-22.
- [29] Sorushanova, A.; Delgado, L.M.; Wu, Z.; Shologu, N.; Kshirsagar, A.; Raghunath, R.; Mullen, A.M.; Bayon, Y.; Pandit, A.; Raghunath, M.; et al. The collagen suprafamily: from biosynthesis to advanced biomaterial development. *Adv. Mater.* **2019**, *31*, 1801651.
- [30] Buehler, M.J. Nature designs tough collagen: explaining the nanostructure of collagen fibrils. *Proc. Natl. Acad. Sci.* **2006**, *103*, 12285-12290.
- [31] Amirrah, I.N.; Lokanathan, Y.; Zulkiflee, I.; Wee, M.M.R.; Motta, A.; Fauzi, M.B. A comprehensive review on collagen type I development of biomaterials for tissue engineering: From biosynthesis to bioscaffold. *Biomedicines.* **2022**, *10*, 2307.
- [32] Kong, W.; Lyu, C.; Liao, H.; Du, Y. Collagen crosslinking: effect on structure, mechanics and fibrosis progression. *Biomed. Mater.* **2021**, *16*, 062005.
- [33] Sallent, I.; Capella-Monsonís, H.; Zeugolis, D.I. Production and characterization of chemically cross-linked collagen scaffolds. In *Collagen: Methods and Protocols*, Springer: Berlin, Germany, **2019**; pp. 23-38.
- [34] Gough, J.E.; Scotchford, C.A.; Downes, S. Cytotoxicity of glutaraldehyde crosslinked collagen/poly (vinyl alcohol) films is by the mechanism of apoptosis. *Journal of Biomedical Materials Research: An Official Journal of The Society for Biomaterials, The Japanese Society for Biomaterials, and The Australian Society for Biomaterials and the Korean Society for Biomaterials* **2002**, *61*, 121-130.
- [35] Moshnikova, A.; Afanasyev, V.; Proussakova, O.; Chernyshov, S.; Gogvadze, V.; Beletsky, I. Cytotoxic activity of 1-ethyl-3-(3-dimethylaminopropyl)-carbodiimide is underlain by DNA interchain cross-linking. *Cell. Mol. Life Sci.* **2006**, *63*, 229-234.

- [36] Sanami, M.; Sweeney, I.; Shtein, Z.; Meirovich, S.; Sorushanova, A.; Mullen, A.M.; Mirafteb, M.; Shoseyov, O.; O'Dowd, C.; Pandit, A. The influence of poly (ethylene glycol) ether tetrasuccinimidyl glutarate on the structural, physical, and biological properties of collagen fibers. *J. Biomed. Mater. Res.* **2016**, 104, 914-922.
- [37] Delgado, L.M.; Fuller, K.; Zeugolis, D.I. Collagen cross-linking: biophysical, biochemical, and biological response analysis. *Tissue Eng. Part A.* **2017**, 23, 1064-1077.
- [38] Monaghan, M.; Browne, S.; Schenke-Layland, K.; Pandit, A. A collagen-based scaffold delivering exogenous microrna-29B to modulate extracellular matrix remodeling. *Mol. Ther.* **2014**, 22, 786-796.
- [39] Collin, E.C.; Grad, S.; Zeugolis, D.I.; Vinatier, C.S.; Clouet, J.R.; Guicheux, J.J.; Weiss, P.; Alini, M.; Pandit, A.S. An injectable vehicle for nucleus pulposus cell-based therapy. *Biomaterials.* **2011**, 32, 2862-2870.
- [40] Hass, V.; Luque-Martinez, I.V.; Gutierrez, M.F.; Moreira, C.G.; Gotti, V.B.; Feitosa, V.P.; Koller, G.; Otuki, M.F.; Loguercio, A.D.; Reis, A. Collagen cross-linkers on dentin bonding: Stability of the adhesive interfaces, degree of conversion of the adhesive, cytotoxicity and in situ MMP inhibition. *Dent. Mater. J.* **2016**, 32, 732-741.
- [41] Capella-Monsonís, H.; Coentro, J.Q.; Graceffa, V.; Wu, Z.; Zeugolis, D.I. An experimental toolbox for characterization of mammalian collagen type I in biological specimens. *Nat. Protoc.* **2018**, 13, 507-529.
- [42] Aker, S.D.; Tamburaci, S.; Tihminlioglu, F. Development of Cissus quadrangularis-Loaded POSS-Reinforced Chitosan-Based Bilayer Sponges for Wound Healing Applications: Drug Release and In Vitro Bioactivity. *ACS Omega.* **2023**, 8, 19674-19691.
- [43] Vyavahare, N.; Kulkarni, M.; Mashelkar, R. Zero order release from swollen hydrogels. *J. Membrane Sci.* **1990**, 54, 221-228.
- [44] Ata, S.; Rasool, A.; Islam, A.; Bibi, I.; Rizwan, M.; Azeem, M.K.; Iqbal, M. Loading of Cefixime to pH sensitive chitosan based hydrogel and investigation of controlled release kinetics. *Int. J. Biol. Macromol.* **2020**, 155, 1236-1244.8
- [45] Siepmann, J.; Peppas, N.A. Higuchi equation: Derivation, applications, use and misuse. *Int. J. Pharm.* **2011**, 418, 6-12.
- [46] Korsmeyer, R.W.; Gurny, R.; Doelker, E.; Buri, P.; Peppas, N.A. Mechanisms of solute release from porous hydrophilic polymers. *Int. J. Pharm.* **1983**, 15, 25-35.

- [47] Rehman, Q.; Akash, M.S.H.; Rasool, M.F.; Rehman, K. Role of kinetic models in drug stability. In *Drug Stability and Chemical Kinetics*, Springer: Berlin, Germany, **2020**; pp. 155-165.
- [48] Voidarou, C.; Antoniadou, M.; Rozos, G.; Alexopoulos, A.; Giorgi, E.; Tzora, A.; Skoufos, I.; Varzakas, T.; Bezirtzoglou, E. An in vitro study of different types of Greek honey as potential natural antimicrobials against dental caries and other oral pathogenic microorganisms. Case study simulation of oral cavity conditions. *Appl. Sci.* **2021**, *11*, 6318.
- [49] Coentro, J.Q.; Di Nubila, A.; May, U.; Prince, S.; Zwaagstra, J.; Järvinen, T.A.; Zeugolis, D.I. Dual drug delivery collagen vehicles for modulation of skin fibrosis in vitro. *Biomed. Mater.* **2022**, *17*, 025017.
- [50] Calderon, L.; Collin, E.; Murphy, M.; O'Halloran, D.; Pandit, A. Type II collagen-hyaluronan hydrogel-a step towards a scaffold for intervertebral disc tissue engineering. *Eur. Cells Mater.* **2010**, *20*, 134-148.
- [51] Murray, C.J.; Ikuta, K.S.; Sharara, F.; Swetschinski, L.; Aguilar, G.R.; Gray, A.; Han, C.; Bisignano, C.; Rao, P.; Wool, E. Global burden of bacterial antimicrobial resistance in 2019: a systematic analysis. *Lancet.* **2022**, *399*, 629-655.
- [52] Reygaert, W.C. An overview of the antimicrobial resistance mechanisms of bacteria. *AIMS Microbiol.* **2018**, *4*, 482.
- [53] Tang, K.W.K.; Millar, B.C.; Moore, J.E. Antimicrobial resistance (AMR). *Br. J. Biomed. Sci.* **2023**, *80*, 11387.
- [54] Jadimurthy, R.; Jagadish, S.; Nayak, S.C.; Kumar, S.; Mohan, C.D.; Rangappa, K.S. Phytochemicals as invaluable sources of potent antimicrobial agents to combat antibiotic resistance. *Life.* **2023**, *13*, 948.
- [55] Antoniadou, M.; Rozos, G.; Vaou, N.; Zaralis, K.; Ersanli, C.; Alexopoulos, A.; Dadamogia, A.; Varzakas, T.; Tzora, A.; Voidarou, C. Comprehensive Bio-Screening of Phytochemistry and Biological Capacity of Oregano (*Origanum vulgare*) and *Salvia triloba* Extracts against Oral Cariogenic and Food-Origin Pathogenic Bacteria. *Biomolecules.* **2024**, *14*, 619.
- [56] Voidarou, C.; Alexopoulos, A.; Tsinas, A.; Rozos, G.; Tzora, A.; Skoufos, I.; Varzakas, T.; Bezirtzoglou, E. Effectiveness of bacteriocin-producing lactic acid bacteria and bifidobacterium isolated from honeycombs against spoilage microorganisms and pathogens isolated from fruits and vegetables. *Appl. Sci.* **2020**, *10*, 7309.

- [57] Sundar, G.; Joseph, J.; John, A.; Abraham, A. Natural collagen bioscaffolds for skin tissue engineering strategies in burns: a critical review. *Int. J. Polym. Mater.* **2021**, *70*, 593-604.
- [58] Ersanli, C.; Tzora, A.; Skoufos, I.; Voidarou, C.; Zeugolis, D.I. Recent advances in collagen antimicrobial biomaterials for tissue engineering applications: a review. *Int. J. Mol. Sci.* **2023**, *24*, 7808.
- [59] Tsekoura, E.; Helling, A.; Wall, J.; Bayon, Y.; Zeugolis, D. Battling bacterial infection with hexamethylene diisocyanate cross-linked and Cefaclor-loaded collagen scaffolds. *Biomed. Mater.* **2017**, *12*, 035013.
- [60] Li, Z.; Lu, F.; Liu, Y. A Review of the Mechanism, Properties, and Applications of Hydrogels Prepared by Enzymatic Cross-linking. *J. Agric. Food Chem.* **2023**, *71*, 10238-10249.
- [61] Xiang, C.; Wang, Z.; Zhang, Q.; Guo, Z.; Li, X.; Chen, W.; Wei, X.; Li, P. Tough physically crosslinked poly (vinyl alcohol)-based hydrogels loaded with collagen type I to promote bone regeneration in vitro and in vivo. *Int. J. Biol. Macromol.* **2024**, *261*, 129847.
- [62] Sánchez-Cid, P.; Alonso-González, M.; Jiménez-Rosado, M.; Benhnia, M.R.E.I.; Ruiz-Mateos, E.; Ostos, F.J.; Romero, A.; Perez-Puyana, V.M. Effect of different crosslinking agents on hybrid chitosan/collagen hydrogels for potential tissue engineering applications. *Int. J. Biol. Macromol.* **2024**, *263*, 129858.
- [63] Dattilo, M.; Patitucci, F.; Prete, S.; Parisi, O.I.; Puoci, F. Polysaccharide-based hydrogels and their application as drug delivery systems in cancer treatment: A review. *J. Funct. Biomater.* **2023**, *14*, 55.
- [64] Bindi, B.; Perioli, A.; Melo, P.; Mattu, C.; Ferreira, A.M. Bioinspired Collagen/Hyaluronic Acid/Fibrin-Based Hydrogels for Soft Tissue Engineering: Design, Synthesis, and In Vitro Characterization. *J. Funct. Biomater.* **2023**, *14*, 495.
- [65] Peppas, N.A.; Khare, A.R. Preparation, structure and diffusional behavior of hydrogels in controlled release. *Adv. Drug Deliv. Rev.* **1993**, *11*, 1-35.
- [66] Unalan, I.; Schrufer, S.; Schubert, D.W.; Boccaccini, A.R. 3D-printed multifunctional hydrogels with phytotherapeutic properties: Development of essential oil-incorporated ALG-XAN hydrogels for wound healing applications. *ACS Biomater. Sci. Eng.* **2023**, *9*, 4149-4167.
- [67] Cheng, C.; Wu, Z.; McClements, D.J.; Zou, L.; Peng, S.; Zhou, W.; Liu, W. Improvement on stability, loading capacity and sustained release of rhamnolipids modified curcumin liposomes. *Colloids Surf. B.* **2019**, *183*, 110460.

- [68] Poolman, J.T.; Anderson, A.S. Escherichia coli and Staphylococcus aureus: leading bacterial pathogens of healthcare associated infections and bacteremia in older-age populations. *Expert Rev. Vaccines*. **2018**, *17*, 607-618.
- [69] Ersanli, C.; Tzora, A.; Voidarou, C.; Skoufos, S.; Zeugolis, D.I.; Skoufos, I. Biodiversity of Skin Microbiota as an Important Biomarker for Wound Healing. *Biology*. **2023**, *12*, 1187.
- [70] Nelli, A.; Voidarou, C.; Venardou, B.; Fotou, K.; Tsinas, A.; Bonos, E.; Fthenakis, G.C.; Skoufos, I.; Tzora, A. Antimicrobial and Methicillin Resistance Pattern of Potential Mastitis-Inducing Staphylococcus aureus and Coagulase-Negative Staphylococci Isolates from the Mammary Secretion of Dairy Goats. *Biology*. **2022**, *11*, 1591.
- [71] Bourgou, S.; Pichette, A.; Marzouk, B.; Legault, J. Bioactivities of black cumin essential oil and its main terpenes from Tunisia. *S. Afr. J. Bot.* **2010**, *76*, 210-216.
- [72] Bakkali, F.; Averbeck, S.; Averbeck, D.; Idaomar, M. Biological effects of essential oils—a review. *Food Chem. Toxicol.* **2008**, *46*, 446-475.
- [73] Teixeira, B.; Marques, A.; Ramos, C.; Neng, N.R.; Nogueira, J.M.; Saraiva, J.A.; Nunes, M.L. Chemical composition and antibacterial and antioxidant properties of commercial essential oils. *Ind. Crop. Prod.* **2013**, *43*, 587-595.
- [74] Aras, C.; Tümay Özer, E.; Göktalay, G.; Saat, G.; Karaca, E. Evaluation of Nigella sativa oil loaded electrospun polyurethane nanofibrous mat as wound dressing. *J. Biomater. Sci. Polym. Ed.* **2021**, *32*, 1718-1735.
- [75] Lo, S.; Fauzi, M.B. Current update of collagen nanomaterials—fabrication, characterisation and its applications: A review. *Pharmaceutics*. **2021**, *13*, 316.
- [76] Antezana, P.E.; Municoy, S.; Pérez, C.J.; Desimone, M.F. Collagen Hydrogels Loaded with Silver Nanoparticles and Cannabis Sativa Oil. *Antibiotics*. **2021**, *10*, 1420.
- [77] Pugliese, E.; Sallent, I.; Ribeiro, S.; Trotier, A.; Korntner, S.H.; Bayon, Y.; Zeugolis, D.I. Development of three-layer collagen scaffolds to spatially direct tissue-specific cell differentiation for enthesis repair. *Mater. Today Bio.* **2023**, *19*, 100584.

## **Chapter 4: Summary, limitations and future perspectives**

#### 4.1. Summary of the study and general conclusions

Antimicrobial resistance (AMR) is one of the drastically increasing global health problem, resulting in the misuse and overuse of the conventional antibiotics which lead to generation of antimicrobial resistant microorganisms [1,2]. AMR has led to increased mortality rates, prolonged stay in hospital, and high healthcare costs [3,4]. AMR has been reported as one of the top ten global health concerns by World Health Organization while emphasizing the urgent need of the development of alternative and safer antimicrobial therapies [5] in order to combat antimicrobial resistant pathogens such as *S. aureus*, and *E.coli*. Among the alternative antimicrobial agents substitute for conventional antibiotics, essential oils have gained attention thanks to their broad-spectrum antimicrobial activity due to various bioactive compounds present in their structure such as terpenes, terpenoids, and phenolic compounds [6-9]. The promising alternative antimicrobial agent candidates, essential oils may exhibit their activity by destroying bacterial cell membrane, preventing cell metabolic activity, eliminating biofilm formation [10,11]. Although they show superior biological activities, their high volatility, low stability, and hydrophobicity may decrease their efficacy and safety [12].

The incorporation of essential oils into biomaterial formulations has gained significant attention in recent years in order to overcome those drawbacks. A developed biomaterial formulation can provide protective environment for the essential oils while enhancing their stability, controlled release and bioavailability. Among a wide variety of biomaterial formulations, collagen hydrogels have been reported as particularly effective for incorporating essential oils to use in tissue engineering applications. Collagen, a natural protein and main component of extracellular matrix of connective tissues, presents superior biodegradability and biocompatibility which make them ideal candidate for biomedical and tissue engineering applications [13-18]. When used in the hydrogel form, collagen can encapsulate essential oils, ensure sustained and controlled release whilst reducing any cytotoxic effect of essential oils. Besides that, this approach not only overcomes the drawbacks of the essential oils but also leverages the inherent properties of collagen to promote tissue regeneration.

Herein, *Thymus sibthorpii* essential oil was incorporated into optimized starPEG crosslinked collagen hydrogels and the properties of developed medical devices were investigated.

Firstly, antimicrobial and anti-biofilm activity of four different essential oils (*Thymus sibthorpii*, *Origanum vulgare*, *Salvia fruticosa*, *Crithmum maritimum*) were screened in detail. The main conclusions obtained from this experimental study (**Chapter 2**) were:

1. *Thymus sibthorpii* was found to be the most effective EO against tested bacterial strains, followed by *Origanum vulgare* EO.
2. *Thymus sibthorpii* and *origanum vulgare* showed higher antibacterial activity than most of the reference antimicrobials.
3. 5 % v/v DMSO which was used for dissolving EOs did not show any inhibitory effect on bacterial growth. Therefore, it can be clearly said that observed antibacterial activities were achieved only by EOs.
4. All EOs displayed significant biofilm inhibition even at their half MIC.
5. Although gentamicin sulfate is mostly used antimicrobial agent in commercial antibacterial dressing products, it could not inhibit biofilm formation.

Afterwards, collagen type I hydrogels were developed by crosslinking six different starPEG molecules which possess different arm numbers, and molecular weights at 0.5, 1, 2, 5 mM concentrations. The optimization study was conducted by assessing the stability of fabricated hydrogels by free amine quantification, and enzymatic degradation assays. Accordingly, the optimally starPEG-crosslinked collagen hydrogels were loaded with 0,5, 1, 2 v% of *Thymus sibthorpii* EO, and the release profile and release kinetics of the EO were examined. Finally, the antimicrobial activity of the developed composite hydrogels was assessed against *S. aureus*, and *E. coli*, whilst their cytocompatibility was examined for NIH-3T3 fibroblasts. The main conclusions obtained from this experimental study (**Chapter 3**) were:

1. 0.5, 1 and 2 mM of starPEG concentrations decreased the free amine percentage more than glutaraldehyde.
2. 5 mM starPEG concentration was found out of the effective concentration range. In other words, an effective plateau was observed between 0.5 and 2 mM of each tested starPEG crosslinker.
3. starPEG functionalized hydrogels did not fully degraded within 24 hours.

4. 0.5 mM of 4SP, pentaerythritol, 10 kDa; 4SP, pentaerythritol, 20 kDa; and 8SP, hexaglycerol, 20 kDa crosslinkers were found the optimal crosslinker to functionalize collagen hydrogels.
5. The non-crosslinked hydrogels demonstrated burst release that was completely released EO within a couple of hours.
6. starPEG functionalized *Thymus sibthorpii* EO-loaded collagen hydrogels demonstrated controlled and sustained release.
7. Hixson-Crowell model did not fit any of the experimental group, whilst the zero-order, first-order, Higuchi and Korsmeyer-Peppas models fitted to different experimental groups.
8. The release mechanism of EO from crosslinked hydrogels obeyed the Fickian diffusion according to the release exponent (n) values calculated by using the Korsmeyer-Peppas model.
9. The EO-loaded composite antibacterial collagen hydrogels showed sufficient antimicrobial activity on *S. aureus* and *E. coli*. However, they showed more resistance to gram-negative *E. coli*.
10. Collagen hydrogels containing 0.5 v% of EO did not show a statistical difference compared to positive control penicillin (for gram-positive bacteria), and enrofloxacin (for gram-negative bacteria) ( $p < 0.05$ ). Hence, 0.5 v% concentration of *Thymus sibthorpii* EO was accepted as the optimal concentration to incorporate collagen scaffolds.
11. All developed 0.5 v% *Thymus sibthorpii* EO including composite hydrogels were found cytocompatible with 3T3-NIH fibroblasts.

Therefore, in this study, we demonstrated the potential of the essential oils as safer and alternative antimicrobial agent substituted for antibiotics, the effectiveness of *Thymus sibthorpii* EO loaded collagen type I hydrogels in purpose of using in tissue engineering applications.

## 4.2. Future studies

The screening performed in our study concluded that *Thymus sibthorpii* EO has great potential as safer antimicrobial and anti-biofilm agent. Besides, this EO showed higher activity on the inhibition of various *S. aureus* strains compared to widely used antimicrobial agent, gentamicin sulfate. These outcomes open new research frontiers in order to assess anti-inflammatory and antioxidant activity of *Thymus sibthorpii* EO to inquire its undiscovered potential. Moreover, understanding of any synergetic effect of this EO with the combination of other antimicrobial agents such as herbal extracts, nanoparticles could open a new research area.

In the present study, we developed *Thymus sibthorpii* EO incorporated collagen type I hydrogel as a potential antibacterial medical device for infected tissue regeneration purposes. In the context of the future perspective of this study, rheological and/or mechanical analyzes of the developed hydrogels might be studied to specialize the antibacterial biomaterials according to the specific target tissue (e.g., skin, bone, cartilage). Besides, this perspective could give better understanding about any positive or negative effect of EO on the mechanical strength of the hydrogels. We achieved great antimicrobial action on gram-positive *S. aureus* and gram-negative *E.coli* thanks to the presence of *Thymus sibthorpii* EO. However, the antimicrobial activity of the developed composite hydrogels might be increased by the addition of secondary polymer which demonstrate antimicrobial activity within its nature such as chitosan.

### 4.3. References

- [1] Harbarth, S.; Balkhy, H.H.; Goossens, H.; Jarlier, V.; Kluytmans, J.; Laxminarayan, R.; Saam, M.; Van Belkum, A.; Pittet, D. Antimicrobial resistance: One world, one fight! *Antimicrob. Resist. Infect. Control.* 2015, 49.
- [2] Rozos, G.; Skoufos, I.; Fotou, K.; Alexopoulos, A.; Tsinas, A.; Bezirtzoglou, E.; Tzora, A.; Voidarou, C. Safety Issues Regarding the Detection of Antibiotics Residues, Microbial Indicators and Somatic Cell Counts in Ewes' and Goats' Milk Reared in Two Different Farming Systems. *Appl. Sci.* 2022, 12, 1009.
- [3] Christaki, E.; Marcou, M.; Tofarides, A. Antimicrobial resistance in bacteria: Mechanisms, evolution, and persistence. *J. Mol. Evol.* 2020, 88, 26–40.
- [4] Liu, W.; Yang, C.; Gao, R.; Zhang, C.; Ou-Yang, W.; Feng, Z.; Zhang, C.; Pan, X.; Huang, P.; Kong, D. Polymer Composite Sponges with Inherent Antibacterial, Hemostatic, Inflammation-Modulating and Proregenerative Performances for Methicil-lin-Resistant *Staphylococcus aureus*-Infected Wound Healing. *Adv. Healthc. Mater* 2021, 10, 2101247.
- [5] Salam, M.A.; Al-Amin, M.Y.; Salam, M.T.; Pawar, J.S.; Akhter, N.; Rabaan, A.A.; Alqumber, M.A. Antimicrobial resistance: a growing serious threat for global public health. *Healthcare.* 2023, 11, 1946.
- [6] Stefanakis, M.K.; Touloupakis, E.; Anastasopoulos, E.; Ghanotakis, D.; Katerinopoulos, H.E.; Makridis, P. Antibacterial activity of essential oils from plants of the genus *Origanum*. *Food Control* 2013, 34, 539–546.
- [7] Cimino, C.; Maurel, O.M.; Musumeci, T.; Bonaccorso, A.; Drago, F.; Souto, E.M.B.; Pignatello, R.; Carbone, C. Essential oils: Pharmaceutical applications and encapsulation strategies into lipid-based delivery systems. *Pharmaceutics* 2021, 13, 327.
- [8] Saad, N.Y.; Muller, C.D.; Lobstein, A. Major bioactivities and mechanism of action of essential oils and their components. *Flavour Fragr. J.* 2013, 28, 269–279.
- [9] Masyita, A.; Sari, R.M.; Astuti, A.D.; Yasir, B.; Rumata, N.R.; Emran, T.B.; Nainu, F.; Simal-Gandara, J. Terpenes and terpe-noids as main bioactive compounds of essential oils, their roles in human health and potential application as natural food preservatives. *Food Chem. X* 2022, 13, 100217.

- [10] da Silva, B.D.; Bernardes, P.C.; Pinheiro, P.F.; Fantuzzi, E.; Roberto, C.D. Chemical composition, extraction sources and action mechanisms of essential oils: Natural preservative and limitations of use in meat products. *Meat Sci.* 2021, 176, 108463.
- [11] Bhavaniramy, S.; Vishnupriya, S.; Al-Aboody, M.S.; Vijayakumar, R.; Baskaran, D. Role of essential oils in food safety: An-timicrobial and antioxidant applications. *GOST* 2019, 2, 49–55.
- [12] Unalan, I.; Endlein, S.J.; Slavik, B.; Buettner, A.; Goldmann, W.H.; Detsch, R.; Boccaccini, A.R. Evaluation of electrospun poly ( $\epsilon$ -caprolactone)/gelatin nanofiber mats containing clove essential oil for antibacterial wound dressing. *Pharmaceutics* 2019, 11, 570.
- [13] Rezvani Ghomi, E.; Nourbakhsh, N.; Akbari Kenari, M.; Zare, M.; Ramakrishna, S. Collagen-based biomaterials for biomedical applications. *J. Biomed. Mater. Res.* 2021, 109, 1986-1999.
- [14] David, G. Collagen-based 3D structures-versatile, efficient materials for biomedical applications. In *Biopolymer-Based Formulations*, 1st ed.; Elsevier: Amsterdam, The Netherlands, 2020; pp. 881-906.
- [15] Miyata, T.; Taira, T.; Noishiki, Y. Collagen engineering for biomaterial use. *Clin. Mater.* 1992, 9, 139-148.
- [16] Lee, C.H.; Singla, A.; Lee, Y. Biomedical applications of collagen. *Int. J. Pharm.* 2001, 221, 1-22.
- [17] Soroushanova, A.; Delgado, L.M.; Wu, Z.; Shologu, N.; Kshirsagar, A.; Raghunath, R.; Mullen, A.M.; Bayon, Y.; Pandit, A.; Raghunath, M.; et al. The collagen suprafamily: from biosynthesis to advanced biomaterial development. *Adv. Mater.* 2019, 31, 1801651.
- [18] Buehler, M.J. Nature designs tough collagen: explaining the nanostructure of collagen fibrils. *Proc. Natl. Acad. Sci.* 2006, 103, 12285-12290.

## **Chapter 5: Scientific outputs**

## 5.1. Published manuscripts

**Ersanli, C.,** Skoufos, I., Fotou, K., Tzora, A., Bayon, Y., Mari, D., Sarafi, E., Nikolaou, K., Zeugolis, D.I., 2025. Release profile and antibacterial activity of Thymus sibthorpii essential oil-incorporated, optimally stabilized type I collagen hydrogels, *Bioengineering* 2025, 12(1), 89. <https://doi.org/10.3390/bioengineering12010089>

**Ersanli, C.,** Voidarou, C., Tzora, A., Fotou, K., Zeugolis, D.I. and Skoufos, I., 2023. Electrospun Scaffolds as Antimicrobial Herbal Extract Delivery Vehicles for Wound Healing. *Journal of Functional Biomaterials*, 14(9), 481. <https://doi.org/10.3390/jfb14090481>

**Ersanli, C.,** Tzora, A., Voidarou, C., Skoufos, S., Zeugolis, D.I. and Skoufos, I., 2023. Biodiversity of skin microbiota as an important biomarker for wound healing. *Biology*, 12(9), 1187. <https://doi.org/10.3390/biology12091187>

**Ersanli, C.,** Tzora, A., Skoufos, I., Voidarou, C. and Zeugolis, D.I., 2023. Recent advances in collagen antimicrobial biomaterials for tissue engineering applications: a review. *International Journal of Molecular Sciences*, 24(9), 7808. <https://doi.org/10.3390/ijms24097808>

**Ersanli, C.,** Tzora, A., Skoufos, I., Fotou, K., Maloupa, E., Grigoriadou, K., Voidarou, C. and Zeugolis, D.I., 2023. The assessment of antimicrobial and anti-biofilm activity of essential oils against *Staphylococcus aureus* strains. *Antibiotics*, 12(2). <https://doi.org/10.3390/antibiotics12020384>

## **5.2. Oral presentations**

**Ersanli, C.**, Bayon, Y., Skoufos, I., Tzora, A., Zeugolis, D. I. Pharmacokinetics, antimicrobial and biological properties of essential oil-loaded collagen hydrogels, United Kingdom Society for Biomaterials Annual Conference 2023, Belfast/Northern Ireland, 20-21 June 2023, book of abstracts, p. 81.

## **5.3. Poster presentations**

**Ersanli, C.**, Bayon, Y., Skoufos, I., Tzora, A., Zeugolis, D. I. Characterization of antimicrobial and physicochemical properties of essential oil-loaded collagen type I hydrogels, 33rd Annual Conference of the European Society for Biomaterials, Davos/Switzerland, 4-8 September 2023, PoB. 1053, p. 110.

## **Appendices**

**A. General workflow**

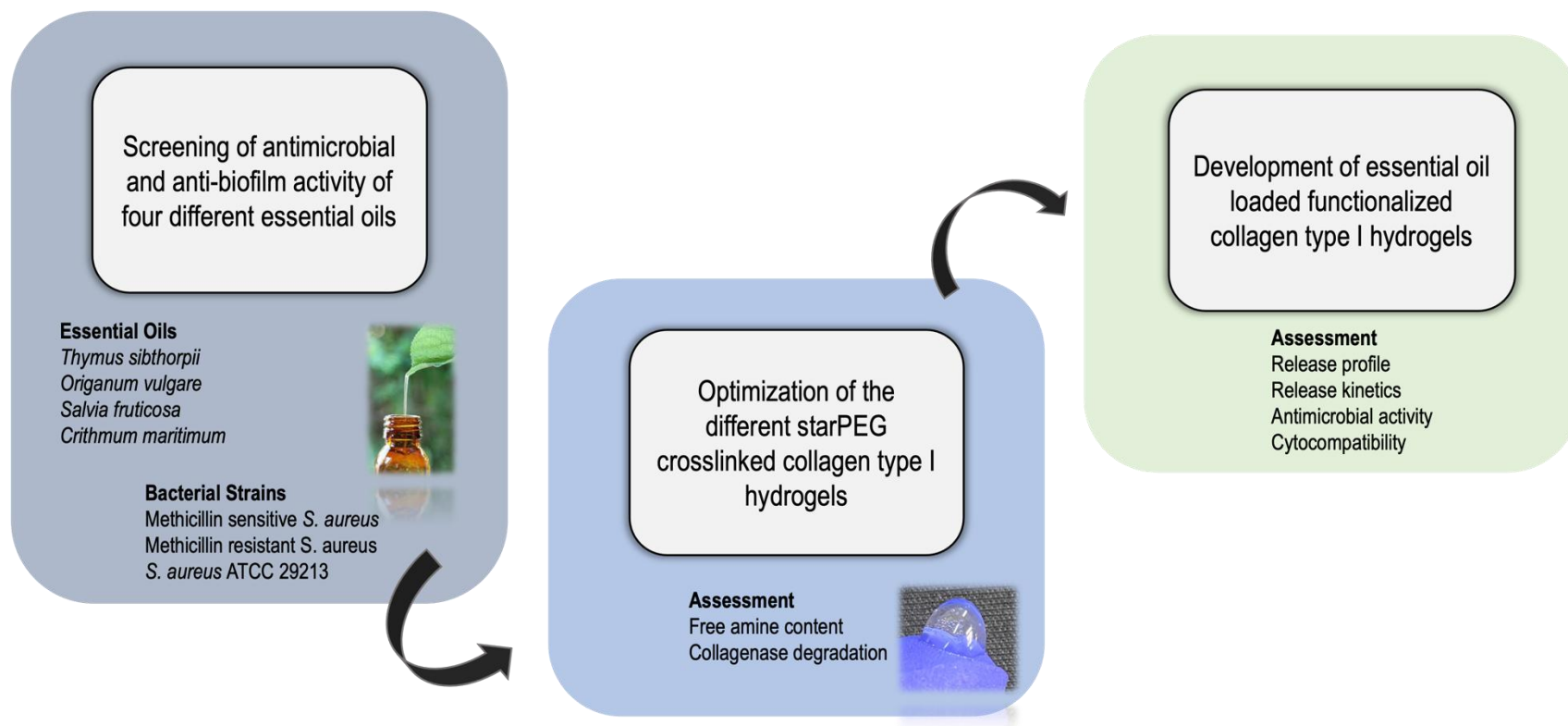


**Figure A.1.** Objectives and overall workflow of the study.

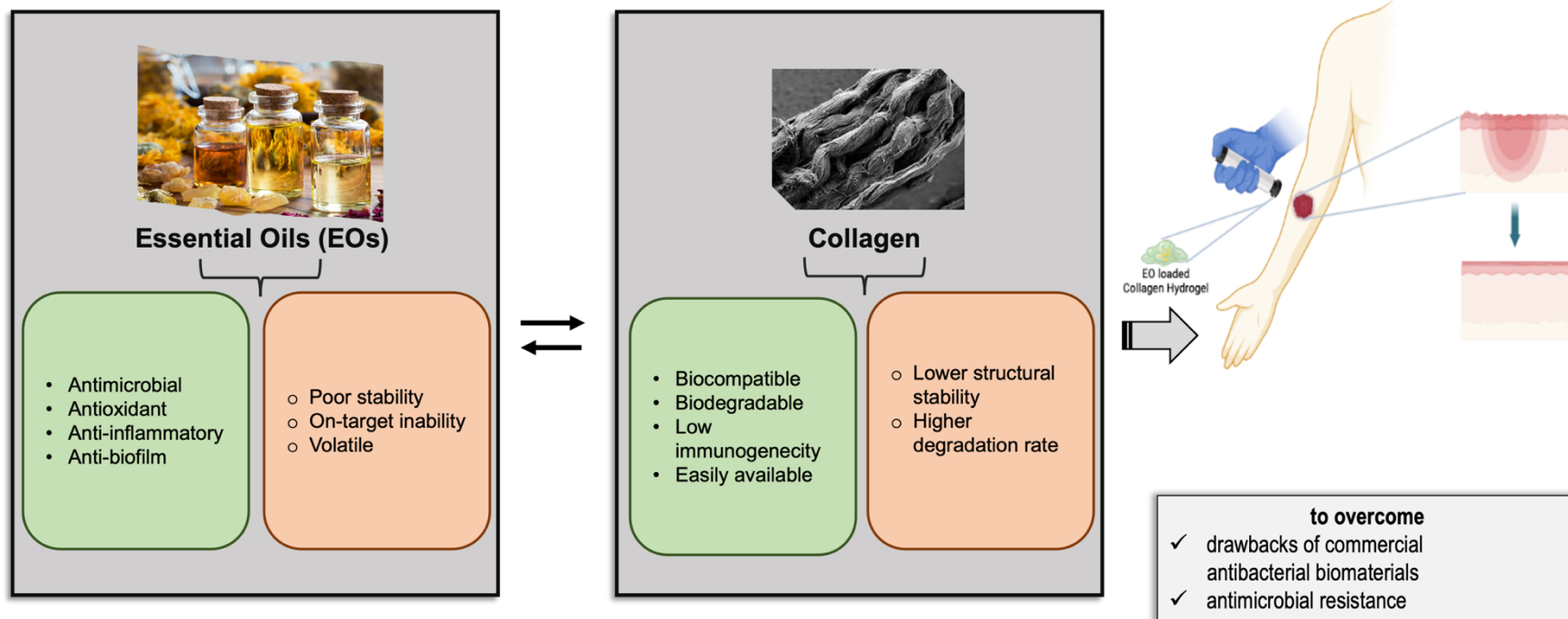


Figure A.2. Schematic illustration of the state of art of the work.

**B. List of consumables**

<b>Reagent</b>	<b>Supplier</b>
Mueller-Hinton broth	Honeywell, Fluka™, Spain
Tryptic soy broth	Sigma Aldrich, Athens, Greece
Mueller-Hinton agar	Oxoid, Hampshire, UK
MacConkey agar	Oxoid, Hampshire, UK
Blood agar base	Honeywell, Fluka™, India
2,3,5-triphenyl tetrazolium chloride	Sigma Aldrich, Athens, Greece
Glucose anhydrous	Sigma Aldrich, Athens, Greece
Gentian violet	Sigma Aldrich, Athens, Greece
Ethanol	Honeywell, Fluka™, Germany
Methanol	Honeywell, Fluka™, Germany
Whatman paper N.1 discs, 6 mm	Cytiva, China
Penicillin G antimicrobial susceptibility discs	Oxoid, Hampshire, UK
Enrofloxacin antimicrobial susceptibility discs	Oxoid, Hampshire, UK
Gentamicin sulfate	Fagron, Austin, TX, USA
Tetracycline antimicrobial susceptibility discs	Oxoid, Hampshire, UK
Cefaclor antimicrobial susceptibility discs	Oxoid, Hampshire, UK
<i>Staphylococcus aureus</i> ATCC® 29213	American Type Culture Collection, USA
<i>Escherichia coli</i> ATCC® 25922	American Type Culture Collection, USA
Collagen type I	Medtronic, France
4arm PEG Succinimidyl Glutarate, pentaerythritol (10 and 20 kDa)	JenKem Technology, Allen, TX, USA
8arm PEG Succinimidyl Glutarate, hexaglycerol (10 and 20 kDa)	JenKem Technology, Allen, TX, USA
8arm PEG Succinimidyl Glutarate, tripentaerythritol (10 and 20 kDa)	JenKem Technology, Allen, TX, USA
Phosphate buffered saline	Sigma Aldrich, Athens, Greece
Sodium hydroxide	Sigma Aldrich, Athens, Greece
Sodium bicarbonate	Sigma Aldrich, Athens, Greece
Calcium chloride	Sigma Aldrich, Athens, Greece
Glutaric dialdehyde	Thermo Fisher Scientific, Athens, Greece
Acetic acid	Honeywell, Fluka™, Germany
Hydrochloric acid	Honeywell, Fluka™, Germany

2,4,6-Trinitrobenzene sulfonic acid, TNBSA	Thermo Fisher Scientific, Athens, Greece
Sodium dodecyl sulfate	Thermo Fisher Scientific, Athens, Greece
Glycine white crystals	Thermo Fisher Scientific, Athens, Greece
Collagenase type II from <i>Clostridium histolyticum</i> , Gibco™	Thermo Fisher Scientific, Athens, Greece
Tris-base	Thermo Fisher Scientific, Athens, Greece
Pierce™ BCA protein assay kit	Thermo Fisher Scientific, Athens, Greece
NIH-3T3 mouse fibroblast cell line	American Type Culture Collection, USA
Dulbecco's Modified Eagle Medium-high glucose	Sigma Aldrich, Athens, Greece
Fetal bovine serum	Sigma Aldrich, Athens, Greece
Penicillin-streptomycin	Sigma Aldrich, Athens, Greece
Trypan blue	Sigma Aldrich, Athens, Greece
Dimethyl sulfoxide	Sigma Aldrich, Athens, Greece
Dulbecco's Phosphate Buffered Saline	Sigma Aldrich, Athens, Greece
Trypsin-EDTA	Thermo Fisher Scientific, Athens, Greece
alamarBlue™ assay kit, Invitrogen™	Thermo Fisher Scientific, Athens, Greece
Quant-iT™ PicoGreen™ dsDNA assay kit, Invitrogen™	Thermo Fisher Scientific, Athens, Greece
Nuclease-free water	Qiagen, Hilden, Germany
T25, T75 and T175 culture flasks	Sarstedt, Nümbrecht, Germany
Microcentrifuge tubes, 1.5 ml and 2ml	Sarstedt, Nümbrecht, Germany
Petri dishes	Sarstedt, Nümbrecht, Germany
24, 48 and 96 well plates	Sarstedt, Nümbrecht, Germany
Falcon® tubes, 15 ml and 50 ml	Sarstedt, Nümbrecht, Germany
Cell culture pipettes, 5, 10, and 25 ml	Sarstedt, Nümbrecht, Germany

## C. List of protocols

### C.1. Antimicrobial activity

#### C.1.1. Kirby-Bauer disc diffusion assay

1. Prepare collagen type I hydrogels (300  $\mu$ L) and sterilize them via UV irradiation for 1 h.
2. Grow *S. aureus* and *E. coli* cells overnight at 37 °C on the blood agar, and MacConkey agar, respectively.
3. Prepare an inoculum in a sterile saline solution by adjusting the McFarland unit to 0.5 ( $\sim 1 \times 10^8$  CFU/mL) with fresh colonies.
4. Immediately spread out the prepared inoculum on dry Mueller–Hinton agar plates.
5. Place the 6 mm diameter sterile Whatman paper N.1 discs on the Mueller–Hinton agar plates.
6. Add 15  $\mu$ L of essential oil to each Whatman paper disc or directly place the sterilized hydrogels on the Mueller–Hinton agar plates.
7. Leave the plates to air dry for half an hour.
8. Incubate the prepared plates at 37 °C 20-22 h.
9. Take the images of each plate, and measure inhibition zone diameters at the end of the incubation period.

#### C.1.2. Broth microdilution assay

1. Grow *S. aureus* and *E. coli* cells overnight at 37 °C on the blood agar, and MacConkey agar, respectively.
2. Prepare inoculum in a sterile saline solution at the final concentration of  $5 \times 10^5$  CFU/mL using fresh colonies.
3. Define the first and last wells in a related row of 96-well plates as sterility and growth control, respectively.
4. Place only tested antimicrobial agent into the sterility control well, and only inoculum into the growth control well.
5. Perform serial dilution by transferring 100  $\mu$ L of well-mixed EO suspension to the other.
6. Add 100  $\mu$ L of freshly prepared inoculum to the wells, except for the sterility control well.
7. Adjust the concentration range between 100% and 0.0488% (v/v) for essential oils and between 128 and 0.000488  $\mu$ g/mL for reference antibiotics.
8. Incubate 96-well plates in a horizontally shaking incubator at 37 °C and 75 rpm for 20 h.

9. Add 1% (w/v) of triphenyl tetrazolium chloride, TTC Gram stain transferring to each well.
10. Re-incubate 96-well plates for 2 h.
11. Record the minimum inhibitory concentration (MIC) of each tested antimicrobial agent as the concentration of the well just before the first red-colored well which indicates the living cells.

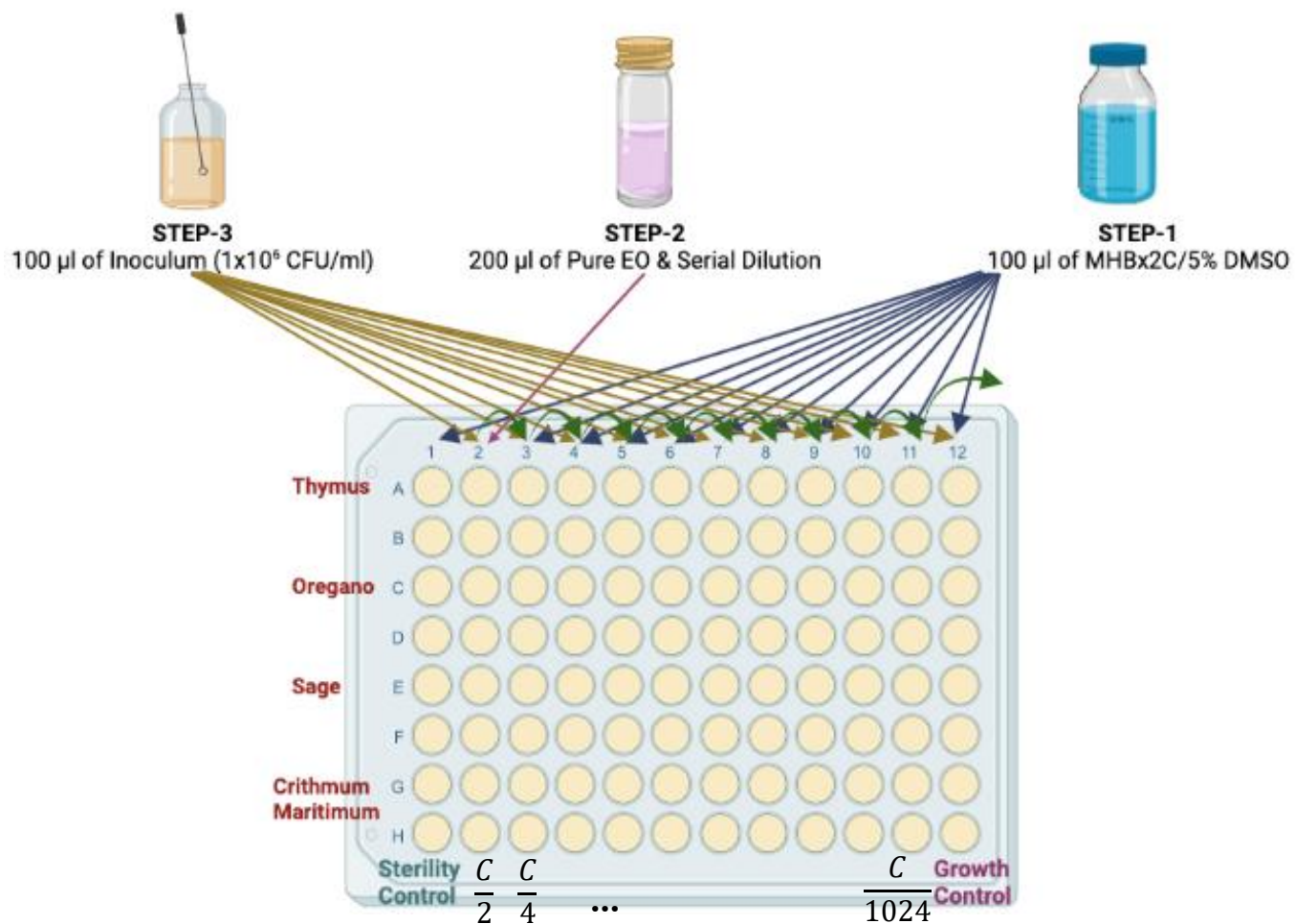


Figure C.1.2.1. Indicative experimental procedure of broth microdilution assay.

## C.2. Anti-biofilm activity

### C.2.1. Microtiter plate biofilm assay

1. Add 100  $\mu\text{L}$  of each essential oil or antibiotics at x4 MIC, x2 MIC, MIC,  $\frac{1}{2}$  MIC concentrations.
2. Add 100  $\mu\text{L}$  of diluted inoculum.
3. Incubate the plates at 37 °C for 20-24 h without agitation, allowing the adherence of bacteria onto the surface/wall of the wells.
4. Dump out cells by turning the plate over and shaking out the liquid on the paper towel.
5. Wash the wells twice with 250  $\mu\text{l}$  of de-ionized water (DIW) in order to remove planktonic bacteria and discard it by turning the plate over and shaking out the water.
6. Fix the attached bacteria with 200  $\mu\text{l}$  of pure methanol for 15 min.
7. Empty the plates and leave them to dry at room temperature for 1 h.
8. Stain the cells with 200  $\mu\text{l}$  of 0.4% w/v crystal violet used for Gram staining per well for 5 min.
9. Rinse off the excess stain by placing the plate under gently running tap water.
10. Resolubilize the dye bound to the adherent *Staphylococcus* cells with 160  $\mu\text{l}$  of 33% (v/v) glacial acetic acid.
11. Mix each well carefully and transfer 100  $\mu\text{l}$  of resolubilized cell suspension to new plate.
12. Take the pictures of plates for qualitative assessment.
13. Read the optical density (OD) of each plate at 570 nm or 630 nm. Readout at 630 nm may help to observe overflow result problems.
14. Evaluate the biofilm inhibition percentages of each antimicrobial agent using the following equation.

$$\text{Inhibition \%} = \frac{OD_{\text{Positive Control}} - OD_{\text{Experimental}}}{OD_{\text{Positive Control}}} \times 100$$

### C.3. Fabrication of collagen type I hydrogels

Note: All steps were carried out on the ice to avoid the denaturation and/or pre-polymerization of the collagen.

1. Prepare collagen stock solution (7.5 mg/mL) by dissolving in 0.05 M of acetic acid.
2. Add 70  $\mu\text{L}$  of 10x PBS in 2 mL microcentrifuge tube which was used as mold.
3. Add 7  $\mu\text{L}$  of 1 N NaOH and mix well by pipetting up and down.
4. Add 200  $\mu\text{L}$  of collagen stock solution (7.5 mg/mL) to have the final collagen concentration of 5 mg/mL. Then, mix well by pipetting up and down.
5. Add required volume of stock crosslinker solution. (For example, for the 0.5 mM of final crosslinker concentration, add 7.5  $\mu\text{L}$  of 20 mM of stock crosslinker solution.)
6. Add the required volume of essential to adjust its desired concentration (0.5, 1, 2 v%).
7. (If needed) Top up the solution to the 300  $\mu\text{L}$ .
8. Check the pH of the solution. If it is not in the range of 7.1-7.4, add 0.5  $\mu\text{L}$  of 1 N NaOH till adjusting the pH.
9. Incubate samples at 37 °C for 1h.

**Table C.3. 1.** Collagen type I hydrogel preparation.

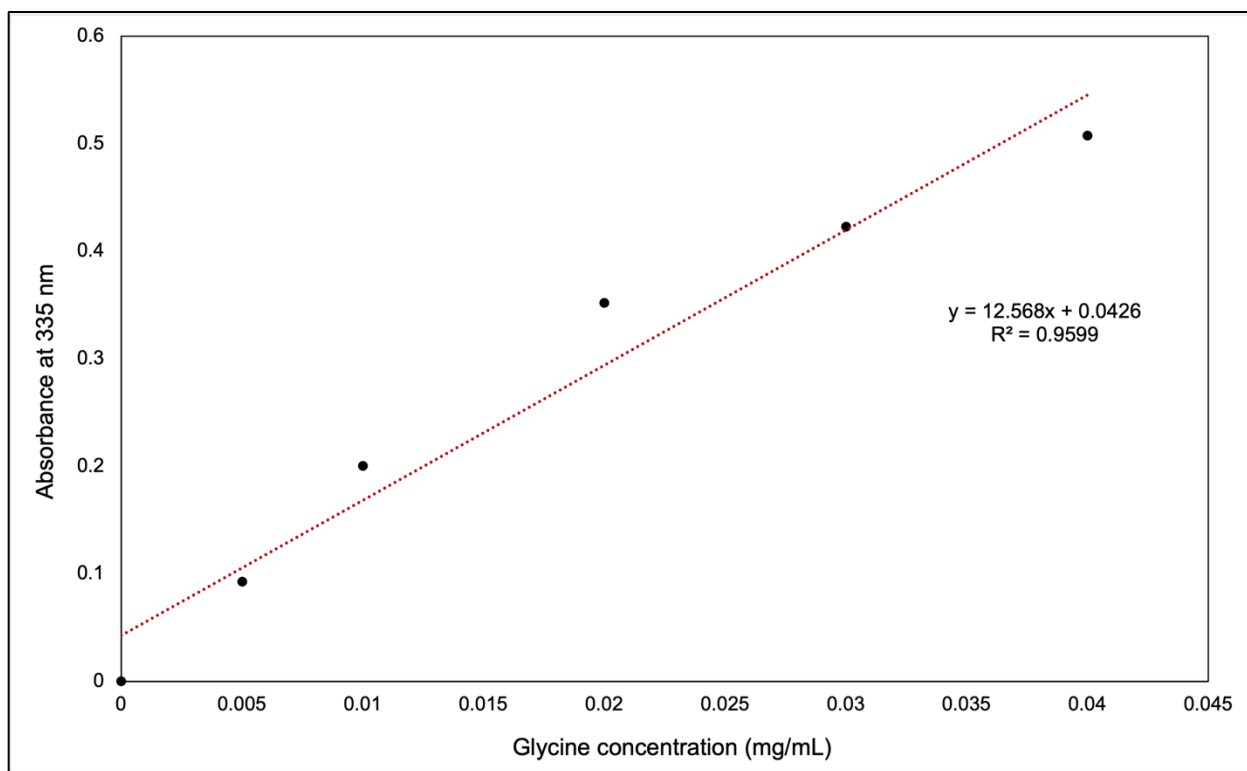
<b>Component</b>	<b>Order</b>	<b>Concentration</b>	<b>Volume</b>
10x PBS	1		70 $\mu$ L
NaOH	2	1 N	7 $\mu$ L
Collagen type I	3	5 mg/mL	200 $\mu$ L
starPEG	4	0.5, 1, 2, 5 mM	10, 20, 40, 100 $\mu$ L
NaOH	5	1 N	Dropwise (if needed)
<i>Thymus sibthorpii</i> EO	6	0.5, 1, 2 v%	1.5, 3, 6 $\mu$ L
1x PBS	7		Remaining volume (if needed)

**C.4. Quantification of free amines by TNBSA assay**

1. Prepare collagen type I hydrogels (300  $\mu$ L).
2. Place hydrogels into labelled 2 mL microcentrifuge tubes.
3. Prepare standard curve solution with the known concentration of glycine (Table C.4.1).
4. Add 500  $\mu$ L of each standard curve solution into labelled 2 mL microcentrifuge tubes.
5. Add 500  $\mu$ L of 0.1 M sodium bicarbonate solution into each hydrogel.
6. Add 500  $\mu$ L of 0.01% w/v TNBSA to each hydrogel and standard curve solution.
7. Mix the microcentrifuge tube content well using benchtop vortex.
8. Incubate the hydrogels and standard curve solutions in a horizontally shaking incubator at 37 °C and 150 rpm for 2 h.
9. Add 250  $\mu$ L of 10% w/v SDS and 125  $\mu$ L of 1 M HCl to each hydrogel and standard curve solution just after incubation period to stop the reaction.
10. Mix the microcentrifuge tube content well using benchtop vortex.
11. Hydrolyze the hydrogels by incubating them in a block heater at 120 °C for 15-30 min if they are not completely dissolved.
12. Transfer 100  $\mu$ L of sample solution of hydrogels and standard curve solutions to labelled 96-well plate.
13. Read the absorbance at 335 nm.

**Table C.4.1.** Standard curve solution preparation for TNBSA assay.

Volume of glycine stock solution, 5 mg/mL ( $\mu$ L)	Volume of 0.1 M sodium bicarbonate solution (mL)	Final glycine concentration (mg/mL)
0	5	0
5	5	0.005
10	5	0.01
20	5	0.02
30	5	0.03
40	5	0.04
50	5	0.05

**Figure C.4. 1.** Calibration curve for TNBSA assay with the known concentrations of glycine.

## C.5. Assessment of the resistance of hydrogels against enzymatic degradation

### C.5.1. Collagenase assay

1. Prepare collagen type I hydrogels (300  $\mu$ L) for each defined time point (2, 4, 8, 24 h).
2. Place hydrogels into labelled 2 mL microcentrifuge tubes.
3. Prepare the buffer solution with 0.1 M Tris-HCl (pH 7.4) and 50 mM CaCl<sub>2</sub>.
4. Prepare a 50 U/mL of collagenase degradation solution in the buffer solution according to the equation below.

$$x = y \cdot \frac{1 \text{ mL buffer}}{1 \text{ sample}} \cdot \frac{50 \text{ U}}{1 \text{ mL buffer}} \cdot \frac{1 \text{ mg of collagenase powder}}{\alpha \text{ U}}$$

where, x is the required amount of collagenase powder in mg, y is the total number of samples, and  $\alpha$  is the U/mg of the collagenase powder specified by the manufacturer.

5. Add 1 mL of degradation solution into each hydrogel.
6. Incubate in a horizontally shaking incubator at 37 °C and 150 rpm for each defined time point.
7. At each time point, take an aliquot of 100  $\mu$ L of each sample, and transfer it into new microcentrifuge tube, and centrifuge at 3,500 g for 10 min at room temperature.
8. Transfer the supernatant into a new microcentrifuge tube, and store at -20 °C till using them for Pierce™ BCA protein assay.

**C.5.2. Pierce™ BCA protein assay**

1. Determine the total volume of working reagent (WR) using the following formula.

Total required WR volume = (#standards + unknowns) × (#replicates) × (volume of WR per sample)

2. Prepare WR by mixing BCA reagent A and BCA reagent B in 50:1 ratio.
3. Transfer 100 µL of standard curve solutions and frozen supernatant into labelled microcentrifuge tubes.
4. Add 2 mL of WR to each tube.
5. Cover the lid of tubes and incubate them at 37 °C for 30 min.
6. Cool all tubes at room temperature.
7. Read the absorbance of samples and standard curve solutions at 562 nm.
8. Subtract the absorbance of blank sample (water) from the absorbance of samples and standard curve solutions.
9. Prepare the standard curve with the known concentrations of bovine serum albumin (BSA).
10. Calculate the concentration of collagen concentration in each sample by interpolating their absorbance using standard curve.

**Table C.5.2.1.** Preparation of standard curve solution for Pierce™ BCA protein assay.

<b>Vial</b>	<b>Volume of diluent (μL)</b>	<b>Volume and source of BSA (μL)</b>	<b>Final BSA concentration (μg/mL)</b>
A	0	300 of stock	2000
B	125	375 of stock	1500
C	325	325 of stock	1000
D	175	175 of vial B dilution	750
E	325	325 of vial C dilution	500
F	325	325 of vial E dilution	250
G	325	325 of vial F dilution	125
H	400	100 of vial G dilution	25
I	400	0	0

## C.6. Release profile and release kinetics of essential oil from hydrogels

### C.6.1. Release profile

1. Determine the specific wavelength of *Thymus sibthorpii* essential oil (**Figure C.6.1.1**).
2. Prepare standard curve with the known concentrations of *Thymus sibthorpii* essential oil using 70% v/v ethanol as a solvent (**Figure C.6.1.2**).
3. Prepare collagen type I hydrogels (300  $\mu$ L).
4. Soak hydrogels into 1 mL of 1x PBS (pH 7.4) and incubate at 37 °C in a horizontal shaker incubator.
5. At each defined time point (0, 0.5, 1, 1.5, 2, 2.5, 3, 3.5, 4, 24, and 48 h), take 100  $\mu$ L of sample and refresh by 100  $\mu$ L fresh 1x PBS.
6. Transfer the samples taken into 96-well plate.
7. Read the absorbance at 365 nm which is specific to *Thymus sibthorpii* essential oil.
8. Calculate the concentration of the released *Thymus sibthorpii* essential oil by interpolation using the linear calibration curve.
9. Calculate the cumulative release percentage of *Thymus sibthorpii* essential oil according to the equation below.

$$\text{Cumulative Release \%} = \sum_{t:0}^t \frac{M_t}{M_0} \times 100$$

where  $M_t$  is the released amount of EO at time  $t$ , and  $M_0$  is the initial EO amount.

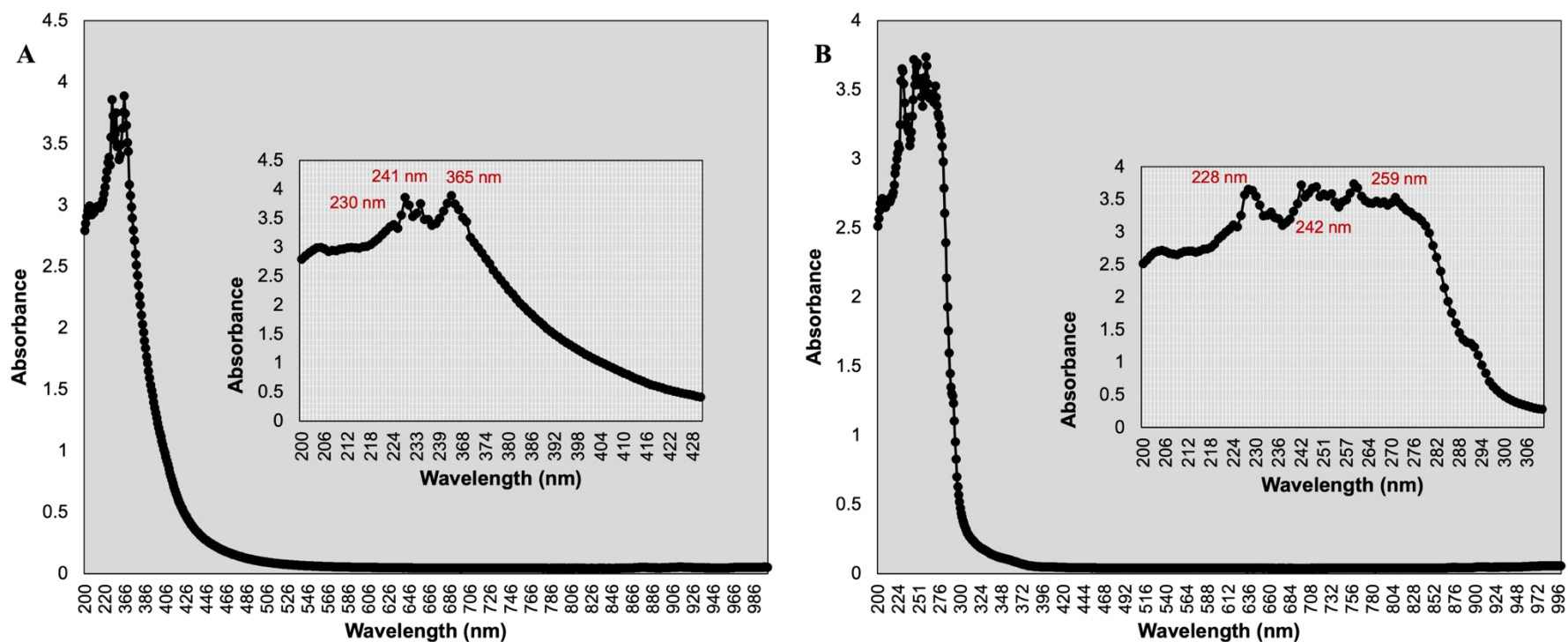


**Figure C.6.1.1.** The scanning of the wavelength of (A) pure *Thymus sibthorpii* essential oil, (B) 70% v/v ethanol in order to assess the specific wavelength of the essential oil. 365 nm was determined as specific to *Thymus sibthorpii* essential oil which gives the maximum peak.

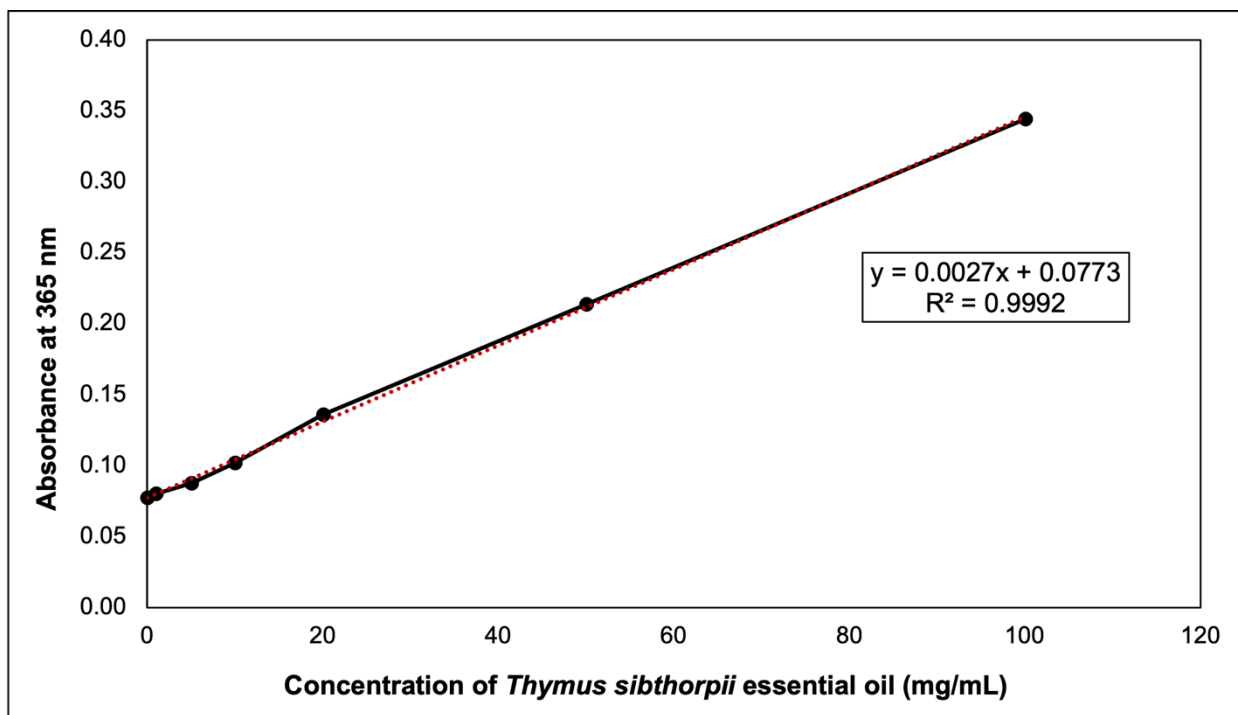


**Figure C.6.1.2.** Calibration curve for release profile assessment with the known concentrations of *Thymus sibthorpii* essential oil.

### C.6.2. Release kinetic mathematical model

In order to assess the release kinetics of *Thymus sibthorpii* essential oil from collagen type I hydrogels, five different mathematical models were applied to the cumulative release amount of essential oil. The mathematical models used are given below.

- Zero-order model:

$$\frac{M_t}{M_\infty} = Kt$$

- First-order model:

$$\ln\left(1 - \frac{M_t}{M_\infty}\right) = -Kt$$

- Higuchi model:

$$\frac{M_t}{M_\infty} = Kt^{1/2}$$

- Korsmeyer-Peppas model:

$$\frac{M_t}{M_\infty} = Kt^n$$

- Hixson-Crowell model:

$$M_0^{1/3} - M_t^{1/3} = Kt$$

where  $M_t$  is the released amount of EO at time  $t$ , and  $M_0$  is the initial EO amount,  $M_\infty$  indicates the amount of EO for the final time of the measurements,  $K$  is the release constant, and  $n$  is the release exponent.

## **C.7. Cell culture**

### **C.7.1. Culture medium for NIH-3T3 fibroblasts**

1. DMEM high glucose (4500 mg/L)
2. 10% v/v FBS
3. 1% v/v Penicillin/streptomycin

### **C.7.2. Cell thawing and passaging**

1. Remove vial from liquid nitrogen container and thaw with the body temperature of in a water bath at 37 °C.
2. Transfer vial content to culture flask of appropriate size containing pre-warmed culture medium.
3. Change culture medium every 2-3 days and observe cell morphology and proliferation with a phase contrast microscope.
4. When cells reach 80% confluency, remove the culture medium, wash cell layer with 1x PBS and add appropriate amount of trypsin/EDTA according to the culture flask size. Incubate at 37 °C, 5% CO<sub>2</sub> for 5 min until cells start detaching from the surface of the flask.
5. Add culture medium with the double volume of added trypsin/EDTA to block the action of trypsin/EDTA.
6. Transfer flask content into a Falcon tube and centrifuge at 1,200 rpm for 5 min.
7. Discard the supernatant and resuspend the cells in desired amount of culture medium.

### **C.7.3. Cell freezing**

1. Remove culture medium and wash cell layer with 1x PBS.
2. Add an appropriate amount of trypsin/EDTA and incubate at 37 °C, 5% CO<sub>2</sub> for 5 min until cells start detaching.
3. Add culture medium with the double volume of added trypsin/EDTA to block the action of trypsin/EDTA.
4. Transfer flask content into a Falcon tube and centrifuge at 1,200 rpm for 5 min.
5. Resuspend cell pellet in a necessary amount of freezing medium (90% v/v of medium with 10% of dimethyl sulfoxide) to have 1 million cells per 1 mL of medium.

6. Add 1 mL of cell suspension per cryogenic vial and place in Mr. Frosty overnight at -80 °C.
7. Move the cryogenic vials to liquid nitrogen container for long term storage.

#### C.7.4. Cell seeding

1. Prepare collagen type I hydrogels (300 µL) and sterilize them via UV irradiation for 1 h.
2. Place the sterilized hydrogel to the wells of 24-well plate for each defined culture day (1, 3, 5 days).
3. Condition the hydrogels with 500 µL of culture medium.
4. Prepare a cell suspension by adjusting 50,000 cells per 20 µL of culture medium.
5. Seed the cells on the top of the hydrogels by adding 20 µL cell suspension.
6. Incubate at 37 °C, 5% CO<sub>2</sub> during the defined culture period.
7. Change medium every 2 days.

#### C.7.5. alamarBlue™ assay

1. Prepare a 10% alamarBlue™ solution in DMEM.
2. Discard culture medium from the cell seeded hydrogels and wash with 1x PBS.
3. Add 500 µL of 10% alamarBlue™ solution to the hydrogels, and 10% alamarBlue™ solution alone as a negative control.
4. To observe the background absorbance, add medium alone to empty wells.
5. Incubate for 2-4 h at 37 °C, 5% CO<sub>2</sub>.
6. Transfer 100 µL of alamarBlue™ solution to the new 96-well plate after reaction.
7. Read the absorbance at 550 and 595 nm. The absorbance values are called as absorbance of the oxidized form at lower wavelength (AO<sub>LW</sub>), and absorbance of the oxidized form at higher wavelength (AO<sub>HW</sub>) for 500 and 595 nm, respectively.
8. Subtract the absorbance of medium from each measured absorbance values if it cannot be negligible.
9. Evaluate the correlation factor (R<sub>0</sub>) according to the equation below:

$$R_0 = \frac{AO_{LW}}{AO_{HW}}$$

10. Calculate the percentage of alamarBlue™ reduction (AR%) by the cells according to the equation below:

$$AR\% = A_{LW} - (A_{HW} \times R_0) \times 100$$

#### **C.7.6. Quant-iT™ PicoGreen™ dsDNA assay**

1. Remove the media and gently wash the hydrogels with 1x PBS.
2. Add 250  $\mu$ L of DNase-free water to each group.
3. Freeze-thaw cell seeded hydrogels three times by freezing at -80 °C for min 15-20 and thawing in the incubator at 37 °C till completely defrosted.
4. Prepare a 1x TE buffer by diluting 20x stock solution with DNase-free water.
5. Prepare standard curve solutions with the known DNA concentration using DNase-free water (**Table C.7.6.1**). Prepare 2  $\mu$ g/mL and 50 ng/mL DNA stock solutions.
6. Make up the PicoGreen™ solution (5.376 mL 1x TE buffer + 27  $\mu$ L concentrated PicoGreen™).
7. Add 100  $\mu$ L of diluted PicoGreen™ solution to each well and gently mix them.
8. Incubate at room temperature for 2-5 minutes in a dark environment.
9. Transfer 100  $\mu$ L of each sample to the new 96 well-plate.
10. Read the fluorescence (excitation: 480 nm, emission: 520 nm).
11. Evaluate the DNA concentration by interpolating the fluorescence values using calibration curve.

**Table C.7.6.1.** Preparation of standard curve solution for Quant-iT™ PicoGreen™ dsDNA assay.

<b>Volume of DNase-free water (μL)</b>	<b>Volume of 2 μg/mL DNA stock solution (μL)</b>	<b>Volume of 50 ng/mL DNA stock solution (μL)</b>	<b>Final DNA concentration (ng/mL)</b>
200	200	0	1000
300	100	0	500
380	20	0	100
0	0	400	50
200	0	200	25
320	0	80	10
360	0	40	5
400	0	0	0